



HOST UNIVERSITY: The University of Edinburgh

FACULTY: College of Science & Engineering

DEPARTMENT: School of Engineering

Academic Year 2020-2021

**STUDY OF THE CHAR FALL-OFF PHENOMENON IN CROSS-LAMINATED TIMBER  
UNDER FIRE CONDITIONS**

Antonela Čolić

Supervisor(s): Prof. Luke Bisby and Dr Juan P. Hidalgo

Co-supervisor: Dr Felix Wiesner

Master thesis submitted in the Erasmus+ Study Programme

**International Master of Science in Fire Safety Engineering**

## Disclaimer

This thesis is submitted in partial fulfilment of the requirements for the degree of *The International Master of Science in Fire Safety Engineering (IMFSE)*. This thesis has never been submitted for any degree or examination to any other University/programme. The author declares that this thesis is original work except where stated. This declaration constitutes an assertion that full and accurate references and citations have been included for all material, directly included and indirectly contributing to the thesis. The author gives permission to make this master thesis available for consultation and to copy parts of this master thesis for personal use. In the case of any other use, the limitations of the copyright have to be respected, in particular with regard to the obligation to state expressly the source when quoting results from this master thesis. The thesis supervisor must be informed when data or results are used.

Read and approved,



Antonela Čolić

Edinburgh, May 11,2021

Total word count: 23,213

## Abstract

Cross-laminated timber (CLT) is a structural composite, in which layers of crosswise oriented lamellae are glued together, and it is prevalently used for walls and slabs. This composite action is restricted at elevated temperatures because the adhesive and timber deteriorate at a different rate. If the adhesive successfully holds the charred layer, then this char will serve as an “insulating” material. This function makes it possible to design for timber auto-extinction. This is crucial for a successful compartmentation fire strategy, which is critical for tall mass timber buildings. The physical separation between two bonded surfaces is called debonding, which in fire conditions is characterised as delamination and char fall-off. In the current state of the art debonding was found to be influenced by various parameters, starting from manufacturing, timber, and adhesive properties, to the methodology or standards used to test these properties, both in ambient and elevated temperatures.

To study debonding, 30 small scale tests were performed on 3 lamellae CLT blocks, from three different European manufacturers. Two different types of one-component-polyurethane (1-C-PUR), and one melamine-urea formaldehyde (MUF) were used. Samples were simultaneously exposed to a structural load (shear stress of 0.15 and 0.20 MPa) and a thermal load (radiant heat flux of 50kW/m<sup>2</sup>). The analysed variables are structural load, bond line temperature at failure, adhesive type, and moisture content.

Four types of failure modes were observed: char fall-off, delamination, local, and mechanical failure. The mean delamination temperatures in the first bond line varied from 78°C (MUF) to 235°C (1-C-PUR). The amount of load placed was only influential for delamination phenomena, where samples experienced delamination at the higher load. Moisture movement was noticed to be an influential factor, but its impact could not be quantified.

The method developed in this work is suitable to observe delamination, there are however some limitations to this approach. To address the issue of char-fall off, the changes in geometry are required (lamellae number and thickness). The high percentage of the local failure at the top of the front lamella also indicated the need for further refinement. The method used in this study can successfully address some of the issues, but more research is needed so that the designer can “*hold the line, hold the bond line!*”.

## Abstract (Sažetak)

Križno-lamelirano drvo je konstrukcijski kompozit u kojem su slojevi križno orijentiranih lamela zalijepljeni i uglavnom se koristi za zidove i ploče. Kompozitno djelovanje ograničeno je na povišenim temperaturama jer ljepilo i drvo gube mehanička svojstva različitom brzinom. Ako ljepilo uspješno zadrži pougljenjeni sloj, tada će taj ugljen služiti kao "izolacijski" materijal. Ova funkcija omogućuje dizajn automatskog gašenja gorućeg drveta, što je presudno za uspješno zoniranje, protupožarnu strategiju za visoke drvene građevine. Fizičko razdvajanje dviju vezanih površina je gubitak prijanjanja (*debonding*), što se u uvjetima požara karakterizira raslojavanjem (delamination) i otpadanjem ugljena (char fall-off). Trenutno stanje područja definira da na gubitak prijanjanja utječu različiti parametri, počevši od svojstava proizvodnje, drva i ljepila, do metodologije ili standarda koji se koriste za ispitivanje tih svojstava na sobnoj temperaturi i na povišenim temperaturama.

Gubitak prijanjanja proučavan je u 30 ispitivanja u malom mjerilu na 3 bloka CLT lamela, od tri različita europska proizvođača. Korištene su dvije različite vrste jedno-komponentnog poliuretana (1-C-PUR) i jedna vrsta melamin-urea formaldehida (MUF). Uzorci su istodobno bili izloženi konstrukcijskom opterećenju (posmično naprezanje od 0,15 i 0,20 MPa) i toplinskom opterećenju (radijacijski toplinski tok od 50kW/m<sup>2</sup>). Analizirane varijable su opterećenje, temperatura u prvoj liniji (površini) ljepila, vrsta ljepila i sadržaj vlage.

Uočene su četiri vrste otkaza: otpadanje ugljena, raslojavanje, lokalni i mehanički lom. Srednje temperature raslojavanja u prvoj površini ljepila varirale su od 78 °C (MUF) do 235 °C (1-C-PUR). Količina postavljenog tereta bila je utjecajna samo za raslojavanje, i to pri većem opterećenju. Kretanje vlage je utjecajan čimbenik, ali ga nije bilo moguće kvantificirati.

Metoda razvijena u ovom radu prikladna je za promatranje raslojavanja, no ovaj pristup ima određena ograničenja. Za proučavanje otpadanja ugljena, potrebne su promjene u geometriji (broj i debljina lamela). Visok postotak lokalnog otkaza na vrhu prednje lamele ukazuje na potrebu daljnjeg usavršavanja. Metoda korištena u ovoj studiji može uspješno riješiti neke probleme, ali potrebno je više istraživanja kako bi dizajner mogao "držati borbenu crtu!".

## Declaration of Covid-19 Impact

It is easy for me to write about the pandemic now that I have finished the thesis and I am writing this section the morning before the submission to reflect on the past couple of months.

At the moment, I was supposed to be in Queensland, Australia, but the travel ban made us slightly change the topic based on the laboratory equipment that was available at The University of Edinburgh. The great support I had from the very start from my supervisors, allowed me to run a large number of experiments throughout the March. The whole process was discussed in detail in our weekly meetings with my two other supervisors in at the University of Queensland.

It did take some time to prepare the experimental setup and to get into the laboratory, due to the restrictions in number of people. But once I was in there, I had the opportunity to run my experiments with no interruption. Being surrounded by the Edinburgh Fire Group members was very helpful to proceed with the Thesis. I was also very lucky to enter the country on time and to have no issues with any administration on the government or university level.

I was able to adjust to the new normal because I knew what it is, and it was more certain than the last year. Every period brings something new. The pandemic did affect three out of my four semesters, but this last one was the least affected because I had people to support me and the opportunity to stay focused, to really *hold my horses* and to get some work done. I think the biggest drawback were the overly ventilated rooms in a very windy city called Edinburgh.

So, to quantify, what was the impact of pandemic, from 0(No impact at all) to 10 (Having the difficulties to submit the Thesis)? It was 3. One for not seeing my siblings, one for not dancing, and one for having to postpone my travel to Australia to meet the amazing UQ Fire group. It would be four had I not have the members of Edinburgh Fire Group around me.

You cannot have it all, but you can plan to have it all!

## Acknowledgements

I consider myself to be a very lucky person for being a part of IMFSE Programme. That is why I am firstly thankful for the given opportunity to study in such a multi-cultural environment, guided by renown but still relaxed and humble professionals. This changed my perspectives and helped me to grow.

This thesis is a product of extreme support from my supervisors Prof. Luke Bisby, Dr Juan P. Hidalgo and Dr Felix Wiesner, and their ability to regularly answer all kinds of creative questions without looking too bored or busy. I am thankful to Luke for encouraging me, for *always making every-single-thing possible* and for make things easier with his famous “*It is all just simple structural mechanics!*”. Thanks to Felix, for translating what the “*simple structural mechanics*” actually is, and for pulling me out of the zillion rabbit holes. And thanks to Juan, for reminding me how to apply my research in practice, for being very responsive and understanding from the other part of the world, for being a great heat-transfer- teacher, and for being a role model as a friend and basically as a human being.

I was fortunate to be a part of the Edinburgh Fire Group and to learn what a small collective can do together. I would like to highlight some individuals and especially thank to Hussein and Tim, the two extremely patient guys, for all the hours of preparation work they spent and the lead ingots (load) they were carrying around the lab with me; to David, a young enthusiastic soul, for being a great friend whose everlasting presence in the lab and willingness to help made my days; to Mike and Michal, two fantastic technicians without whom this all would be impossible, for adjusting my shear rig and fixing my H-TRIS in no time; and finally to Simon, George and Grunde, three very positive and encouraging individuals.

Nothing would be possible without my friends. I am thankful: to my Laura, for her significant support, understanding, love and never-ending video calls; to Darko, for pushing me forward and encouraging me to do the IMFSE; to Dan, my favourite Australian, for every balloon game, biking trip, slow run, jump in the bushes, and for making my life cheerful; to Cathleen, for every dance and for teaching me how to spend the money on everything and nothing; to

my Tuur, Rona and Lucas, for all of our travels, dinners, talks about sustainability, future plans and gossips in general; and finally to my Edinburgh family, Anna, Ali and Mina, for endless talks in the kitchen, for not complaining about my showers at 2 am and for respecting my sensitivity to any type of smell.

And thanks to my V., for all the hugs and long walks, for every *hold your horses* meme, for making fun of my English, for teaching me that articles exist and that species is only plural, for all of his Oxford commas, and for talking to me about the new released albums, when all I wanted to do is to talk about timber.

I know that this is a long section but it is important to say thank you.

Nothing would be the same without my Balkan crew; my Mergim, Ivana, Miha, Tonta, Teodora and Nikola to whom I am thankful for never changing, for sharing all the cold summer coffees and for all the support they gave me throughout this journey.

And most importantly, I am grateful for the help from my siblings and my parents. For their jokes, their Tik Tok non-sense, and for all the singing videos they sent me during the exam period. I am very happy to have my Ana, who teaches me how to wake up after 7 and my Josip for every Balkan vegetarian meal he cooked for me (by taking out the meat with a spoon).

I truly think that this all made a huge contribution to finishing my Master and doing my thesis. Because, to be creative you need to get rid of the frustrations, and there is so much more that contributes to it, rather than just being able to enter the lab during the pandemic.

## Table of Contents

Chapter 1	Introduction.....	17
1.1	What is debonding? .....	19
1.2	Research aim and objectives .....	21
Chapter 2	Literature review.....	23
2.1.1	Manufacturing.....	23
2.1.2	Adhesive properties .....	27
2.1.3	Timber properties .....	34
2.1.4	Understanding the adhesive and timber interaction in specific EWP .....	36
2.2	Thermal load effects on debonding.....	37
2.2.1	Char layer formation.....	37
2.2.2	Bond line temperature and thermal penetration depth.....	41
2.3	Structural load effects on debonding.....	42
2.3.1	Loss of shear strength.....	45
2.3.2	Failure mode and wood failure percentage .....	50
2.3.3	Temperature induced creep .....	55
2.4	Summary: structural and thermal response of adhesives.....	56
2.5	Important methodology drivers .....	57
2.5.1	Impact of non-harmonised testing standards.....	58
2.5.2	System size .....	59
2.5.3	Thermal exposure (steady-state/transient heating/pre-heating) .....	60
2.5.4	Importance of structural load .....	61
2.5.5	System orientation (Horizontal or vertical) and fuel distribution.....	62



2.5.6	Layer setup and importance of edge-gluing .....	62
Chapter 3	Methodology .....	64
3.1	Materials.....	65
3.2	Experimental conditions .....	67
3.2.1	Structural loading conditions.....	68
3.2.2	Thermal loading conditions.....	70
3.2.3	Duration of tests.....	71
3.2.4	Experimental matrix .....	71
3.3	Experimental apparatus, instrumentation and procedure .....	72
3.3.1	Ambient shear strength tests .....	73
3.3.2	Moisture content tests.....	73
3.3.3	Shear strength tests under fire conditions.....	73
Chapter 4	Results and discussion .....	79
4.1	Ambient shear strength tests .....	79
4.2	Shear strength tests in fire conditions .....	81
4.2.1	Thermal behaviour of the tested samples .....	81
4.2.2	Type of failure modes identified .....	84
4.2.3	Failure time and temperature at the first bond line.....	87
4.2.4	Factors relevant to failure modes.....	91
Chapter 5	Conclusions and future work .....	105
References	.....	108
Appendix A	.....	126
Appendix B	.....	129
Appendix C	.....	135

Appendix D ..... 148  
Appendix E ..... 156

## List of Figures

Figure 1. Example of EWP products in Hereford college of arts, England, UK; © Lance McNulty Photography [2] ..... 17  
Figure 2. Debonding – the difference between char fall-off and delamination, and failure description at the bond line ..... 19  
Figure 3. Use of PUR and MUF among CLT manufacturers in Europe ..... 25  
Figure 4. Use of PUR and MUF among GLT manufacturers in Austria and Germany ..... 25  
Figure 5. SEM images of MUF (left) and PRF (right) adhesive at 20°C [88]. Bond line thickness includes wood interphase (1) and adhesive bulk (2) - adhesive can penetrate the cell (cavity, primary wall) and the space between cells (middle lamella) ..... 28  
Figure 6. Overview of glass transition temperatures from Witowski et al. [99], Nicolaidis et al. [21], Richter et al. [46], Verdet et al. [104], Cruz et al. [89] and Technical Sheets from Sika [83] ..... 33  
Figure 7. Difference in cellular structure for hardwood and softwood made with a scanning electron microscope [107]. Hardwood (Black Walnut (1), Red Oak (2)), Softwood (Eastern White Pine (3), Southern yellow Pine (4)). ..... 35  
Figure 8. Debonding of unloaded Radiata Pine (softwood) sample exposed to 65 kW/m<sup>2</sup>, modified from Emberley et al. [10] ..... 38  
Figure 9. Charring non-uniformity. Layer orientation (left): L-longitudinal, C-crosswise. Thermocouples output data (right) for specimen 3 (Adhesive: PRF, Layer setup: LCL); Adapted from Hasburgh et al. [23] ..... 40

Figure 10. Failure mode change in the beam tested in three-point test. Timber failure at ambient temperatures (left) and bond line failure at elevated temperatures (65-80C, right) [26] ..... 43

Figure 11. Shear stresses when loaded in-plane (wall-) and out-of-plane (slab-). Rolling shear in tangential direction  $\tau_{TR}$  and in radial direction  $\tau_{RT}$  . Adapted from Erhart and Brandner [132]..... 43

Figure 12. Reduction of shear strength at elevated temperatures. Formaldehyde adhesives – data adapted from Clauß et al.. [22], Frangi et al. [45], Liu et al. [88] and Zelinka et al. [127] ..... 48

Figure 13. Reduction of shear strength at elevated temperatures. Polyurethane adhesives – data adapted from Clauß et al.. [22], Frangi et al. [45], and Zelinka et al. [127]..... 49

Figure 14. Change in failure mode in ambient and elevated temperature observed in small-scale single-lap shear test (left)[21] and intermediate-scale three point bending beam test (right) [26]..... 50

Figure 15. Failure mode: A/T-Bonding interface (left)[140], (centre) [22]; A-Adhesive (centre); T-Timber (right)[45] ..... 51

Figure 16. Wood failure percentage for different Polyurethanes (upper) and Formaldehydes (lower) at 20C, adapted from Clauß et al [22], Niemz et al. [29], Frangi et al. [45], Clauß et al [51], Liu et al. [88], Zelinka et al. [127]and Lim et al. [141]..... 52

Figure 17. Wood failure percentage for formaldehydes, based on studies from Liu et al. [88], Clauß et al [51] and Zelinka et al. [127]..... 54

Figure 18. SEM images. Type of failure at 220°C: MUF loss of cohesion - A (1), PRF bonding interface failure A/T (2). Bond line thickness at 280°C: MUF (3), PRF (4). Adapted from Liu et al. [88]..... 54

Figure 19. Flowchart with the methodology used for this research..... 65

Figure 20. Series A: Large sample before slicing (left), Bond lines’ front view (centre), side view (right). ..... 66

Figure 21. Series B and C: Large sample before slicing (left), Bond lines' front view for PUR2 (centre), and MUF (right).....	66
Figure 22. In-depth cuts in the shearing bond line.....	67
Figure 23. Illustration of the steps taken to define structural load in experimental matrix	69
Figure 24. Time to ignition for all samples.....	71
Figure 25. Apparatuses used for ambient tests to failure (1,2) and for shear strength test under fire conditions .....	72
Figure 26. Shear rig geometry – 3D view with dimensions (left), side view (right).....	74
Figure 27. Position of thermocouples installed from the back of the sample (Series A and B). Dimensions are in mm. ....	75
Figure 28. Instrumentation for shear strength test under fire conditions.....	76
Figure 29. Stress vs. displacement curve for the ambient shear strength tests.....	79
Figure 30. Failure modes for ambient tests. From left to right: High wood failure percentage A2, B1, B2, C1; Partial adhesive cohesion failure C2.....	80
Figure 31. Average thermocouple reading at the first bond-line. Temperature-time curve for all specimens bonded with 1-C-PUR at the bond-line between layers and combination of Hotmelt and PVAc between single lamellae (narrow bonding).....	82
Figure 32. Average thermocouple reading at the first bond-line. Temperature-time curve for all specimens bonded with 1-C-PUR at the bond-line between layers and between single lamellae (narrow bonding) .....	82
Figure 33. Average thermocouple reading at the first bond-line. Temperature-time curve for all specimens bonded with MUF at the bond-line between layers and between single lamellae (narrow bonding).....	82
Figure 34. Samples loaded with 100kg (left) and 200 kg (right). Comparison of thermal profiles for PUR1 adhesive at 20min (blue), 30 min (green) and at the point of failure (F).83	

Figure 35. Failure modes: 1-2 Local failure, 3-4 Delamination, 5 Char fall off at the adhesive line, 6 Char fall off after the adhesive line .....	84
Figure 36. Local failure caused by eccentricity of load and eventual charring .....	85
Figure 37. Adhesive degradation (A12) and peeling forces(C4) caused by local failure at the top .....	86
Figure 38. Failure time for three groups of adhesive and different setup.....	87
Figure 39. Median failure temperatures in the first bond-line for three groups of an adhesive and different setup. The orange area represents range of temperatures for timber pyrolysis. Samples in bold indicate delamination.....	88
Figure 40. Thermal penetration for non-dried and dried samples 5s before the failure for A3, A7, B6, B7, C5 and C7 .....	90
Figure 41. Delamination: Adhesive-timber failure: bond-line interface with timber residues from the second lamella. From left to right: PUR2 B12; MUF C7, C8.....	96
Figure 42. Delamination: Timber failure: sliding of fibres in the first lamella. From left to right: B9, B14, A14 .....	96
Figure 43. Failure variation within one sample. From left to right: B9, B14.....	97
Figure 44. MUF and PUR2 main bond-line holding the charred lamella despite the developed cracks.....	98
Figure 45. Narrow bond-line failure for PUR2 (B) and MUF (C) adhesive. From left to right: B9, B12 (delamination), C6 (local failure).....	102
Figure 46. Narrow bond-line failure and specific wood failure for Hotmelt formaldehyde-free and PVAc adhesive From left to right: A6, A7, A9 (char fall-off).....	102
Figure 47. Buckled char fall-off residue.....	104

## List of Tables

Table 1. Different adhesives used for production of load-bearing (grey) and non-bearing (white) EWP products.....	24
Table 2. Adhesive properties that affect manufacturing.....	24
Table 3. Small scale shear tests in ambient temperatures .....	45
Table 4. Small scale shear tests at elevated temperatures .....	47
Table 5. Series of material samples, including information regarding timber species, adhesive and lamellae configuration.....	66
Table 6. Experimental matrix.....	72
Table 7. Thermal penetration for non-dried and dried samples 5s before the failure .....	90
Table 8. Visual observation of samples before/after mechanical failure (MF), and after cooling.....	92
Table 9. Visual observation of samples before and at char fall-off (CF).....	93
Table 10. Visual observation of samples before wood failure, at the moment of wood failure, and after cooling.....	95
Table 11. Visual observation of samples before or/and at delamination, and after cooling.....	95
Table 12. Change in failure modes based on the adhesive type, the structural load applied and moisture content.....	98

## Notation

### Terminology

$T_g$	glass transition temperature [°C]
$f_{r,k}$	characteristic rolling shear strength [MPa]
$L$	length [m]
$W$	width [m]

### Greek letters

$\tau_{RL}$	radial-longitudinal shear stress [MPa]
$\tau_{TL}$	tangential-longitudinal shear stress [MPa]
$\tau_{RT}$	radial-tangential rolling shear stress [MPa]

### Acronym

EWP	Engineered wood products
CLT	Cross-laminated timber
OSB	Oriented Strand Board
PB	Particleboard
FB	Fibreboard
GLT	Glue-laminated timber
LVL	Laminated veneer lumber
PSL	Parallel strand lumber – Parallam
LSL	Laminated strand lumber – Intrallam
PF	Phenol formaldehyde
RF	Resorcinol formaldehyde
PRF	Phenol Resorcinol formaldehyde
UF	Urea formaldehyde
MF	Melamine formaldehyde
MUF	Melamine-urea formaldehyde

PUR	Polyurethane adhesive
1-C-	One component
EPI	Emulsion Polymer Isocyanate adhesive
EPX	Epoxy adhesive
HRR	Heat release rate
WFP	Wood failure percentage
BSS	Block shear strength
LSS	Lap shear strength
HMR	Hydroxymethylated Resorcinol primer
MCA-C	Micronized Copper Azole preservative
MC	moisture content
TGA	thermogravimetric analysis
T	timber failure
A	adhesive cohesion failure
A/T	failure at the adhesive/timber interface



## Chapter 1 Introduction

Adhesives in the timber industry are mostly used for connecting wooden parts of differing properties towards a unified product, i.e. composite. Applications are mainly focused on joints (Finger-joints, Glued-in-rods, I-joists), non-structural wood-based panels (Oriented Strand Board (OSB), Particleboard (PB), Fibreboard (FB)), and structural Engineered Wood Products (EWP). With the increased use of CLT for loadbearing purposes, there is a knowledge gap about how adhesives perform in elements with a structural role. In this thesis, the interaction between timber and adhesive in EWP will be studied for cross-laminated timber (CLT), presented in Figure 1. Some other types of EWP products where adhesive technology is also used are (glue-laminated timber (GLT), laminated veneer lumber (LVL), parallel strand lumber – Parallam (PSL), or laminated strand lumber – Intrallam (LSL)) [1].

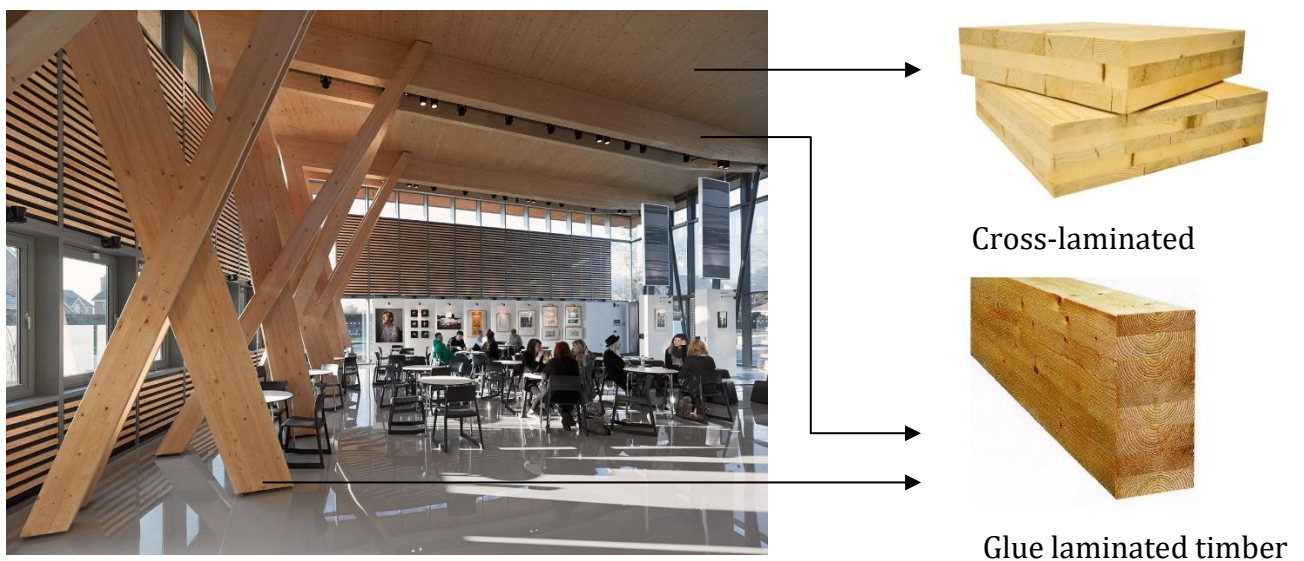


Figure 1. Example of EWP products in Hereford college of arts, England, UK; © Lance McNulty Photography [2]

The mechanical strength of timber is affected by numerous factors such as moisture content, density, grain slope, and natural imperfections. By splitting larger timber parts into lamellas and then re-joining them, as in EWP, more control is present in the production process and the variance is reduced [3].

The structural response of EWP, in both ambient -and elevated temperatures, relies on the successful composite action, which depends on the adhesive-timber interaction [4]. An extensive summary about timber behaviour in fire can be found in recent review from

Bartlett *et al.* [5], while Barber and Gerard [6] indicated challenges in fire safety for specifically EWP products as LVL, SCL, GLT and CLT in tall timber buildings (e.g. contribution of CLT to room fires, transient fire testing, compartment burnout and CLT delamination and char fall-off).

Adhesives are designed to have the same or higher strength than the adjoining timber. However, adhesive strength deteriorates at temperatures above ambient [7]. When EWPs are exposed to a compartment fire, it is assumed that debonding is influenced by the performance of the adhesive. As EWP manufacturers in different parts of the world use various polymer adhesives, failure modes at the timber-to-timber bonding interfaces in case of heating must be adequately understood for credible fire safety engineering design to be performed by practitioners.

In recently published work by Law and Hadden [8], together with a talk given at the Institution of Structural Engineers by Law [9], the authors tried to shed light on the engineer's professional responsibility when using structural timber in tall timber buildings, and not taking into consideration any advantages or disadvantages of the material. Four hazard mitigation strategies were presented: (1) encapsulation, (2) demonstration of auto-extinction by full-scale testing, and (3) demonstration of auto-extinction by solving the energy balance. Successful implementation of one of the three above will allow for compartmentation and (4) restricted fire spread (externally and internally, horizontally and vertically) safe firefighting operations, and structural integrity and stability during and after the decay phase [10], where the structure is still standing to satisfy the functional requirements set out in the regulations.

(1) Encapsulating the timber with a thermal barrier, leads to an insignificant contribution of timber to the compartment fire [11] with delayed charring onset of the first lamella behind the protection [5][12]. Potential integrity failure of the encapsulation [13] leaves the unprotected timber exposed and leads to an increase in heat release rate (HRR), charring rate and the possibility of flashover onset [11,14].

(2,3) Tall mass timber structures ought to be designed to achieve auto-extinction. This is a part of compartmentation fire strategy where construction itself as a fuel needs to cease flaming and achieve burnout. As discussed by Crielaard *et al.* [15] it happens when: (i) there is no sufficient energy for the timber to continue burning (5-6 kW/m<sup>2</sup>) [16], (ii) the

char fall-off is prevented, and (iii) when the ventilation conditions do not allow for sufficient thermal penetration [13,17] for continuous smouldering of the element. To achieve this, encapsulation should not fail, the ratio of exposed CLT surfaces should be limited [13,17,18] and the adhesive between the lamellae should not fail.

If the adhesive fails, the (semi) charred lamella will debond, allowing for the new virgin timber to be consumed as a fuel and preventing in that way the auto-extinction. If the adhesive successfully holds the charred lamellae, charred layer will serve as an “insulating” material. By predicting, postponing, or even preventing debonding, it may be possible to design for the auto-extinction of timber, supporting the main concept of compartmentation.

### 1.1 What is debonding?

Debonding is a process of separation between any two bonded surfaces caused by any type of mechanism [19]. As explained by different authors [10,20–22], debonding of EWP can be caused through three different mechanisms. (1) the failure within the timber (lamellae), (2) through the loss of cohesion within the adhesive, and (3) loss of adhesion between the timber and adhesive at the bonding interface. These mechanisms are presented visually in Figure 2. The terminology used to describe this phenomenon varies greatly among researchers, and often terms such as *delamination* [1,7,29–32,11,21,23–28], *char fall-off* [6,33–36], or *loss of stickability* [36,37] are used interchangeably to describe the fall-off of both, completely or partially charred lamellae. Figure 2 shows the difference between the two concepts of debonding, char fall-off and delamination, and the classification used in this study.

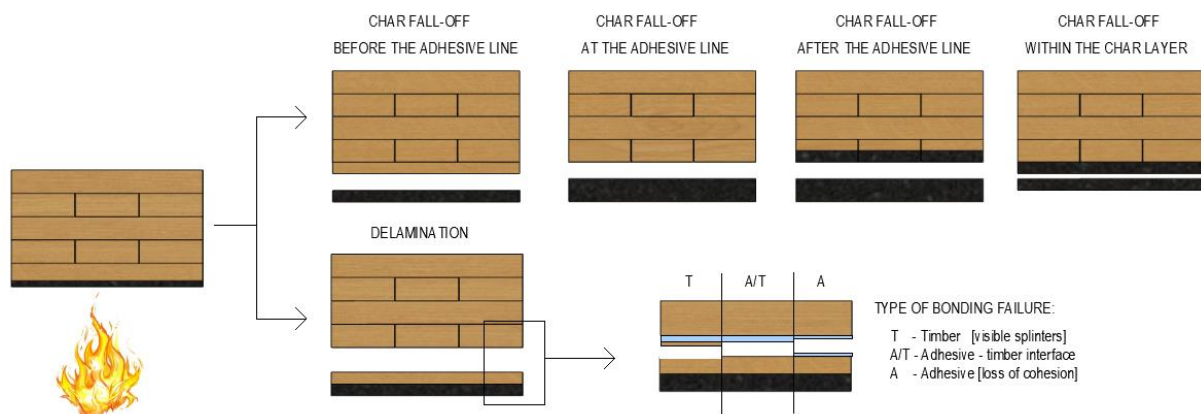


Figure 2. Debonding – the difference between char fall-off and delamination, and failure description at the bond line

The occurrence of debonding in EWP's under fire conditions can have effects on the fire dynamics and the structural performance:

- Fire dynamics. New fuel becomes available for the fire, thus causing a sufficient thermal feedback to the timber structure for prolonged steady and/or cyclic burning [10]. Prolonged burning inhibits auto-extinction and the subsequent burnout of the compartment.
- Structural performance due to the exposure of uncharred timber. The development of a layer of char is typically responsible for a decay in the heat transfer to the underlying timber, and thus a slower movement of the pyrolysis front. Reignition of newly exposed virgin timber in the post-flashover phase, caused by any type of debonding, could result in faster loss of cross-section, possible instability, and equivalently faster in-depth heating which can lead to reduced mechanical properties [20,38].

The concepts of char fall-off and delamination are explicitly defined for clear interpretation of the work presented within this thesis.

### **Char fall-off**

As shown in Figure 2, the fall of charred timber can occur before, at and after reaching the adhesive line. The occurrence of *char fall-off at the and after reaching the adhesive line* can be considered to depend on the performance of the adhesive. Conversely, the occurrence of *char fall-off before reaching the adhesive line* or *within the char layer* can be considered as an timber integrity failure of the charring lamella caused by debonding between charred and uncharred timber. In this thesis, the latter two are considered to be out of the scope.

If CLT experiences char fall-off *before or at the adhesive line*, the protective material in front of the virgin wood is completely lost, pyrolysis rate increases renewing the charring of the cross-section, and subsequent growth in the compartment fire's HRR and duration is achieved [5,24]. If CLT experiences char fall-off *within the char layer*, or *after the char depth reaching the adhesive line*, this effect on the fire dynamics can still occur, albeit with less intensity as there still exists a protective char layer slowing down the heat transfer to the virgin timber [10].

Char fall-off is sometimes described as *loss of stickability* [36], which is defined/described as the “ability of a fire protection material to remain sufficiently coherent and in position without failure due to detachment of a significant area (0.25 m<sup>2</sup>) or sudden significant temperature rise upon the initially protected timber surface” [37]. This term originates from the use of passive fire protection solutions (e.g. plasterboard). However, the term is not suitable for timber as char fall-off can also occur because of the loss of char integrity, *within the char layer*, uninfluenced by the adhesive.

### **Delamination**

In the US standard ASTM PRG 320-2019 [39] *delamination* is described as “the separation of layers in a laminate due to a failure of the adhesive either in the adhesive itself or at the interface between the adhesive and adherent” and can be used for both, delamination in ambient and fire conditions. Delamination in non-fire situations reflects only the response from applied structural load or/and environmental changes (i.e. exterior usage of EWP products exposed to several dry and wet cycles can result in splitting along the lamellas [1,40,41]). From studies in ambient conditions, one can define general adhesive properties, but for this study, the main interest is delamination caused by large preheating times that can cause risk of failure in the adhesive line before any charring propagates to the bond line [25,42], as explained in Figure 2. Example of both, char fall-off and delamination, was observed in the full-scale compartment tests from Hadden *et al.* [13]. When delamination occurred, the char did not penetrate the full thickness of the first lamella.

## **1.2 Research aim and objectives**

The aim of this study is to better understand the performance and response of different adhesives in fire conditions and their effect on delamination and char fall-off.

The objective is to perform small scale CLT experiments for three types of adhesives, to observe and describe how debonding prevents participation of the affected cross section in the element load transfer in shear through:

- Discussion about and comparison of the adhesive’s shear strength and the load transfer between two lamellae when exposed to ambient temperatures or

simultaneous application of thermal load from the radiant panel and different structural load.

- Assessment of influence of the thermal penetration on the delamination or char fall-off at the adhesive line. In-depth positioned thermocouples will be used to find the thermal gradient beneath the char line and the critical bond line temperature range that affects the bonding performance and failure mode.
- Discussion about the lamella thickness influence on the thermal wave delay the and the adhesive protection.
- Reflection on the impact of moisture content on the adhesive structural performance.
- Visual evaluation of the char fall-off and delamination phenomena during the tests and their influence on structural performance.

This can improve understanding and design of the EWP's auto-extinction, which plays a crucial part in the forming of fire strategies in multistorey, multi-occupancy, and complex mass timber buildings

## Chapter 2 Literature review

Time, temperature, and moisture content thresholds in fire define the composite action between CLT layers and their corresponding structural and thermal response. These thresholds depend on: (1) manufacturing properties, (2) adhesive and timber material properties, (3) developed bond line temperatures, (4) char depth, (5) the structural load applied, and other yet unexplored variables. All of them will be discussed within this literature review and the summary is presented as a diagram in Appendix A. Emphasis will be given on the properties that could be directly measured from the results of the experiments within this study.

The standards used by researches will be noted to emphasise the need for harmonised EWP standards, with well-defined and unified performance criteria for specific combinations of adhesives and timber species. (All experimental studies used are tabulated in Appendix B).

### 2.1.1 Manufacturing

Adhesive types applied in EWP can be classified as traditional or new (non-traditional) [1]. Traditional adhesives are formaldehyde adhesives, phenolic, and aminoplastic: Phenol – (PF), Resorcinol – (RF), Phenol Resorcinol – (PRF), Urea – (UF), Melamine – (MF) and Melamine-urea Formaldehyde (MUF). New adhesives are Polyurethane- (PUR), Emulsion Polymer Isocyanate- (EPI), and Epoxy adhesives (EPX) [43]. It is also common to differentiate adhesives based on the type of EWP they are used for. Such differentiation is presented in Table 1 to distinguish the structural applications (load-bearing) from non-structural (wood composites such as fibre and particle boards [44]).

Table 1. Different adhesives used for production of load-bearing (grey) and non-bearing (white) EWP products

Adhesive	EWP and connections		Ref	Adhesive	EWP and connections		Ref
	Structural	Non-structural			Structural	Non-structural	
<b>PUR</b>	GLT, CLT, LVL	PB, FB, OSB	[34,45,46]	<b>UF</b>	LVL	PB, OSB	[3,47]
<b>EPI</b>	GLT, CLT, LSL	I-joints, Finger joints	[1,23,48]	<b>MF/MUF</b>	GLT, CLT, LVL	PB, FB, OSB	[3,22,23]
<b>PF</b>	LVL, PSL	Glued-in-rods	[1,3]	<b>EPX</b>	N/A	Wood and non-wood products	[45,46]
<b>PRF</b>	GLT	Glued-in-rods	[23,45]	<b>PVAc</b>	N/A	Solid Wood Panels, Veneers	[47]

The application of adhesives depends on their properties. Table 2 summarises properties that can affect the production of specific EWP, being colour, adhesive emission, and complexity of curing process.

The production of CLT with one component polyurethane (1-C-PUR) is easier, and thus more widespread because it does not require to be mixed with other components before its application. The **curing process** of 1-C-PUR is the cross-linking reaction of pre-polymers, driven by the influence of water from adherent timber or ambient humidity [46]. Formaldehydes do not need water, but they require the application of heat, hardeners or post-curing (Table 2).

Table 2. Adhesive properties that affect manufacturing

	Colour	Pre-mixing	Curing process		Environmental impact	Struct. response affected by:
<b>1-C-PUR</b>	(T)	No [49]	Chemical	Moisture, Heat [50] Isocyanate [46]	Low [1,12,50]	CC <sup>1</sup> , PA <sup>2</sup> [45,50,51], CO <sub>2</sub> [48]
<b>EPI</b>		Yes [48]		Isocyanate [3]	Low [1]	CC <sup>1</sup> [48]
<b>PF</b>	(D)	Yes [50]	Combined	PF: Heat [3]	Formaldehyde emission – harmful, not easily removable, or recyclable [1]	PRF: Air gaps CO <sub>2</sub> [47] UF: Crumbling [44]
<b>PRF</b>				PRF, RF, MUF, MF: Added salt, or hardener, or change in pH [3,47]		
<b>RF</b>						
<b>UF</b>						
<b>MUF</b>						
<b>MF</b>	T			PRF: Post-curing [22]		
<b>1-C-EPX</b>	T/D	Yes	Chemical	Reacting hardener [46]	Not documented	PA <sup>2</sup> [50]

<sup>1</sup> Chemical composition; <sup>2</sup> Primer application;  
(T) Transparent, (D) Dark



The most common adhesives among CLT manufacturers are 1-C-PUR and MUF. In a recent CLT global industry study from 2017 [52], 66% of respondent companies use 1-C-PUR as primary adhesive and 24% of them use MUF. PRF adhesive has good structural response at elevated temperatures, but its biggest drawbacks are the dark colour and complexity of the manufacturing process, so it is not widely used.

The extent of application of MUF and 1-C-PUR in CLT production is reviewed in Figure 3 on a European scale [46]. But, it is present worldwide, as in North America (Nordic Structures [53], Smartlam Technologies [54], Structurlam [55]), Australia and New Zealand (XLam [56]), and in the Asian market [48] (with the highest application of EPI adhesives - i.e. Length Cooperative, Meiken Lamwood, Yamasa Mokuzai [57]).

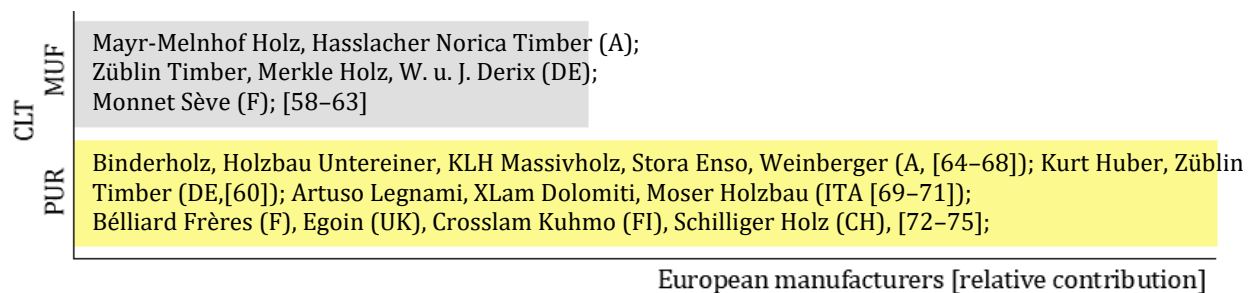


Figure 3. Use of PUR and MUF among CLT manufacturers in Europe

Application of the same adhesives in GLT is only discussed within Germany and Austria in Figure 4 (as the biggest producers in Europe) since a more extensive review, due to its high number of producers, would be out of scope for this study

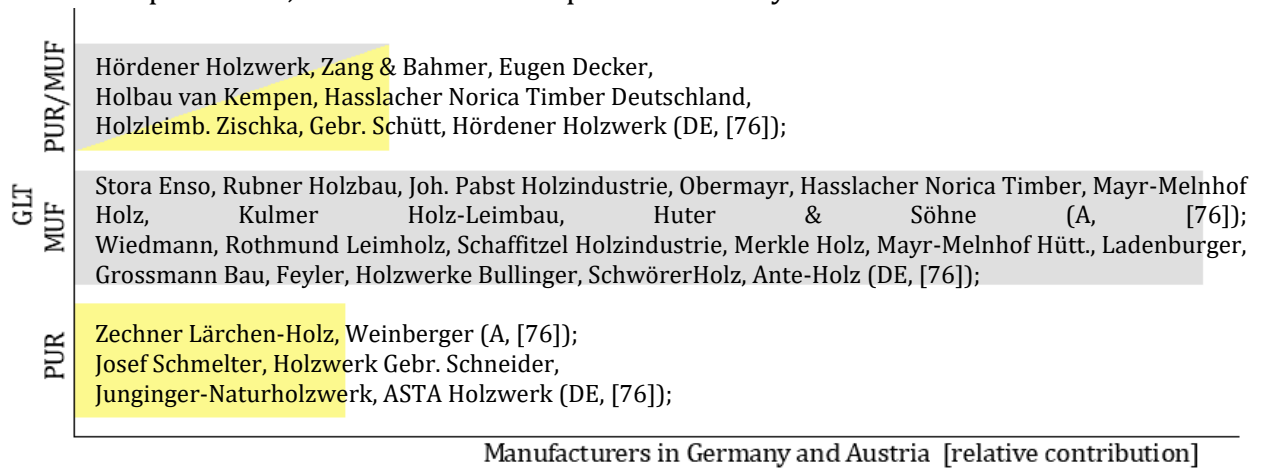


Figure 4. Use of PUR and MUF among GLT manufacturers in Austria and Germany

The primary rationale for a wider application of 1-C-PUR in CLT could be in manufacturing difficulties, because it can be energy-consuming to produce large CLT by hot pressing, used for formaldehydes [48,52].

Secondary issue is **formaldehyde emission**, especially because CLT elements demand larger amount of adhesive than GLT. Formaldehydes, as air pollutants mainly entering the body through respiration, could have a carcinogenic effect on humans [77]. The risk defined by World Health Organisation [78], is well-regulated in wood industry [43,79–81]. However, the release of formaldehydes is not only directed by manufactures, but also by a consumer [78]. In energy efficient insulated houses, specific air-tightness and ventilation conditions set by user define the air exchange. Formaldehyde emission makes no difference when it comes to debonding, but if one adhesive has a good performance in fire, environmental impact is still an important parameter for a sustainable built environment.

**The manufacturing technique** can influence the structural response of EWP. Some of the factors are low wetting, high moisture of wood, too dry wood, disturbances in the machine, long assembly time, uniformity of adhesive application [82], the thickness of adhesive applied [43], and production temperature and pressure [29]. For polyurethanes, the film thickness higher than 1mm can lead to cohesion failure [46], while less than 0.3 mm can reduce the cavities induced from CO<sub>2</sub> foaming during production [1]. CO<sub>2</sub> in bond line might have an influence on debonding due to the reduction in strength by limiting the elastic modulus. While adhesive producers as Sika [83] and AkzoNobel [84] emphasise the importance of sufficient curing and pressure time to achieve a strong bonding interface for the use in non-fire conditions, formaldehyde adhesives (especially MF and PRF) tend to have a longer press time (4-5 h) [22,51] than PUR (1-3 h) [45]. It is still unknown how this affects the mechanical performance at elevated temperatures, but it will not be addressed within this study.

System size, lamella thickness, and the presence of longitudinal narrow bond line between two lamellae in the same plane influence the charring behaviour. Small cracks in the char work as channels where combustible gases' concentration increases and mix with air, leading to the formation of flames if the fire point is reached. Flame penetration can then

locally accelerate the heating and charring of the next layer and increase the charring rate. Austrian and German CLT producers (Figure 4) offer different specifications for “*Top layers narrow side bonding*”: (1) they do not specify if narrow bonding is possible [58,65,66], (2) it is possible on request [59,60,68], or (3) they use it regularly. For the latter, the adhesive in this narrow bond line can be the same as the main bond line adhesive between the layers, e.g. 1-C-PUR[67], MUF[61]. When it differs, adhesive used in main bond line is 1-C-PUR, but MUF for the narrow bond line [64]. The adhesive can also differ when used for the main bond line and in finger joints (perpendicular joint of two lamellas). In this study, some tested samples have a *narrow side bonding* and its possible influence on the results will be discussed.

All this is complemented with a diversity of testing technologies and methodologies used among manufacturers and researchers to assess an adhesive’s bonding performance.

### **2.1.2 Adhesive properties**

Strong adhesion between adhesive and wood is achieved by appropriate adhesive application, penetration, wetting and curing [85]. Application and penetration are discussed with physical properties. Chemical thermosetting and thermoplastic properties define curing which can be a physical process (solidification), a chemical process (polymerisation), or a combination of both [86], as summarised in Table 2.

To assess bonding performance at ambient temperatures, two tests are usually used: (1) the mechanical strength test, with the application of short and long-term duration load, which defines the sample’s wood failure percentage (WFP) and shear strength (BSS) in dry conditions, and (2) bond line quality delamination test, which shows the length of debonding over the bond line in wet conditions, as a response to environmental change in boundary conditions and stresses caused by wood shrinking or swelling.

#### **Physical properties**

**Bond line thickness** includes the adhesive and the penetrated wood tissue [87]. When the adhesive penetrates the cellular lumina (cavity) (Figure 5), it increases the specific area for adhesive contact and improves the mechanical interlocking, but it has no influence on cell

swelling. Once it penetrates the middle lamella (space between the cells) and primary wall of the cell (Figure 5), the adhesive can react with the cell wall polymers and create an interpenetrating network. In Figure 5, Liu *et al.* [88] shows that PRF fills more uniformly both cellular lumina, middle lamella and primary wall of the cell.

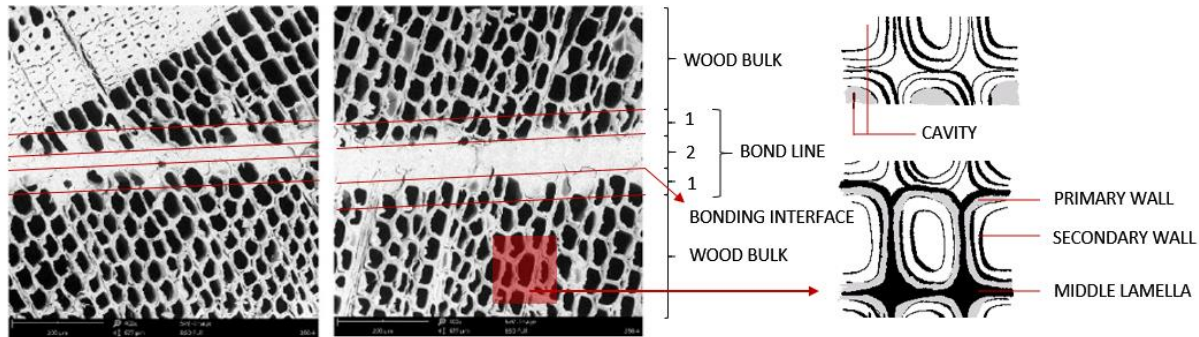


Figure 5. SEM images of MUF (left) and PRF (right) adhesive at 20°C [88]. Bond line thickness includes wood interphase (1) and adhesive bulk (2) - adhesive can penetrate the cell (cavity, primary wall) and the space between cells (middle lamella)

The bond line thickness defines the composite action and failure mode. Its importance for the debonding caused by the loss of cohesion was supported by Richter *et al.* [46], who showed that a weak zone in the thick glue is in the centre of the adhesive film (Figure 5 – (2)). For 1-C-PUR adhesive, at elevated temperatures, a close bond (0.1 mm) has a less pronounced drop in shear modulus because the temperature cannot be distributed across the wood-adhesive bonding interface (Figure 5 (1-2)). Bond line thickness also depends on the chosen timber species [87]. For hardwoods with larger cavities (Figure 7), *bond line starvation* (i.e. lack of adhesive) can occur when adhesive penetration is too strong, which can then weaken the composite action. Cruz *et al.* [89] reported that the bonding strength of high elongation EPX adhesives is less dependent on the thickness of the bond line.

Within the future research, it would be good to assess how the penetration depth might be affected by the type of adhesive and timber, but also by the pressure and curing time (i.e. very fast curing adhesive cannot penetrate as deep as a slower curing one).

Frihart [86] has put an emphasis on the importance of adhesive penetration (and therefore thickness) for the bond line performance in moisture content changes. In fire conditions, water in timber evaporates and pushes the moisture front away from the charring front towards the adhesive. It diffuses through the permeable wood structure and then migrates

with capillary action in cracks within the adhesive, posing a threat to the adhesive and bonding interface. Custodio *et al.* [82] discussed that some adhesives can have a critical water concentration above which weakening becomes irreversible. Burchardt *et al.* [50] supported this by noting that once the moisture diffuses into the adhesive, it acts as a plasticiser (making it more flexible), lowers the glass transition temperature, or has a long-term influence on the adherent adhesion.

**Moisture** also influences creep behaviour. At ambient temperatures, PUR adhesives tend to be waterproof and show good behaviour at high wood moisture content [1,46]. EPI adhesives show low creep in the adhesive [23,47,48]. The behaviour for the formaldehyde family varies: PF experiences distinct softening [44], UF has reduced modulus, brittle failure and tends to crack in creep tests [3,44,47]. MUF adhesive is improved compared to UF, but it also experiences reduced modulus, while RF, PF, and PRF adhesives are highly resistant to moisture variation [3,22,44]. For example, PRF adhesive films measured for creep at high humidity behave in the range of wood swelling, which minimises and therefore distributes the interfacial strain [44]. EPX have a high resistance to moisture as long as the temperature is kept stable [82].

Knorz *et al.* [90] observed, in the long-duration tensile shear lap test with MUF, that when MC was reduced at 90°C, the failure mode changed from wood to adhesive failure. This was assumed to be either due to adhesive hydrolysis, or the weakening of physical bonds between wood and adhesive. Hydrolysis of UF or MUF was also observed by Dunky and Neimz [91]. Therefore, it is expected that the adhesive behaviour in fire conditions can be influenced by the moisture movement.

### **The effect of added components:**

Added components that may influence the bond performance (e.g. elastic modulus, increased creep, or higher fracture energy) include additives and catalysts, hardeners, fillers and primers. When it comes to debonding, as shown in subsequent paragraphs, at ambient temperature, the application of primers and catalysts does not always improve mechanical performance and shear strength of PUR adhesives, whereas fillers can be beneficial for shear strength and thermal stability of 1-C-PUR and EPX. There is no agreement on hardeners

impact on debonding. At elevated temperatures, there is unfortunately insufficient data available regarding the effect of these components to debonding.

Clauß *et al.* [51] tested 1-C-PUR pre-polymers and adhesives properties with the following mechanical tests: adhesive film tensile test (ISO 527-1:2012 [92]<sup>1</sup>) and longitudinal tensile shear strength test (EN 302-1:2004 [93]<sup>2</sup>). **Additives and catalysts** were added to pre-polymers to achieve the chemical composition of adhesives. Cohesion performance in adhesive film test was the same, but the adhesives showed an improved shear behaviour because the prepolymers formed a discontinuous bond line thickness. However, catalyst can also accelerate the reaction of the adhesive's isocyanate (NCO) groups with water, causing the faster curing, but restricted penetration into the wood cells. With a greater concentration of the adhesive in the bond line delamination caused by cohesion failure is more likely [90].

**Hardeners** can be used to increase the 1-C-PUR adhesive strength [50]. However, for formaldehydes, the mixing ratio of adhesive and hardener varies within different studies (MUF: [28][51], PRF: [12,28,51]) and sometimes the same producers offers very different mixing ration depending on pressure time [84] (i.e. 100:20 (6h) to 100:100 (65')). Knorz *et al.* [90] showed that hardener amount had no influence on delamination and creep behaviour of bond line in wet conditions which contradicts the finding from Dunky and Niemz [91] who explained that since hardeners contain PVAc they can affect the adhesive moisture resistance. PVAc is a thermoplastic adhesive, which effects performance in fire.

When it comes to **primers**, composite action depends on the wood species [27,94] and wet/dry conditions. In wet conditions, bonding quality of PUR with hardwood (ash, oak, beech) was improved with PUROBOND primer application, as assessed in delamination test (EN 391:2002 [95]<sup>3</sup>). The same adhesive with no primer in softwood (spruce) had the same bonding performance [87]. In dry conditions and shear test (EN 392:1995 [96]<sup>3</sup>), primer application had negligible effect on BSS and WFP. Another example is primer

---

Superseded by:

<sup>1</sup> ISO 527-1: 2019 [137];

Superseded by:

<sup>2</sup> EN 302-1:2013 [101];

<sup>3</sup> EN 14080:2013 [43].

Hydroxymethylated Resorcinol (HMR), used with EPX, EPI, 1-C-PUR and PRF in hardwood Eucalyptus. When tested in dry conditions, it showed negative effects for PUR and EPI, and positive for PRF and EPX adhesive, resulting in higher BSS [94] according to block shear tests (ASTM D2559-04 [97]<sup>4</sup>). Delamination rate in wet conditions for PUR and PRF adhesive dropped to 0 % (AITC Test T110-2007 [98]). With no trend in ambient conditions, it is hard to design for shear strength in fire conditions, necessary to prevent debonding.

**Fillers** are assumed to be beneficial for thermal stability (i.e. the cohesiveness will not degrade with the change of time and temperature). Richter *et al.* [46] and Witkowski *et al.* [99] observed this for EPX adhesives. Clauß *et al.* [100] reported that the addition of 30% of chalk to adhesive mixture increased shear strength by 52% in 1-C-PUR adhesive. They performed dried the samples to 100°C and 150°C and then loaded them according to mechanical strength test EN 302-1:2004 [101].

Change of chemical properties in ambient and elevated temperatures is defined by an adhesive's chemical composition, which is controlled by the addition of *additives, catalysts* [51], *hardeners, and fillers* [22].

### **Chemical properties:**

**The chemical composition** varies greatly among and within adhesive families. The biggest discrepancy in performance based on the chemical composition, in terms of adhesion to wood, viscosity, strength and stiffness, was observed for PUR [22,33,47,50,51,102], EPX [82] and EPI adhesives [48]

Adhesive viscosity, molecular size, and chemical composition can also influence the penetration depth and mechanical interlocking of adherents (plies) [27]. Keywords used to describe the change in chemical properties at elevated temperatures are: *thermosetting/thermoplastic, thermal degradation, thermal decomposition, and glass transition temperature.*

---

<sup>4</sup> ASTM D2559 12D-18 [143]

Polymeric adhesives are classified as **thermoplastic or thermosets** depending on their respectively linear or crosslinked molecular structure of monomers. The main difference is in their behaviour at heat exposure. **Thermal degradation** includes only chemical processes occurring before 1% of the mass is lost [99] and it can start in lower temperatures. During **thermal decomposition**, heat causes extensive chemical change, change in cross-link density (i.e. the new hard and soft phases of the bond line [51]), followed by a change in mass and the loss of physical and mechanical properties. **The glass transition temperature** is a criterion for a transition in mechanical properties at elevated temperatures. Formaldehydes and epoxies are thermosets [49,82,89], historically cured by using heat and pressure together with hardeners and catalysts. However, some polyurethanes are thermosets that cure at room temperatures. Thermoplastic polyurethanes are not used for structural application [99]. EPI can also behave as both, thermoplastic and thermoset [47,48]. PVAc is thermoplastic material [22].

A thermoset material first strengthens when heated, and that is one of the reasons for its higher thermal and dimensional stability, and resistance to creep. A thermoplastic material will soften and melt, while for a thermoset, before even crossing the glass transition temperature  $T_g$  (explained below), will decompose directly from solid to vapour through pyrolysis. However, this makes thermosets more brittle, less ductile, with lower tensile strength compared to thermoplastics. Thermoplastic materials often have a low melting point and tend to “creep” over time when loaded. Also, for thermosets the process is irreversible while thermoplastics can re-solidify when cooled without experiencing a chemical change [103]. This ability to reheat and remould thermoplastics makes them recyclable [99], but their low melting point makes them less convenient for structures exposed to fire conditions.

**The glass transition temperature** value depends on the particular adhesive's formulation, its thermal history, and age [89]. At ambient temperatures in the solid phase, molecules in polymers are in a state of constant vibration (i.e. glassy state). As the temperature increases, the vibrations become more intense. A critical temperature is reached when there is sufficient kinetic energy to rupture one of the bonds that make the monomers into a polymer. Before a material reaches its glass transition temperature  $T_g$ , the expected failure mode is



brittle. Once that point is reached the chains have acquired sufficient thermal energy to undergo significant translational motion to a liquid or rubbery state, e.g. thermoplastics [99]. If one wants to use flexible and elastic properties of a material, it is important that they remain above  $T_g$ . But for composites,  $T_g$  is a threshold and when reached, one can experience a decreased elastic and shear modulus.

The thermal decomposition thresholds are higher than  $T_g$  [99] for adhesives and designing for thermal decomposition could lead to non-conservative solutions.  $T_g$  varies greatly [99], being 0- 160°C for EPX, 20-40 °C for UF, 60-100°C for PF resin, 20-60°C for MF, and 10-220°C for PUR adhesives. For polyurethanes  $T_g$  is usually a range and not a discrete temperature due to different molecular weights and cross-linking. The difference in reported ranges is presented in Figure 6.

Richter et al. [46] performed DTMA for shear tension mode and tested beech joint with six different **1-C-PUR** adhesives to study temperature-dependent creep (from -120°C to 180°C). For PUR adhesives,  **$T_g$  was not discernible**. Nicolaidis et al. [21] did not test  $T_g$  directly but they mentioned that it ranges from 80°C to 100°C for 1-C-PUR adhesive, and when reached, failure modes within the bond line temperatures are assumed to be governed by the adhesive.

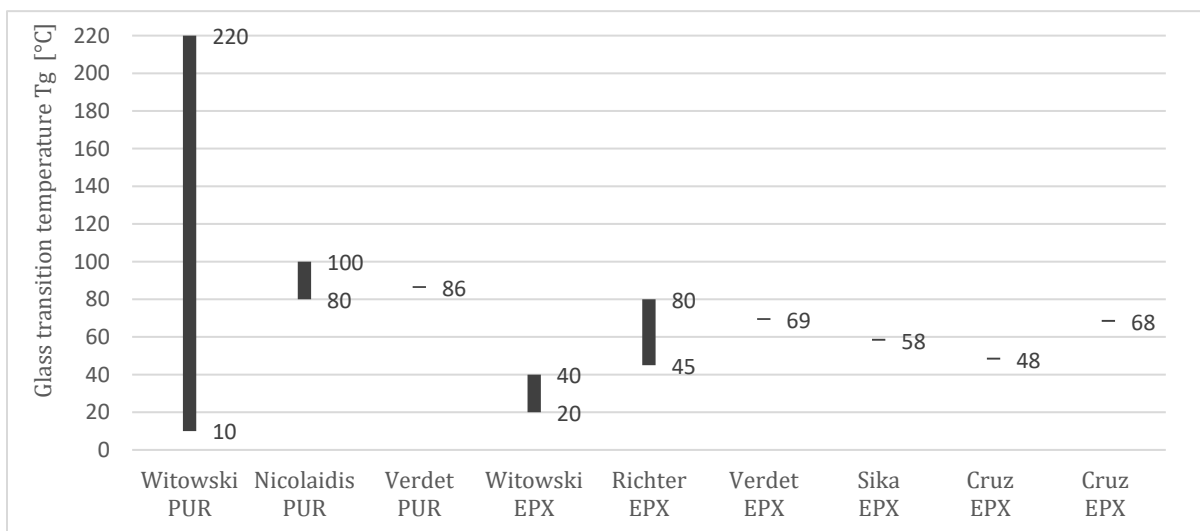


Figure 6. Overview of glass transition temperatures from Witowski et al. [99], Nicolaidis et al. [21], Richter et al. [46], Verdet et al. [104], Cruz et al. [89] and Technical Sheets from Sika [83]

Burchard et al. [50] advised that **Tg is not a reliable parameter** for predicting an adhesive's failure because many **PUR adhesives work very well above their Tg**. Instead, the load which the adhesive can sustain over its lifetime under service that should be observed more carefully. Cruz et al. [89] observed the same but for 2-C-EPX adhesives.

Thermoplastic properties of materials are not always easily identifiable. There is also little information available on how the Tg of the different emulsions and adhesive components can influence the Tg of the final adhesive [48]. Based on the studies presented in Figure 6, Tg cannot be taken as a criterion for transition in mechanical properties and debonding in CLT elements tested in this thesis.

However, composite action, and the interphase between the adherend (timber) and adhesive plays an important role in the system ductility [105]. Therefore, in the following section timber properties and their interaction with adhesives will be analysed.

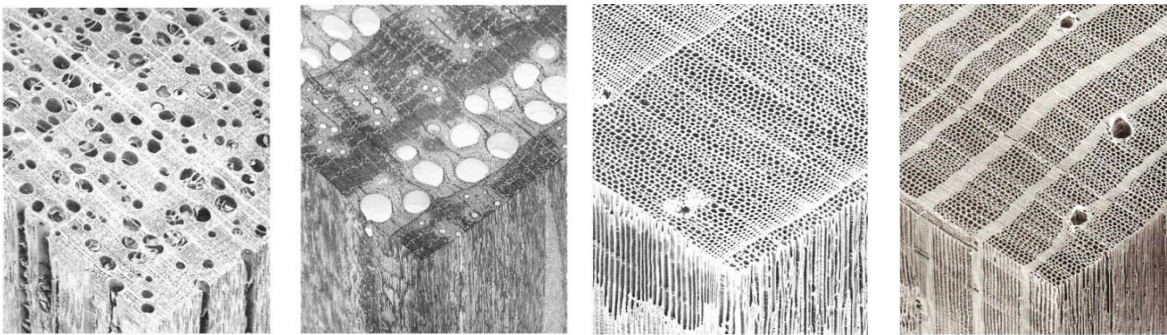
### 2.1.3 Timber properties

Timber can be depicted as a bundle of plastic straws. When exposed to some load, this bundle will behave differently depending on: the thickness of each straw (wood cell thickness), the glue in between the straws that keeps them together (lignin between wood cells), the direction of applied load on the bundle, which can be perpendicular or in the direction of straws (parallel or perpendicular to the wood grain). Therefore, distinct natural variability of the two adherent lamellae in longitudinal (radial and tangential) direction can also be responsible for the large scattering of bond line performance [44]. Apart from this, its structural performance in fire can be affected by the variable chemical composition defined by species, its density, and moisture content [5]. These properties will be discussed within this section.

Surface pH and acidity differ for deciduous and coniferous **species**, hardwood and softwood. Even one species and its specific part could differ in this property (e.g. heart and sapwood). In case of delamination in wet conditions, softwood performs better than hardwood. Compared to other softwoods, spruce showed to be prone to debonding [27], but it is also widely used in structural design and therefore tested the most, which makes it hard to draw

a definite comparison. For this study, only spruce was used and discussion about the species would be out of scope.

The minimal required timber **density** (approx.  $350 \text{ kg/m}^3$ ) for structural applications in CLT and GLT is discussed in [106] and it depends on the countries' jurisdiction. Density is defined by porosity visible in Figure 7 and species with lower density, as softwoods (e.g. spruce  $400\text{-}500 \text{ kg/m}^3$  [66]), typically have lower thermal conductivity than hardwoods (i.e. beach, ash, oak  $670\text{-}770 \text{ kg/m}^3$ [27]).



(1) (2) (3) (4)  
 Figure 7. Difference in cellular structure for hardwood and softwood made with a scanning electron microscope [107].  
 Hardwood (Black Walnut (1), Red Oak (2)), Softwood (Eastern White Pine (3), Southern yellow Pine (4)).

The choice of specific timber species and adhesive influences debonding in ambient wet conditions. In case of delamination in wet conditions, softwood performs better than hardwood. However, in fire conditions, the timber species does not solely influence debonding.

Preferred wood **moisture content (MC)** in wood is  $<15\%$ , but for serviceability class 1 and the softwood used indoors according to European jurisdiction [3], it should be lower than  $12\%$ . Moisture movement can be affected by the wood species (e.g. European Beech swelling and shrinkage compared to Oak, Black Locust, and Spruce[27]). Too high MC  $>20\%$  can resolve the adhesive, increase thermal conductivity, cause stiffness and strength decrease, and increase creep deformation. In fire conditions, increased MC can also decrease the charring rate (with no general agreement to which extent [5]), but for composites, this would also mean that there is more water moving towards the bond line which can then be more detrimental than the heat itself.

Too low MC <10% can cause high adhesive penetration into the wood [1]. Having a low moisture content during fire testing (i.e. 5% [28]) represents a worse scenario in fire because it leads to faster drying, ignition, increased charring rate, and heat penetration to the bond line. For polyurethane adhesives the sensitivity to low wood moisture (below 8% [29]) varies widely. However, it might be beneficial for some formaldehyde adhesive as there is less water “moving” in the timber and at the bond line surface that can affect the adhesive due to hydrolysis (e.g. formaldehydes). As moisture in timber cells evaporates and/or migrates to cooler regions, it also causes differential shrinkage, parallel and perpendicular to the longitudinal timber fibres. This “contraction” of timber cells can cause internal stresses at the bonding interface of CLT elements that can be an alternative cause of debonding [20] and probably facilitate the delamination or char fall-off in fire conditions.

Moisture content in timber is not a variable that can be strictly controlled—it will be dictated by the ambient temperature and relative humidity, which in turn will depend on geographical location and building management practice [5]. On the other side, manufacturers can decide on species (density). In this case, higher timber density reveals lower adhesive penetration due to the smaller number of cavity cells [51] which results in limited interlocking of the adhesive, and higher internal stresses from increased swelling and shrinking caused by moisture movement around the bond line. Apart from density, the most important choice is the right combination of adhesive and timber for specific EWP.

#### **2.1.4 Understanding the adhesive and timber interaction in specific EWP**

Interaction of adhesive and timber cannot be generalised for CLT, GLT, and finger joints because they have different stress distribution mechanisms [108].

In ambient conditions, a combination of nine European species (seven hardwoods and two softwoods) and three different adhesives (MUF, 1-C-PUR and PRF) in GLT were examined by Konnerth et al. [27] by using the tensile shear lap test (EN 302-1:2013 [101]), and delamination test (EN 302-2: 2013[109]<sup>5</sup>). Two softwoods performed differently: Norway Spruce with 1-C-PUR, MUF was not affected while European Larch showed delamination

---

<sup>5</sup> Superseded by EN 302-2:2017[40]

higher than 10% of the length of the bond line. From hardwood species, only beech with 1-C-PUR passed both the aforementioned tests. The latter finding deviated from the one from Schmidt et al. [110]. Light-optical micrograph examinations showed that the curing process of the hardwood beech and another 1-C-PUR, was retarded by wood and resulted in failure in both delamination (EN 302-2: 2002<sup>1</sup>) and shear lap tests (EN 392:1995[96]<sup>6</sup>), proving the variance in behaviour within one product (GLT).

In fire conditions, in the modified flame test CSA O177, Annex A2 [111]<sup>7</sup> from Dagenais and Ragner [112], CLT samples exhibited cracks at the glue lines, whereas GLT had smoothly penetrated the charred layer. When 1-C-PUR was used, delamination in fire conditions was observed to be much higher for CLT than GLT specimens, while MF and PRF adhesive showed no delamination, nor in CLT nor in GLT. Notwithstanding the applicability of this standard only for GLT products, the same adhesive would pass for one EWP and fail for another.

The following section will discuss the interaction of wood and adhesive further, in terms of thermal and structural response.

## 2.2 Thermal load effects on debonding

The aim of this section is to question if debonding (char fall-off and delamination) could be predicted by observing the charring and thermal penetration in different fire studies (at different scales as noted in Appendix B).

### 2.2.1 Char layer formation

Figure 8 presents the non-uniformity of char formation and subsequent *delamination*, where correlated temperatures were taken from the heat transfer model by Schmidt [19]. Virgin timber (V) starts to lose its properties above 65 to 100°C, affecting its structural capacity [113]. Thermal penetration depth (H) is the distance from pyrolysis front (P) to virgin timber (V) and it corresponds to preheated wood. This is the zone where *delamination* can appear, before the charring front penetrates to the glue line, assumingly due to the weakening of

---

<sup>6</sup> Superseded by EN 14080:2013 [43]

<sup>7</sup> This standard is used as a qualification code for manufacturers of structural GLT in Canada to ensure bond line performance in fire.

adhesive [114], but also the loss of interaction between adhesive and timber. For *char fall-off at or after the adhesive line*, the pyrolysis front (P) has reached the adhesive exposing it to temperatures above 300°C. When the formulated char oxidises between 400 and 550°C, the surface starts to regress [115], implying that the adhesive cannot be protected above these temperatures.

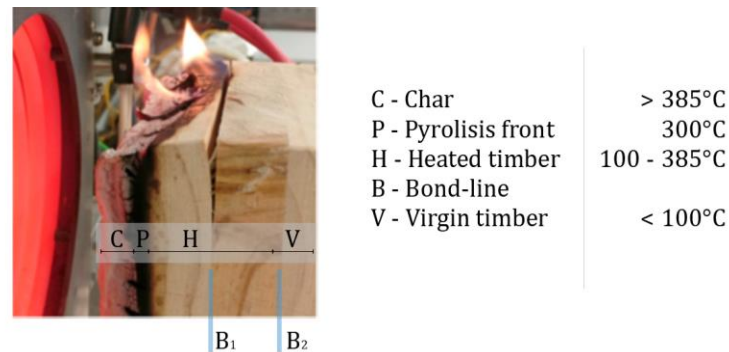


Figure 8. Debonding of unloaded *Radiata Pine* (softwood) sample exposed to 65 kW/m<sup>2</sup>, modified from Emberley et al. [10]

Pyrolysis is the reason for the rapid reduction of strength in wood, which starts between 200 and 220°C [22], but the pyrolysis front (P) cannot simply be defined with one “magic number”, similar to the glass transition temperature. When considering thermogravimetric analysis (TGA), where mass loss is plotted against temperature for wood, the curve is wide from 200 to 350°C (Figure 5.12., [116]). Specific wood components pyrolyse at different temperatures (200-400°C) but it does not make a big difference in char depth [47,116]. Therefore, 300°C is often taken as a representative value for an onset of char formation [6,14,23,24,32,33,45,117–119].

The charring rate is a one-dimensional measure in-depth char propagation over time. Although it is often taken as a constant, realistically it is a transient property influenced by:

- compartment fire dynamics,
- incident heat flux,
- heating duration [10],
- timber species with specific material properties (density and moisture content) [5,28],

- depth of already formed char [59,66,67,120] which is dependent on EWP layout and lamella thickness (in CLT) [36,121], initial element protection (encapsulation), and horizontal (ceiling) and vertical (walls) orientation [64].

In the literature and standards, the charring rate is taken as a constant value because once the specific char depth is formed, the constant charring rate and steady state heat transfer should be ensured [5]. Some representative values are 0.65 mm/min for solid wood (not composite) and GLT [120] and 1 mm/min for Plywood [34]. However, non-uniformity in charring (as presented Figure 9 [23], and by Frangi et al. in [35]) makes it harder to define a constant value for CLT. CLT manufacturers in Europe make a distinction between vertical and horizontal elements, where for walls it is 0.75 mm/min and for ceilings it is 0.90 mm/min [64], but they also use different charring rate for first- 0.65 mm/min and second layer: 0.80 mm/min [59], 0.90 mm/min [66]. Klippel et al. [122,123] proposed the use of so-called *Stepped charring model*, with 0.65 mm/min from EN 1995-1-2 [120] for initial charring, and a doubled value for notional charring which is also implemented in different handbooks [124–126]. To calculate the fire resistance of CLT elements, Canadian standard CSA O86-14, Annex B proposes the same, 0.65 mm/min for one dimensional char depth, but 0.80 mm/min for notional charring. Adding different charring rates for additional layers (notional charring) is taken with an assumption that the first lamella has failed due to *delamination or char fall of at the adhesive line* [35,122,123].

Non-uniform charring is presented in Figure 9. For two CLT layers oriented in the opposite direction (LCL), one out of four thermocouples in the 1<sup>st</sup> glue line indicated that the char front has passed the bond line while at the other side of the panel, temperatures were around 120°C (fluctuation in temperatures above 400°C indicate the direct exposure to flaming combustion). When oriented in the same direction (LLC) charring was uniform.

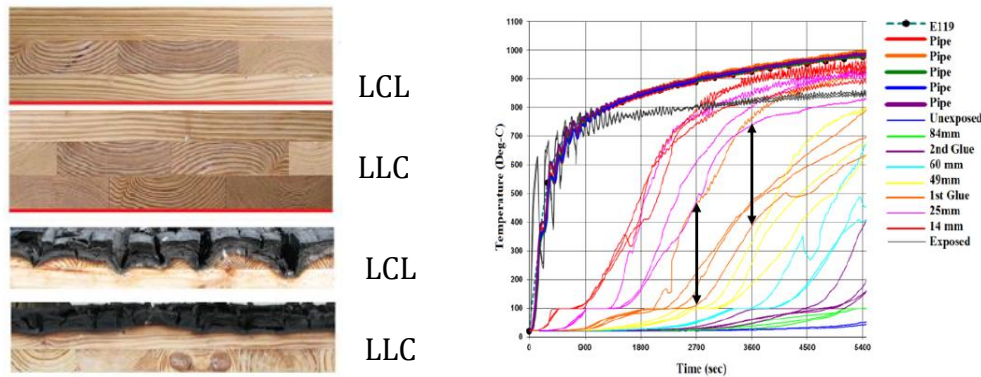


Figure 9. Charring non-uniformity. Layer orientation (left): L-longitudinal, C-crosswise. Thermocouples output data (right) for specimen 3 (Adhesive: PRF, Layer setup: LCL); Adapted from Hasburgh et al. [23]

Important finding from this work is that the charring rate was similar for all specimens, independent from adhesive, which suggests that adhesive type did not enhance nor prevent char propagation beyond the adhesive line [23]. From this, one can assume that the adhesive cannot influence the char propagation, but the extend of char propagation can influence an adhesive's performance because it defines the onset of thermal penetration. It all comes down to whether there is a specific temperature or moisture threshold that adhesive sustain and hold its performance.

With 'adequate' adhesive, even with the faster propagating char, it can pass the first lamella and continue to char the second one. That new char on the second lamella will protect that layer at the point when the first lamella falls off. The questions are "How deep should char propagate into new lamella before the *char fall-off after adhesive line* (Figure 2) appears?", "Which adhesives can allow this?" and "What is the thickness of lamella that can delay the thermal wave and protect the adhesive layer?"

In the recent study from Klippel et al. [123], a new European method was proposed for adhesive assessment, by performing 14 furnace tests with 1-C-PUR and MUF. One of the adhesives was the *non-delaminating* 1-C-PUR (tested with ANSI/APA PRG 320-2018 [39] in study by Su et al. [11]). Authors suggested that the adhesive should, after reaching the charring temperatures, be able to hold the charred layer, until at least 25 mm of new carbonised layer in the second lamella is created. When MUF adhesive was used, char fall-off was not observed. Sample with *non-delaminating* adhesive experienced char fall-off when



lamella was 10 or 25 mm thick, but for 35 mm lamella it did not appear suggesting that it could be enough to delay the thermal wave and protect the adhesive layer in a standard fire. Since charring in CLT is very non-uniform, it is hard to measure the charring depth and to take charring rate and char front movement as the sole indicator of debonding. It also matters to which extent is the specific bond line area affected. Wiesner et al. [114] concluded from their full scale compartment tests that the HRR and the auto-extinction are the function of the area of char fall-off and the thickness of the lamella.

Finally, the biggest drawback of the study by Klippel et al. [123], for the purposes of this thesis, is that the specimens were not loaded and that the fire scenarios did not include a cooling phase when the adhesive can be affected by long-term temperature effects. As presented in Figure 8, debonding as delamination could occur due to the thermal penetration, where the char does not reach the bond line [10,11,51,127].

### **2.2.2 Bond line temperature and thermal penetration depth**

In fire conditions, the adhesive strength is not the same as (or higher than) the timber strength, as it is in ambient conditions due to preserved composite action. Hence, the adhesive cannot undergo charring temperatures as high as 300°C and resist both the heat, and the normal and shear stresses from wood because the bond line strength deteriorates at temperatures above ambient [7]. These bond line temperatures differ for *char fall-off at the adhesive line* and *delamination* (Figure 2). It would be useful to observe debonding as a causal phenomenon and establish which temperature range has caused debonding.

Wiesner et al. [114] observed the thermal penetration depth through the 100mm thick, 5 ply CLT wall and ceiling elements tested by Hadden et al. [13]. When auto-extinction was achieved, 100°C isotherm progressed into the element for 30 minutes. The first *delamination* occurred in 20' when the char depth was only 11 mm and the first glue line at 20mm was exposed to 100°C.

In US standard, PRG 320-2019, for unprotected ceiling the maximal allowable temperature in the first glue line for 150' exposure is 510°C (B12.2, [39]).

One criterion that can be used to determine delamination is based on full-scale experiments, where the 100°C temperature gradient in adhesive surrounding, lasting for 1', indicates that the thermocouple became suddenly exposed to the fire [31]. However, in the decay phase this increase is less rapid as the difference between gas temperatures and bond line temperatures is potentially smaller.

If the *char falls off at the adhesive line*, a conservative criterion could be that the failure was induced by 200°C temperature because the char front is not expected to exist at lower temperatures. However, if *delamination* occurs the temperature could be lower.

From full scale tests 200°C [30], [128] in the first glue line could be taken as a reference point. Small scale experiments with steady-state uniform heating, where adhesive was exposed to lower temperatures 100-150°C for certain amount of time, also showed a delamination tendency [21,22,47,114,129]. It was observed in multiple studies that CLT failure above 150°C can be predominately in the bond line [4,22,36,45,51,88,118].

### **2.3 Structural load effects on debonding**

In load-bearing constructions, adhesives must transfer high static and dynamic mechanical load. The aim of this section is to understand how the structural performance of CLT relies on the composite action between two adjacent timber plies, but differs in ambient and fire conditions.

In the case of a one sided fire scenario, element heating causes a reduction of the wood's stiffness, and the glue line's weakening. Combined with the char formation, they cause the neutral axis to shift toward the unheated cool side. To preserve the composite action, bond lines have to be able to resist not only the normal and shear stress redistribution in the reduced cross-section with the drop in the timber's elastic modulus, but also the increased temperatures within the adhesive. [130]

For the structural design of CLT, composite is assumed to behave as one, with strong bond adherence, and no slip in the bond line between the plies [7]. However, when exposed to higher temperatures, the failure mode is changed from wood to adhesive failure as observed by Nicolaidis et al. [21] and Emberley et al. [24] in Figure 10.



Figure 10. Failure mode change in the beam tested in three-point test. Timber failure at ambient temperatures (left) and bond line failure at elevated temperatures (65-80C, right) [26]

Since wood is an orthotropic material (different properties in three mutually perpendicular directions), the shear strength of timber varies in different directions depending on the application of load relative to the grain; in-plane (wall) or out-of-plane (slab). As presented in Figure 11, there are three types of shear present in EWP: in direction parallel to the grain as radial-longitudinal  $\tau_{RL}$  and tangential-longitudinal  $\tau_{TL}$  shear, and in direction perpendicular to the grain as rolling  $\tau_{RT}$  and  $\tau_{TR}$  shear. Shear strength is highest in the longitudinal direction, where  $\tau_{TL}$  is weaker than  $\tau_{RL}$  because the failure plane can follow only the weaker, younger rings of the section whereas to fail in radial direction it has to go through all, older (strong) and younger (weak) rings. The younger part is the one closer to the heartwood (pith) [131].

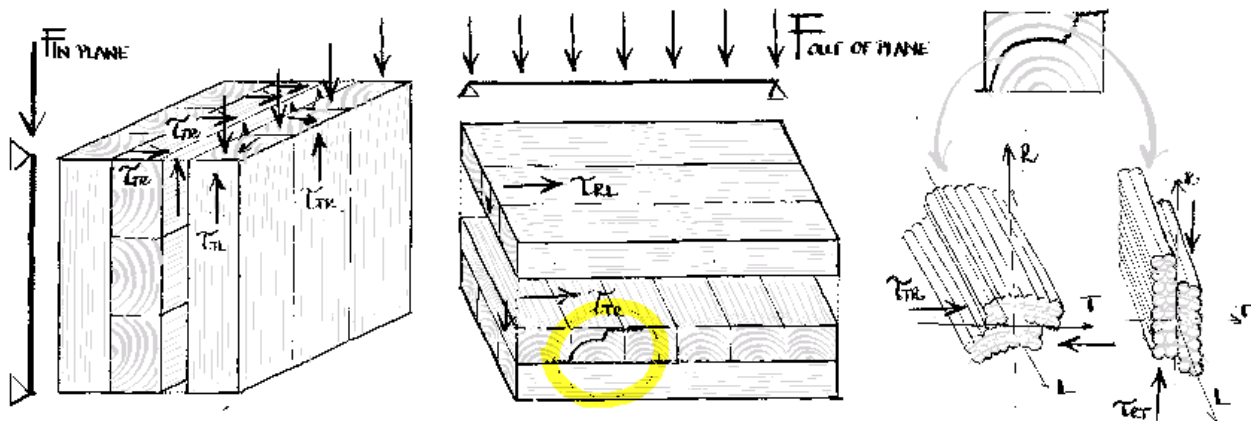


Figure 11. Shear stresses when loaded in-plane (wall-) and out-of-plane (slab-). Rolling shear in tangential direction  $\tau_{TR}$  and in radial direction  $\tau_{RT}$ . Adapted from Erhart and Brandner [132].

When loaded out of plane, rolling shear can be the weakest link for CLT composites because the shear modulus perpendicular to the grain can be an order of magnitude lower than along the grain [1]. It is called rolling because two grains are rolling against each other. For EWP applications, it is very important that the bonding is exposed as much as possible to the longitudinal shear because when designing for serviceability, rolling shear can make a big contribution to the global deflections. In EN 16351:2015 [81], rolling shear strength is a function of layup, span, timber species geometry, sewing pattern, edge bonding and most detrimentally, lamella width/thickness ratio (e.g. the smaller the ratio, lower the strength).

To test the shear properties of the composite one can relate to test methods for base material (wood) and/or for the CLT specifically [132]. However, approval of new adhesives is often based on two small-scale tests independently from final EWP application: mechanical response in dry conditions and delamination in wet conditions. Mechanical response is measured with block shear strength (BSS) test (compression) or lap shear strength (LSS) test (tension) as the quick quality tests to check surface preparation and the control of adhesive batches in ambient conditions [50]. Pure cohesion failure in adhesive is generally regarded as proof of poor gluing because wood has the same or lower strength than the adhesive, meaning that the failure should normally be in the wood-adhesive interface region or in the wood itself. Wiesner et al. [20] noted that the low shear module could be expected for PVAc, phenolic resin (PF), resorcinol resin (RF), Casein (natural adhesive) and urea resins (UF).

This section will describe bond behaviour through the degradation of the adhesive's mechanical properties and change in failure mode type at ambient and elevated temperatures. Studies are presented in Appendix B.

### 2.3.1 Loss of shear strength

#### Ambient temperature

Small scale shear tests, presented in Table 3 were performed by Lu et al. [94] (BSS) and Clauß et al. [51] (LSS). A comparison of these two studies is vital because it shows that even at ambient temperatures, the adhesive shear strength varies depending on the test type.

There was no big difference in BSS [94] among EPI, PRF, and 1-C-PUR. WFP and BSS strength could not be correlated. In LSS [51], PRF had 15% higher tensile shear strength than commercial 1-C-PUR and when only the adhesive film tensile test was performed, PRF had almost three times higher strength than 1-C-PUR. Delamination rate<sup>8</sup> in wet conditions [94], was the highest for EPI adhesive (15.7 %) and the lowest for 1-C-PUR (7.6%).

These two studies are presented to highlight the considerable difference in the adhesive's performance throughout the application of four different test methods. Since the product layout can be completely different (e.g. GLT vs CLT), the use of one small scale test method is not representative to define an adhesive's properties in all EWP products.

Table 3. Small scale shear tests in ambient temperatures

Author *year*	Test description	Test standard, *superseded by*	Adhesive *production*	Timber species	EWP	H/ L <sup>1</sup>	Sample dim. [mm]
SMALL-SCALE   AMBIENT TEMPERATURE							
Lu et al. [94] *2017*	1. Block shear test 2. Cyclic temp. delamination test 3. Short span centre point bending test	1. ASTM D905-03 [133], *[134]* 2. AITC T110-2007 [98] 3. ASTM D3737-03 [135], *[136]*	EPI PRF 1-C-PUR *commercial*	Eucalyptus 580kg/m <sup>3</sup>	CLT, 3 plies	L	1: 100x100x54 2: 100x100x54 3: 580x150x54 Ply: t = 18
Clauß et al. [51] *2011*	1. Longit. tensile shear strength 2. Tensile tests: Adhesive films 3. Nanoindentation: micro-mechanical properties	1. EN 302-1:2004 [93], *[101]* 2. ISO 527-1:2012 [92], *[137]* 3. Hysitron Triboindenter	MUF, PRF, 1-C-PUR (1) *commercial* 1-C-PUR (3) *lab. pre-polymer* 1-C-PUR (3) *lab. synthesised*	Beech 735 kg/m <sup>3</sup>	Joints Films	L	1. 20x150x5 Overlap 10 [93] 2. t = 25 3. Cubes: 10
<sup>1</sup> H – thermal load; L – structural load							

<sup>8</sup> Delamination must be lower than 10% to pass the requirements in AITC Test T110-2007 in order to be used in GLT products.




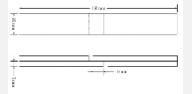
### **Elevated uniform temperature**

In studies presented in Table 4, after heating to temperatures under 300°C to avoid charring of the timber, the authors loaded the samples to test their shear strength (LSS, displacement 1mm/min). Only Zelinka et al. [127] preheated the samples to 103°C to avoid the drying effect of wood and save in testing time. Zelinka et al. [127] and Liu et al. [88] tested the samples in the same machine where it was heated and held at constant temperature. Clauß et al. [22] and Frangi et al. [45] first heated specimens in the oven and then transferred it to an untempered load-cell, which according to the authors, might cause a possible decrease in the temperature of the specimens. This might be important when specific temperature ranges for adhesive failure are discussed. Although adhesives do belong to the same families, they come from different manufacturers and vary in their chemical composition. Additionally, different timber species were used in the above studies, so a direct comparison is not possible.

Zelinka et al. [127], Liu et al. [88] and Clauß et al. [22] compared shear tests with solid wood tests. Up to 260°C, only PRF adhesive had the same shear strength deterioration as Douglas Fir solid wood [127]. Same was found for (different) MUF and PRF adhesives when compared to Larch [88] and Beech [22].

Figure 12 shows the normalised deterioration of shear strength at representative elevated temperatures for Formaldehyde adhesives. Figure 13 presents the same for Polyurethane and EPX adhesives. Plotting all adhesives on one graph would introduce unclarity, making it hard to discuss and analyse studies. Results for UF, RF, and 2-C-EPX adhesive are just presented for the completeness, but they will not be further discussed as they are usually not used for EWPs.

Table 4. Small scale shear tests at elevated temperatures

Author *year*	Test description	Test standard, *superseded by*	Adhesive *producer*	Timber species	EWP	Heat/ Load	Sample dimensions [mm]
SMALL-SCALE   ELEVATED TEMPERATURE							
Zelinka et al. [127] *2019*	1. Tensile tests solid wood 2. Lap shear tests (preheated at 103°C)	1. ASTM D143-14 [138] 2. Not standard. Geometry from 1.	1-C-PUR (2) MF PRF *commercial*	1. S.Y. pine, D. fir, SPF 2. D. fir	Solid wood, Glued joints	H/L <300°C (uniform)	2. 139 x 22 x 2 Overlap: 25 
Liu et al. [88], *2020*	1. Tensile tests solid wood 2. Double lap shear strength test 3. FTIR: Adhesive cured, grounded, and heated.	1,2. Not standard. Geometry from EN 301:2017 [49] 3. Not standardised	PRF *Dynea, China* MUF *lab. synthesised*	Larch 604 kg/m <sup>3</sup>	Solid wood, Glued joints	H/L <300°C (uniform)	2. 20 x 80 x 5 Overlap: 10 
Frangi et al. [45] *2004*	Three point bending test	Not standardised	RF (1) <sup>1</sup> 1-C-PUR (5) <sup>2</sup> 2-C-EPX (1) <sup>3</sup>	Spruce 456-533 kg/m <sup>3</sup>	GLT MS17	H/L <300°C (uniform)	112 x 40 x 40 
Clauß et al. [22] *2010*	1: Lap shear tests 2: Solid wood shear strength test	1. EN 302-1:2004 [93], *[101]* 2. DIN 52187:1979 [139]	1-C-PUR (3) PVAc, UF, MUF, MF, PRF, EPI	Beech 756 kg/m <sup>3</sup>	Glued joints	H/L <300°C (uniform)	1. 150x20x5 [101] 
<sup>1</sup> RF: Kauresin 460 + Hardener 466 - Türmerleim AG, CH-Basel <sup>2</sup> 1-C-PUR: Kauranat 970   1-C-PUR: Balcotan 107 TR, Balcotan 60 190 - Forbo CTU AG, CH-Schönenwerd   1-C-PUR: Purbond HB 110, Purbond VN 1033 - Collano AG, CH-Sempach-Station <sup>3</sup> 2-C-EPX: Araldite AW 136 H, Hardener HY 991 - ASTORit AG, CH-Einsiedeln							

Three main Formaldehyde adhesives discussed are MF, MUF, and PRF. Since Zelinka et al. [127] did not test the specimens below 100°C, strength decrease is taken as 0% at that point which might affect the comparison with other studies where MUF and PRF adhesives have already lost up to 30% of their initial strength at ambient temperature.

After 100°C, there is a big scatter in data among researchers. It is also noticeable that from 100°C to 180°C most of the adhesives tend to hold the plateau or their strength decreases only up to 10%, possibly due to the drying out of the specimen. At 140°C, residual strength varies from 76 to 86% (MF), 61 to 72% (MUF) and 56 to 96% (PRF). However, from PRF showed 10-20% higher strength than MF and MUF in individual studies (for the same timber species) [22,127].

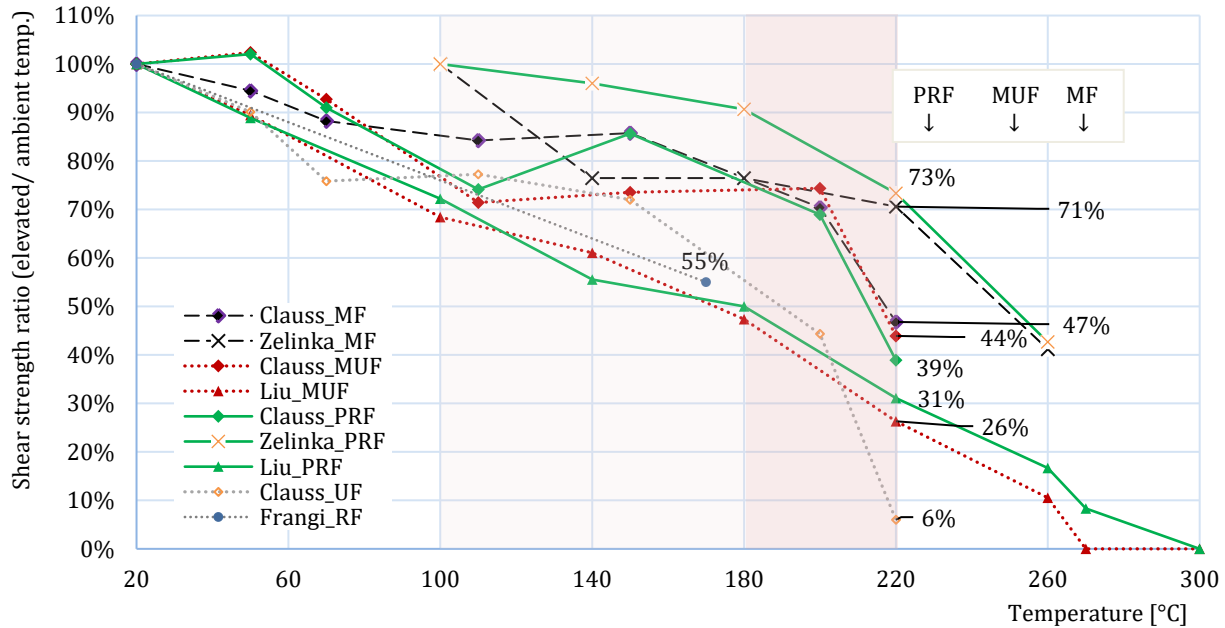


Figure 12. Reduction of shear strength at elevated temperatures. Formaldehyde adhesives – data adapted from Clauß et al. [22], Frangi et al. [45], Liu et al. [88] and Zelinka et al. [127]

After 180°C shear strength decreases sharply in all studies. At the final reference point, 220°C, adhesives show similar residual strength, approximately 30% [88], 40% [22] and 70% [127] of the initial ambient shear strength. However, shear strength loss is not solely indicator of adhesive behaviour because timber starts to lose the mechanical properties before 100°C.

1-C-PUR adhesive behaviour strongly depends on the chemical composition, as presented in Figure 13. Results from Zelinka et al. [127] are scattered, strength deteriorations follows no trend, with no definite conclusions up to 220°C when noticeable strength reduction commences.

Clauß et al. [22] and Frangi et al. [45] observed similarities in trend only up to 60°C, with a decrease in strength up to 30%, as comparable to Formaldehydes. From 60°C to 170°C, Frangi et al. [45] observes linear strength decrease ranging up to 50%, while 1-C-PUR adhesives from Clauß et al. [22] show a plateau in their behaviour with a minimum 70% of initial strength at 170°C. At 220 °C residual strength of 1-C-PUR adhesives ranges from 18% to 70%, suggesting the complexity of this adhesive composition [22,127].



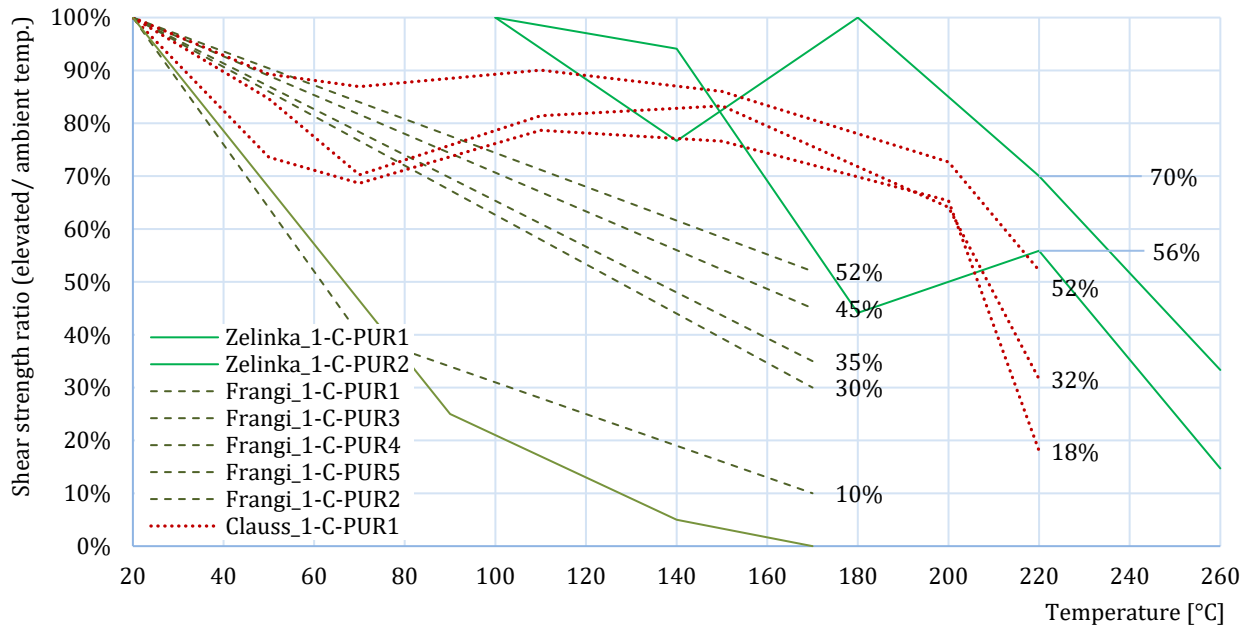


Figure 13. Reduction of shear strength at elevated temperatures. Polyurethane adhesives – data adapted from Clauß et al. [22], Frangi et al. [45], and Zelinka et al. [127]

However, since the trends do show similarities with Formaldehyde studies in Figure 12, the test outcome could be determined by the methodology applied by the specific author.

To conclude, decrease in shear strength with increased temperature was observed in all studies. Up to 180°C Formaldehydes tend to experience a lower and more predictable drop in strength than Polyurethanes, but at 220°C the reduction is similar. PRF shows the best performance. 1-C-PUR shows the biggest drops in strength and the highest variations even within one study. Many test variables could have an impact on the adhesive performance in the observed studies (e.g. methodology, bond line length, and timber species). Frangi et al. [102] discussed that oven tests at stationary elevated temperature tend to give higher strength values in comparison to transient fire tests, due to the loading rate and change in wood moisture.

Performance of Radiata Pine with 1-C-PUR under uniform temperatures was assessed in three subsequent studies in small and intermediate tests. Nicolaidis et al. [21] performed LSS tests and observed a difference in displacement of the bond line behaviour between ambient and elevated temperatures. In ambient temperature, the load-displacement curve reaches a peak and then drops sharply resulting in timber failure. At elevated temperatures, the

curve in Figure 14 shows the same trend up to 20-30% of maximal ambient displacement, after which the softening of the bonding interface leads to increased elongation and temperature induced creep (80°C), or brittle failure (150°C). Debonding started in the end region of the bond line when stresses dropped to zero and then plateaued with damage propagating into the both, bond line and timber. The temperatures used for steady state heating were obtained from temperature profiles developed in study from Emberley et al. [24] who exposed CLT blocks to different heat fluxes. To support the latter small-scale tests from Nicolaidis et al. [21], in their follow up study Emberley et al. [26] used the results to perform three point bend test on intermediate-scale beams (L=1.5 m) at 6kW/m<sup>2</sup> and the temperature induced creep temperatures 65-80°C in the bond line. Similar results were observed, as presented in Figure 14.

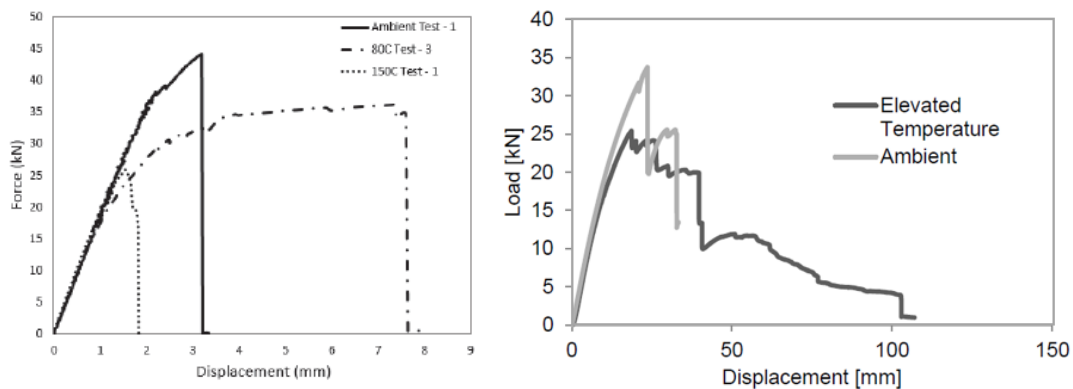


Figure 14. Change in failure mode in ambient and elevated temperature observed in small-scale single-lap shear test (left)[21] and intermediate-scale three point bending beam test (right) [26].

Deterioration of mechanical properties for timber can be also expected at lower temperatures (i.e. from approximately 60°C) [114]. Therefore, bonding performance is explained also through the type of the failure mode, because it is not always the case that the high shear strength of the adhesive is followed by high wood failure percentage.

### 2.3.2 Failure mode and wood failure percentage

The highest BSS does not necessarily mean the highest WFP. This lack of correlation is caused by the different deterioration pace of wood and adhesive. When wood softens or changes its properties, it will cause less shear in the bond line. At that point the specimen's behaviour depends on what diminishes faster – the wood stiffness or the adhesive strength. If the wood

stiffness decreases rapidly, the high adhesive shear strength alone is not very valuable because the shear stresses are released in the wood.

As presented Introduction, for the case of *delamination* or *char fall off before the adhesive line*, bonding failure can be expected solely in Timber (T) resulting in WFP being 100%. For a good adhesive, this is usually the case in ambient temperatures. Drop in WFP will result in the failure of the adhesive-timber (A/T) interface where one can see a rough surface with both wood splinters and adhesive residual. When WFP is 0% it implies pure adhesive failure (A), loss of cohesion and a smooth surface. All is presented in Figure 15.

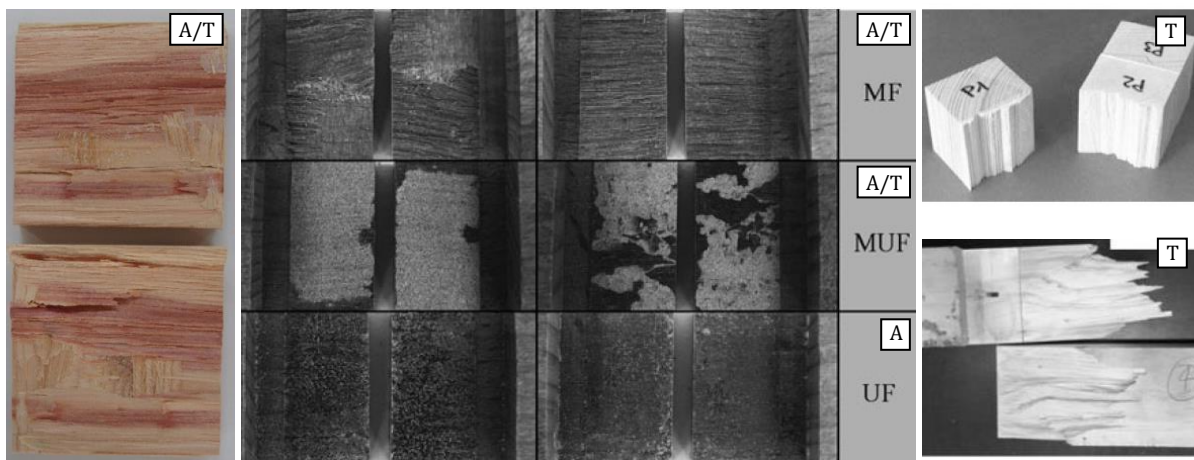


Figure 15. Failure mode: A/T-Bonding interface (left)[140], (centre) [22]; A-Adhesive (centre); T-Timber (right)[45]

Wood failure percentage is mostly measured visually, or combined with some sort of image analysis [20,51,88,140]. In the following paragraphs, WFP is assessed from the shear strength experiments described in the previous section, with some additional studies. Summary of WFP for the tests performed at 20 °C, is presented in Figure 16 for formaldehydes (lower) and polyurethanes (upper). While formaldehydes show trend, indicated scattered behaviour for PUR making it impossible to predict the failure mode.



Figure 16. Wood failure percentage for different Polyurethanes (upper) and Formaldehydes (lower) at 20°C, adapted from Clauß et al [22], Niemz et al. [29], Frangi et al. [45], Clauß et al [51], Liu et al. [88], Zelinka et al. [127] and Lim et al. [141]

### **Ambient temperature**

In study from Clauß et al.[51], formaldehydes had higher strength than the wood which also resulted in much higher WFP, being 100% for MUF and PRF, but 40% for commercial 1-C-PUR. This was also confirmed by other authors [22,29,142]. One of the conclusions from this study was that the high gross penetration of the ductile 1-C-PUR adhesive possibly contributes to delaying wood failure by reinforcing the wood, while intracellular PRF and MUF adhesive penetration in the interphase region can change the wood properties, decrease the ductility of the cell wall and promoting wood failure.

Lim et al. [141] tested the impact on WFP depending on the application of Micronized Copper Azole MCA-C preservative on wood which protects it from degradation, makes it resistant to attack by termites, and fungi decay. Shear strength was tested according to ASTM D905-08 [134] with non/treated and treated samples (high and low retention level of preservative)

for 1-C-PUR, MF and RF. 1-C-PUR and MF showed the decrease in WFP for retention specimens (from 93 to 89 %, and 99 to 93%). RF showed the same results. Shear strength was similar for all.

Lower WFP in 1-C-PUR does not indicate a weaker adhesive bond. When a delamination test was performed with three accelerated aging cycles as specified in ASTM D2559 [143], formaldehyde adhesives proved to be more rigid and brittle than polyurethanes. 1-C-PUR absorbed additional energy upon deformation and withstood moisture-driven dimensional changes. This could be a good property when wood is exposed to repeated cycles of wetting and redrying, which could be the case when the moisture front is moving away from a surface exposed to fire. Delamination rates from Lim et al. [141] specifically suggested that 1-C-PUR is the most suitable adhesive for assembling CLT panels, treated with low and high retentions of MCA-C preservative.

### **Elevated uniform temperature**

Frangi et al. [45] described the temperature range at which A/T-failure changes to cohesion A-failure. For these tests, all the adhesive specifications were provided in the study, which is not usually the case in the literature (Table 4). One RF and three 1-C-PUR experienced A-failure above 150°C and other two 1-C-PUR and one 2-C-EPX adhesive in a range from 50°C to 70°C. Polyurethanes show scattered behaviour, where the change in the failure mode can appear from 50°C to 200°C [24,90], followed by the noticeable plasticisation [127], which is an unpredictable and non-desirable phenomenon when it comes to fire design.

Change of failure mode can also depend on the test duration [90]. For MUF specimens immersed in water at 60°C and 90°C, and tensile test according to EN 14292:2005 [144], the wood failure was consistently 100 % for short term test and 70-90% load long-term test. However, authors could not assess if debonding was caused by hydrolysis of the adhesive (caused by longer exposure), which is noted behaviour for MUF [91].

For formaldehydes, Clauß et al. [51] and Zelinka et al. [127] also observed that up to 200°C the lowest rate of WFP is 70%, but Liu et al. [88] noticed significant change in failure mode already after 150°C as presented in Figure 17, being only 30% at 200°C because the

melamine "ring" broke (formaldehydes are cross-linked), as confirmed by Fourier-transform spectroscopy (FTIR). PRF adhesive started to decrease significantly only after 250°C was reached.

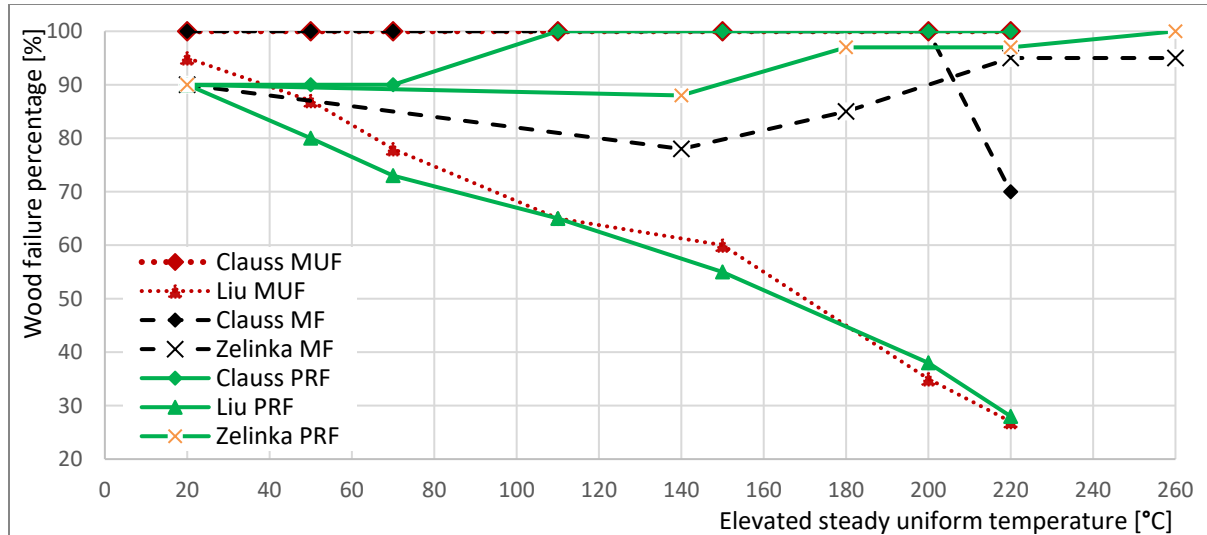


Figure 17. Wood failure percentage for formaldehydes, based on studies from Liu et al. [88], Clauß et al [51] and Zelinka et al. [127]

A SEM analysis in Figure 18 shows that at 220°C MUF has no cracks at the bond line interface (like PRF does). Holes appeared in the bond line which suggests the loss of cohesion. However, at 280°C, the thickness of the PRF glue-line increased and penetrated deeper into the specimen.

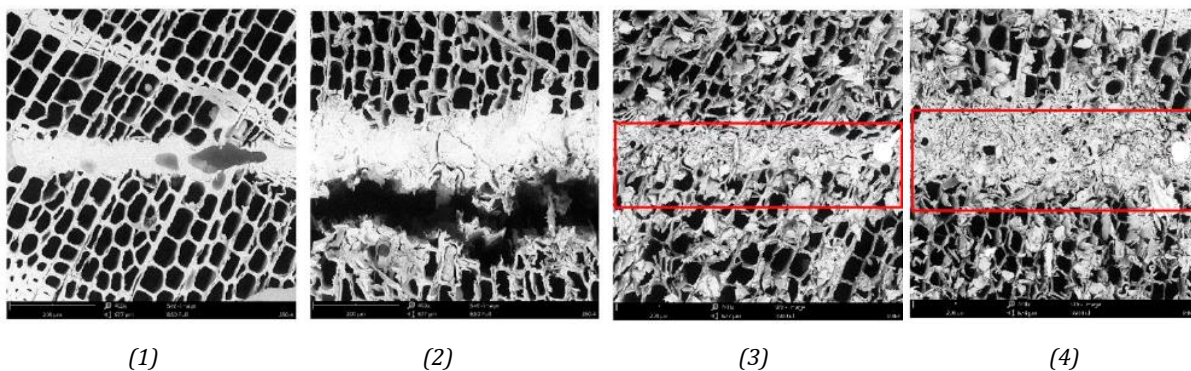


Figure 18. SEM images. Type of failure at 220°C: MUF loss of cohesion - A (1), PRF bonding interface failure A/T (2). Bond line thickness at 280°C: MUF (3), PRF (4). Adapted from Liu et al. [88]

Finally, adhesives and finger joints at elevated and fire temperatures were observed by Frangi et al. [45,102], Craft et al. [145], Lehringer et al. [87], Clauß et al. [22,51] and Klippel et al. [47,146]. Finger joints are out of scope for this study, so only one research showing a

clear difference between formaldehydes and polyurethanes is discussed. Based on the three reviewed tests (shear test, creep test, and bending test), Craft et al. [145] wanted to create a new elevated temperature adhesive tension test where they applied simultaneous thermal (220°C for 2 hours) and structural tension load. PRF and MF adhesives never showed failure in the bonding line or in adhesive during the 2 hours. When they eventually did, it was a wood failure. Seven different 1-C-PUR adhesives failed at temperatures between 90°C and 175°C within 30 minutes with a low WFP. The gradient from the oven to the middle of the sample was 50°C. However, Lehringer et al. [87] noted that this method was too conservative because the thermal gradient in a real fire scenario would be so steep that the finger joint would hardly experience this temperature.

From the studies above, a steadier behaviour of formaldehydes with a high WFP is noted at ambient temperatures. Polyurethanes vary in performance, being highly dependent on their chemical composition. At elevated temperatures, deterioration of adhesive is present for both, and influenced by load duration. Between two lamellas, change in failure mode can be experienced for polyurethanes in wider temperature range (50°C to 200°C) than for formaldehydes (from 150°C). Temperature range in finger joints is comparable to polyurethanes (90°C to 175°C).

### **2.3.3 Temperature induced creep**

As already observed, thermal load affects the mechanical performance, bonding quality, creep, and fatigue of the composite wood product [82]. Usually, creep behaviour of wood-adhesive bonds are observed with small scale compression shear test ASTM D3535-07a at 180°C [147], EN 302-8 at 90°C±2°C [148], and bending test EN 15416-3 at 45±2°C [149].

Chemical cross-link density is important factor for creep. Highly crossed linked adhesive PRF has a high thermal stability with stiff but brittle behaviour. On the other side, some adhesives with weaker cross-linked density as PUR reach lower strength values but they are more ductile. Some adhesives deteriorate intermittently, but others continuously when exposed to temperatures greater than only 38°C, but for long periods [150]. For example, for 1-C-PUR adhesive Klippel et al. [34] findings expect the creep to start from 40 to 80°C.

Rammer et al. [108] observed the creep performance of finger joints at elevated temperature (185°C) in the four point bending test. Deformations throughout the 2h test were normalised to initial deformations. Eight different adhesives from three manufacturers were tested: four 1-C-PUR, two PVAc, one MF and one PRF adhesive. All finger joints with 1-C-PUR experienced failure in the bonding, while MF and PRF experienced only wood failure and showed the same creep behaviour as the control wood sample (not bonded). Results from this study correlate to the findings from Lim et al. [141], who also showed that for the long test, behaviour of 1-C-PUR is significantly worsening because the viscoelastic properties decline rapidly at high temperatures.

However, all established test methods have determined that it is difficult to draw quantifiable conclusions about the expected service life of a bond in practice.

#### **2.4 Summary: structural and thermal response of adhesives**

Results from the discussed studies are supported with the review written by Stoeckel et al. [44], which covers mechanical properties of some adhesives used for wood bonding. Some of the main conclusions based on the adhesive type are presented within Appendix A. Since polyurethanes and melamine – urea formaldehyde is used in this study, only their properties are presented here:

##### Polyurethanes

- ductile, high fracture energy [1] [51],
- the long-term durability of PUR adhesives is not well known [1],
- resistance to heat poorer than for formaldehydes [23],
- structural performance highly reliant on its chemical composition, manufacturer and fillers [22,44,46,47], and the methodology used to test the specimen [46,47],
- if well adapted it can reach the PRF adhesive strength and WFP [22],
- based on the small-scale shear tests, increased elongation, WFP reduction, and temperature induced creep is expected from 80°C to 150°C [21,26,108],
- low heat flux as 6 kW/m<sup>2</sup> can also cause 1-C-PUR adhesive failure [24],
- char fall-off observed in several full-scale tests [11,13,30,31,38],
- “Non-delaminating” PUR [11,30,31] could be used to avoid CLT delamination in furnace tests,



- shows good results when combined with 35 mm thick lamella, but not with 25 mm where it experienced char fall-off [123] in furnace tests.

### Melamine-urea-formaldehyde (MUF)

- High shear strength, brittle behaviour, and the high wood percentage failure,
- compared to PRF, it can absorb more deformation energy, but strength and stiffness in tensile shear test tends to be higher than for all 1-C PUR adhesives [88],[51],
- change in failure mode expected after 150°C [88], but can also depend on the test duration [90],
- at 220°C can undergo significant chemical breakdown [88],
- no reports of char fall-off for MUF were found [131].

### Fire performance

One repeatable relation was found for the tests in studies observed for this thesis. In small scale tests, failure in the adhesive (A) or at the bonding interface (AT) was often observed for 1-C-PUR adhesive, while MUF adhesive tend to have a higher wood failure percentage. In compartment tests, 1-C-PUR adhesive experienced regularly delamination and char fall of at the adhesive line, causing the reignition, while MUF showed better behaviour with no increase in HRR and eventual auto-extinction. Although linking the specific bond line temperatures is challenging, performance can still be related.

## 2.5 Important methodology drivers

From the studies presented, the following parameters are noted as important for debonding:

- standard and method used for testing,
- time (duration),
- mode (steady-state or transient heat application, presence and amount of load applied),
- cause (material properties assessment, real case scenario simulation, specific phenomena observation - i.e. char fall-off),
- reproducibility (number of tested specimens),
- geometry (small-, intermediate-, large- or full-scale test),
- vertical or horizontal orientation,
- CLT layer setup (crosswise or longitudinally oriented adherent lamellae).

### 2.5.1 Impact of non-harmonised testing standards

CLT guidance is under development globally to address issues with char fall-off and delamination. There is still no harmonised methodology with a defined set of testing procedures to assess the adhesive performance in fire and get repeatable results.

For example, Craft et al. [145] reviewed three small-scale tests in use. The first to be assessed was a shear lap strength test ASTM D7247-06 [151]<sup>9</sup>. After the specimen was tempered to a specific temperature (up to 220°C), a tensile force was applied on the bond line. The main disadvantage of this test is that it is not heated under load as it would be in reality. The second was the CSA O112.9-10 B2 Creep test [152]<sup>10</sup> where the specimen is simultaneously loaded under compression and heated up to 180°C for 2 hours. It is the authors' position that this temperature is not conservative enough because an adhesive that passes this test fails in the full-scale furnace test [112]. The third method observed was (at the time, 2008)) in the developing phase from Forest Products Lab (FPL)<sup>11</sup>. In the latter, specimens are loaded in four-point bending test while heated to 220°C, but conditioned to 103°C before testing. Conditioning is the main deficiency of the last method because it does not represent the real case scenario and the impact of moisture movement.

It can be said that, with respect to adhesive performance in fire, North America (ANSI/APA PRG-320 [39]) currently displays the furthest developed and most onerous requirements for CLT manufacturing. Additional to the small-scale tests, full-scale testing needs to be performed to ensure that the CLT does not exhibit fire re-growth when subjected to severe exposures. That is because it is allowed to have installed exposed surfaces, other countries' codes allow only encapsulation. In Europe, Australia, New Zealand, and Japan the adhesive requirements are still in a developing phase. Performance is assessed through a lap shear strength test, and tests where delamination is induced by cycles of hot-cold and wet-dry environmental conditions, without taking fire explicitly into account. However, there is no agreement between those two tests [27].

---

<sup>9</sup> superseded by ASTM D7247-17 [172]

<sup>10</sup> revised by CSA O112.9-10 [173]

<sup>11</sup> United States Department of Agriculture (USDA)

## 2.5.2 System size

Disadvantages and comparison of small and large scale testing are also discussed by Klippel et al. [36], where it is explained that compartment and large scale furnace tests are very costly and subjected to more scatter, while for small-scale tests, the validity and significance of the results are questioned. When it comes to CLT element specifically, it is hard to replicate the conditions of the real fire scenario in a small-scale test because in reality the element is exposed to eccentric thermal and mechanical loads [108].

By testing in a smaller scale, a test method can be much more refined. Thereby, repeatability and reproducibility are increased, and the cost is reduced dramatically. Furthermore, the tests can be completed by the manufacturer, conducted in any laboratory, which could accelerate product development (when applied responsibly) [145]. Small scale tests can mitigate full-scale nonlinear interactions, adhesive performance can be quantified, and tested under load which is often disregarded with full scale testing [127].

On the other hand, Dagenais et al. [112] concluded that qualifying adhesives by some small scale tests (e.g. CSA O112.9 creep test at 180°C, CSA O112.10 shear delamination test in cyclic environmental conditions) does not necessarily confirms the fire performance in larger scale. High elevated temperature do not necessarily increase the level of safety of the full size glued member [106], but the author found a good correlation of compartment tests with small scale flame test CSA O117 Annex A2 [111].

Currently it is still hard to extrapolate the small-scale tests results to predict the char fall-off mechanism observed in large scale tests. But continuous development of small-scale methods is necessary and should not be overlooked because once established, a screening algorithm between two scales could be implemented to predict the bond behaviour. This could be very useful for the developer and new adhesives entering the market. The importance of system-level testing was highlighted in the review about the fire safety challenges in tall wood buildings [6]. It is not enough to test only the element but the whole system which shares the load, meaning that different load ratios can cause different outcome.

### 2.5.3 Thermal exposure (steady-state/transient heating/pre-heating)

Steady state testing is often discussed [4,21,22,45,47,88,127] because it allows for observation of material mechanical properties at the uniform cross section temperatures without any thermal gradients. Hence, the specific combination of applied load and heat (and to it correlated failure mode) can be found. The main deficiency of this method is that in reality a temperature gradient cannot be avoided unless the sample is being heated so slow that the heating rate is irrelevant. Also, dehydration that causes shrinkage and moisture movement is not observed. Finally, if the sample is loaded only after it has been heated, sample is not self – stressing, and the internal stresses and temperature induced creep are ignored so the failure mode obtained with steady state is not applicable. To represent real fire scenario (e.g. flashover), one needs to apply high heat fluxes, which allows the specimen to pass quickly through the lower temperatures.

Niemz et al. [29] showed that due to the increase of temperature and change of moisture content, complex stresses can appear in both adhesive and wood. Tension between glue and wood due to impaired shrinkage was recognised, especially in the event of changes in humidity. With transient heat applied, the moisture content and temperature gradient that causes moisture movement and internal pressure can be discussed. Applicability of transient tests is explained with finger joints and lamella bond-lines. Finger joint in reality must maintain the load as the cross section is reduced and the temperature of the remaining cross section is increased. This could be better represented by a creep test with transient heat because joints are oriented in the same direction as the thermal wave and they experience an immediate temperature gradient. Delamination could be assessed by performing a shear lap test in a chamber with constant load and increasing heat. The temperature at which the sample fails could then be compared with the temperature at which wood chars.

However, when the specimen is firstly loaded and then heated (transient conditions) one cannot assess the temperature at which specimen fails due to the present temperature gradient between the surface and inside the specimen. This can be characterised by placing the thermocouples in multiple positions in the specimen, but it is harder to define the

location with corresponding level of mechanical stress, internal stress, and temperature at the point of failure.

To avoid the effect of moisture movement, some authors preheat specimens a little bit above 100°C [102,108,127]. However, a study from Craft et al. [145] shows that heating and “curing” under no load in formaldehydes has a big impact on the results because it causes the cross-linking of the phenolic component, which can then increase the elevated temperature performance of the adhesive. For example, PVAc adhesive tested in tension test failed at 90°C when it was not pre-heated and at 190°C when it was dried in the oven for 24 hours before the test at 103°C.

A convenient approach would be to do both, load and then heat (transient behaviour) and heat and then load (steady-state behaviour) as it was done by Wiesner [20]. Also, it is recommended to perform both, large and small testing. By doing that, one can at least qualitatively describe the performance. A difficulty in performing such comparison could be a lack of time or equipment. This is in agreement with Klippel [34] who stated that there is no clear correlation between uniform testing and real fire behaviour and that to get one, it is necessary to study more specimen scales in both steady-state and transient state fire conditions.

#### **2.5.4 Importance of structural load**

It is important to consider application and amount of structural load in testing. In example, when assessing CLT wall elements performance, adhesive behaviour in fire is a function of the deflection of the wall [145]. Therefore, it is inconvenient to make conclusions about adhesive performance from full scale tests where there is no load, but only heat applied.

In EN 1995 -1-2 [120] fire load is considered as rare event and the design load is therefore reduced to 60% of the ambient design load. Wiesner [20] tested his specimens with 0.50 of the ultimate load that specimen could sustain at ambient conditions. To assess the adhesive performance in PRG-320-2019 [39] a floor-ceiling slab is exposed to a vertical load which is 0.25 of allowable stress design (ASD) . That load should be sustained for 240 minutes in

specified fire conditions without the char fall-off that could result in significant temperature rise during the cooling phase.

In most of the studies observed, the rationale for the load applied are rarely clarified. When testing in fire conditions, authors are encouraged to represent if the specific load percentage obtained from tests in ambient conditions was defined from maximal stresses at the surface, design ultimate load, or actual failure strength.

### **2.5.5 System orientation (Horizontal or vertical) and fuel distribution**

In the developing European method [123] to assess CLT behaviour in fire, authors presented the intermediate-scale furnace test for horizontally placed elements. Some authors agree that the vertical structural members (walls) may show a better fire behaviour in comparison to horizontal members (slabs) [34,36] because char fall of in horizontal elements is influenced by gravity.

However, in a study from Gorska et al. [18], where 24 intermediate compartment fire tests with eight different configurations of exposed wall and ceiling surfaces were tested to analyse the fire dynamics, it was noted that exposing the ceiling in the compartment is the safest option for the design, compared to other elements. The ceiling area experiences the lowest burning rate because oxygen cannot penetrate easily due to the high concentration of smoke, which makes the charring less efficient, with lower surface regression. Similar results in temperature profiles and HRR rates were observed between a setup with two walls and ceiling exposed and a setup with two walls and no ceiling exposed., Hadden et al. also noted lower charring depths on the ceiling compared to the back wall, attributed to lower oxygen concentration near the ceiling, resulting in a lower pyrolysis rate [13]. In a recent review of factors that affect burning behaviour in tall timber construction [5], it was discussed that the charring rates are expected to be greater for vertically orientated samples due to increased radiation from the flame.

### **2.5.6 Layer setup and importance of edge-gluing**

Wood is an orthotropic material and when it dries, shrinkage can be greater for one direction (i.e. tangential compared to radial and longitudinal), which can lead to stresses developed at

the bond lines. For GLT products where all lamellas are oriented in the same direction this is not of high importance, but for the case of CLT, stresses between two orthogonal layers are introduced because both shrink in the opposite direction. This can accelerate delamination, as it was studied by Dagenais et al. [112]. During the flame test, observable cracks opened at the glue lines in CLT, while for GLT a smooth charred layer could be seen. Total delamination length ratio for 1-C-PUR was for CLT approx. 11% and but for GLT it was 2%.

Hasburgh et al. [23] where in horizontally oriented CLT samples deep grooves and non-uniform charring appeared for LCL oriented specimen (3: longitudinal-crosswise-longitudinal) while for the specimen with two adjacent longitudinal layers (LLC) charring was uniform. Author assumes that the smooth char layer front ensures more uniform heat distribution.

*Edge-gluing* of lamellas between the two parallel layers is important. Narrow bond line offers a passage for gases and flames penetration which can then locally accelerate the heating and charring of the next layer (timber behind the gap) and then increase the charring rates.

Number of layers (layer setup), i.e. the difference between three and five ply CLT configuration, was discussed by Wiesner [20]. Choosing more than three layers offers a solution for both scenarios (ambient and fire) but more research should be done to cover the impact of layer setup (layer thickness and orientation). Five ply sample ensures better stresses distribution, whereas three layers with two thicker outside layers, from a structural point of view, ensures stability because the load bearing part of cross section is near to the neutral axis. For fire conditions, using the thicker outer plies delays the thermal penetration and postpones debonding, thus increasing the chances of achieving burnout and auto-extinction before the new virgin wood is involved. However, with only three lamellae, 50% of the total available load-bearing material is exposed to fire at an early stage. In contrast, in five-ply walls, when the first layer is exposed it is only one third that is affected, which prevents instability for a longer period.

## **Chapter 3      Methodology**

The Literature review described that the structural behaviour of a (timber) composite depends on the properties of both timber and adhesive, along with their interaction. In bending, shear parallel to the grain in longitudinal layers and shear perpendicular to the grain perpendicular in orthogonal layers are developed, which are then distributed between the timber and the bond line. With simultaneous application of the thermal and structural load, their interplay weakens and this can potentially cause debonding. This chapter presents the methodology developed in this study to test the element load transfer – only in shear – at elevated temperatures. This was used to expose the bond line to the most severe conditions. Higher load was applied to avoid the randomness from the thermal load. With no load applied, bond line behaviour would depend on thermal deformation and the temperature in the glue, where the results tend to be more inconsistent and not representative.

The following sections describe the materials and experimental methods used in this thesis. A summary of this methodology is presented in Figure 19. Stage 1 covers the method design, where the materials used, tested moisture content, calculated structural load and specified thermal load define the experimental matrix. Stage 2 presents the testing procedure, which is presented together with instrumentation and apparatus. Stage 3 shows the outcome obtained from the applied instrumentation in Stage 2, which will here be noted and later presented within Chapter 4.



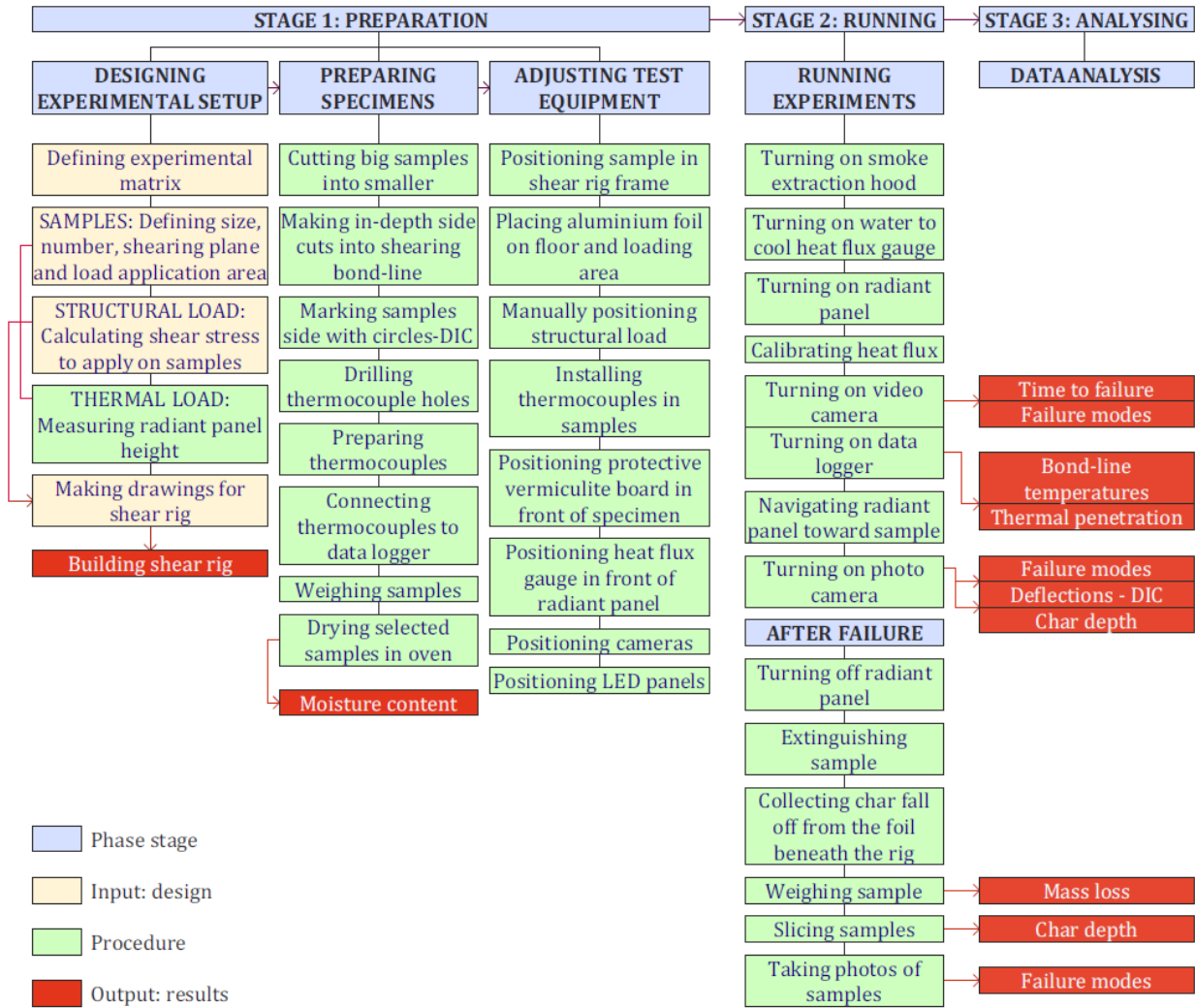


Figure 19. Flowchart with the methodology used for this research.

### 3.1 Materials

Three series of samples from three different European CLT manufacturers were studied, as presented in Table 5. All of them use the same Spruce timber species but with only slightly differences in density (i.e. (A) 450, (B) 470, (C) 420 kg/m<sup>3</sup>), while the adhesive used in each series varies. In the main bond line, Series A and B use two different one-component polyurethanes (1-C-PUR), while Series C uses melamine-urea formaldehyde (MUF). The exact adhesive producer is known only for the glue used in the main bond line in Series A. The colour code of the highlighted cells in Table 5 corresponds to the bond lines in Figure 20.

Each original sample source was cut from a large CLT samples of dimensions 30x30x20 cm to eight smaller samples of 15x15x10 cm. In total, 36 samples were tested, 6 in ambient and 30 in fire conditions, as presented in the experimental matrix in Table 6.

Table 5. Series of material samples, including information regarding timber species, adhesive and lamellae configuration.

Series	Manufacturer	Main bond line	Narrow bond line		Layers [from front to back]	
			(decking and inner layers)		Number	Thickness [cm]
A	Binderholz BBS	1-C-PUR1 <sup>1</sup>	MUF1 <sup>2</sup>	H+PVAc <sup>3</sup>	4	2,2,4,2
B	Stora Enso	1-C-PUR2 <sup>3</sup>	PUR2 <sup>3</sup>	PUR2 <sup>3</sup>	3	4,4,2
C	Hasslacher	MUF2 <sup>3</sup>	MUF2 <sup>3</sup>	MUF2 <sup>3</sup>	3	4,4,2

<sup>1</sup> PUR1: Henkel Loctide Purobond HB S line, <sup>2</sup> MUF1: Casco Akzo Nobel, <sup>3</sup> Not specified

The position of the middle cut in the large samples (Figure 20Figure 21) pre-defines if the sample has a narrow bond line exposed to the radiant panel, which could potentially lead to a different failure mode and time to failure. The manufacturer of Series A uses different adhesive for the narrow bond line between decking layers and inner layers (see Figure 20 (left)). In Series A, the sample was rotated and the usually inner layers were exposed to the radiant panel. The exposed narrow bond line and main bond line for Series A are shown in Figure 20, whereas these features in Series B and C are shown in Figure 21.

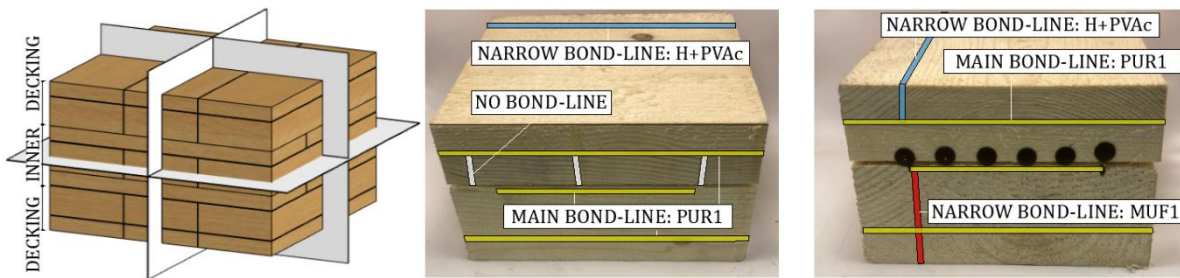


Figure 20. Series A: Large sample before slicing (left), Bond lines' front view (centre), side view (right).

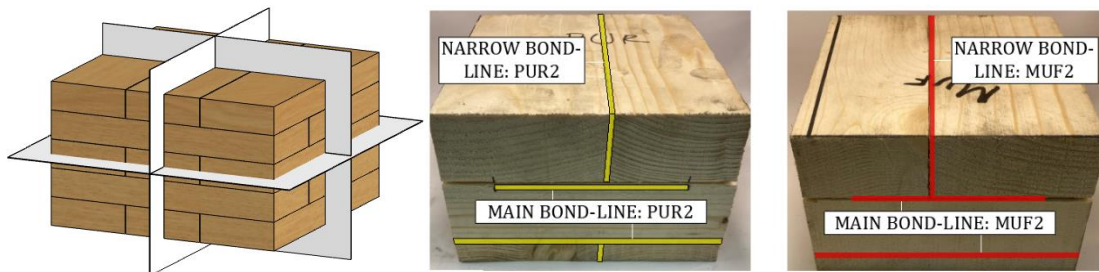


Figure 21. Series B and C: Large sample before slicing (left), Bond lines' front view for PUR2 (centre), and MUF (right).

Series A small samples were rotated to reduce the number of comparing variables since the two decking lamellae together have a thickness of 6 cm. This was a result of logistic issues at the time when the samples were ordered. By exposing two inner (thinner) lamellae for Series A, the area of 4 x 150 cm was exposed to compression for all three cases. However, thinner lamellae also serve to observe the importance of lamella thickness for char fall-off phenomena. This was done to observe the trends and not estimate Binderholz BBS CLT as a product since the conditions to which the sample was exposed are not representative of the real case scenario.

To obtain a uniform distribution of heat around the bond line area when tested under fire conditions, it was decided to make a side in-depth cut of 2.5 cm in the shearing bond line at all four sides. Restricting the expected edge effect from the flame enables the assumption of one-dimensional conduction heat transfer through the bond line. By doing this, the effective bonding area was reduced from 15x15 cm to 10x10 cm for all samples as presented in Figure 22.

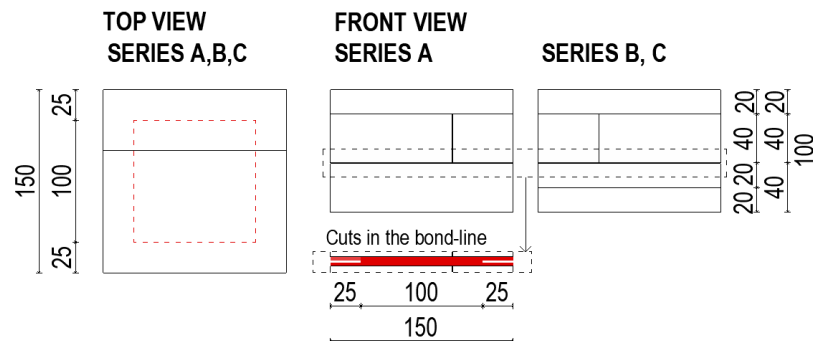


Figure 22. In-depth cuts in the shearing bond line

### 3.2 Experimental conditions

Samples in Series A have a different layer configuration than Series B and C. For Series A, 2x2 cm front lamellae, and for Series B and C 1x4 cm front lamella was exposed to structural and thermal load, as specified in Table 5. The loaded shearing plane was distanced 4 cm from the front side in all conditions.

Three types of tests were performed: (1) ambient shear strength tests; (2) moisture content measurements; and (3) shear strength tests under thermal radiant exposure conditions. This section provides rationale for the choice of structural and thermal load used in the latter.

### 3.2.1 Structural loading conditions

By exposing the bond line to shear, the intention was to trigger the weak link of the composite manifested in rolling shear. The load used in the shear tests in fire conditions is calculated as a fraction of the characteristic rolling shear strength prescribed by European Standards [1, 5.2.3.2],  $f_{r,k} = 0.7$  MPa for 100x100 mm bond line area. Once the ratio of that stress was calculated, it was translated into the mass in kilograms. That mass was then applied on the steel plate which was hanging from the front lamella. Geometry of the shear rig is presented and explained later in Figure 26. Hereby, one is acquainted with basic principles of the design calculations, and the detailed process is presented within Appendix C.

The design of CLT in ambient conditions is rarely governed by the ultimate limit state (ULS). It is rather the serviceability limit state (SLS) and the stiffness, deflections, and vibrational limitations that are critical to design structures [126]. Therefore, to define that fraction of the shear stress, a range of single-span floor slabs in bending at ambient conditions were designed. The aim was to find the deflections in the largest possible span for 1m wide, 20 cm thick slab - Series A Stora Enso 5 layer CLT (5x40mm). For that deflection, the maximal developed shear stress and utilisation of rolling shear strength was found. That stress was then finally transferred the tested bond line area to back track the needed structural load. The design process is illustrated in Figure 23.

The design load consists of the dead load (self-weight based on the specified geometry) and live load (imposed load based on the purpose-shopping centre). After a couple of iteration, a span of 5.5 m was representative of 88% of the capacity for deflection, maximum allowed vibrations. Calculated shear stress in three longitudinal layers has to be lower than the shear strength, whereas in two orthogonal layers it has to be lower than the rolling shear strength. Shear strength is according to European Standards five times higher than rolling shear

strength. This led to 22% of the rolling shear strength capacity being utilised. This is approximately a mass of 152 kg ( $\approx 1.5 \text{ kN}$ ) distributed over 100 x 100 mm bond line area.

However, in case of fire, char will form an “insulating” layer, which is no more load-bearing. This means that after a specific time when the first lamella chars, only two longitudinal layers, will act as load-bearing because the perpendicularly oriented layers (to the span direction) are not accounted for. Therefore, shear stress distribution will change as presented in Figure 23.

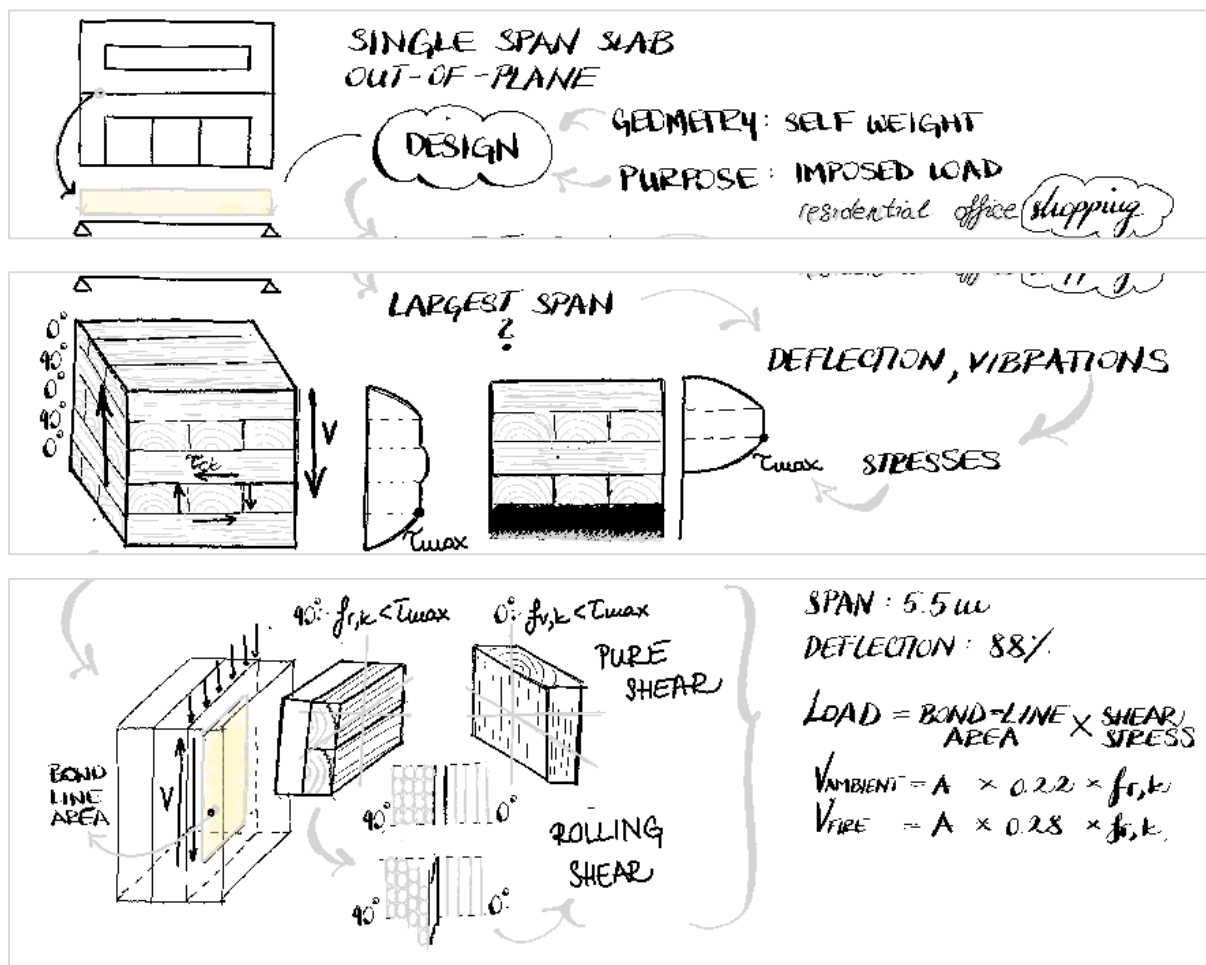


Figure 23. Illustration of the steps taken to define structural load in experimental matrix

An increase in the shear stress, now 28% of the rolling shear strength in the next bond line, will then correspond to a higher load, approximately 199 kg ( $\approx 2 \text{ kN}$ ).

Therefore, two load values will be used in the tests, lower load (100 kg) and higher load (200 kg), representative of the 22% and 28% of the used rolling shear strength capacity.

Approach in this study deviates from the normal design principles used in European jurisdiction. Shear strength calculated in this study in case of fire has a higher percentage of utilization than in ambient. This results from the design combination, which was the same as for the ambient conditions, but applied on the reduced cross section. Actions were not taken with the lower values of coefficients for variable actions  $\psi$  and partial safety factors  $g$  for accidental situation (fire), but rather the same as for persistent situation in ambient conditions. This is a conservative approach which allows for direct comparison of ambient and fire conditions.

### **3.2.2 Thermal loading conditions**

The thermal load applied by the radiant panel was 50 kW/m<sup>2</sup>. The intention was to achieve a rapid auto-ignition and continuous flaming combustion of the exposed timber during the test, such that the incident heat flux during the test remains as steady as possible. In small scale cone experiments developed by Emberley et al. [153], flaming combustion and no self-extinction was present for heat fluxes higher than 45 kW/m<sup>2</sup>, while debonding was indicated above 55 kW/m<sup>2</sup>. Cuevas et al. showed that self-extinction in FPA tests, with 21% O<sub>2</sub> concentration, is not present over 40 kW/m<sup>2</sup> [154]. Critical mass loss rate found in the latter corresponds to the one from Bartlett et al. in FPA tests with ambient oxygen concentration [155].

Additionally, the application of this heat flux was chosen due to its widespread use for small and intermediate testing. In the future, this can also allow for a comparison of results with other developing studies which observe delamination in similar conditions [156].

### 3.2.3 Duration of tests

Shear strength in ambient conditions was tested until failure. Test starts once the stress starts to grow with a duration of 30 to 103 seconds. After the stress has reached the peak and experiences a significant drop, indicated by a loud sound of a brittle failure in the bond line, experiment was terminated.

Change of mass was measured for 60 hours in moisture content tests. Ten measures were taken throughout the first five working hours. Samples were then left in the oven during the night for 15 hours. Ten measures were taken during the ten hours of the following day after which they were consolidated for 30 more hours. The change between the two last mass readings was 0.01%. The oven temperature was then kept on 30°C to consolidate samples for shear strength tests in fire conditions.

The shear strength tests in fire conditions was initiated by placing the radiant panel in front of the sample. The average ignition time for non-dried samples was  $13 \pm 3$  s and for dried samples  $10 \pm 2$  s as presented in Figure 24. Once the loading frame dropped together with the (part of) front lamella drops, the experiment was terminated. These experiments lasted from 16 to 52 minutes, depending on the adhesive, moisture content and structural load applied.

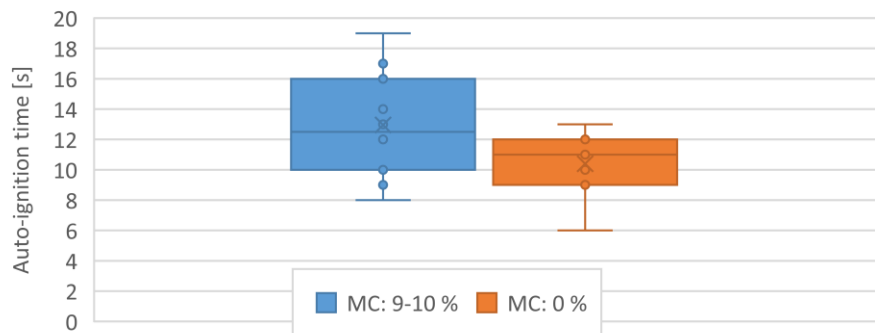


Figure 24. Time to ignition for all samples

### 3.2.4 Experimental matrix

As presented in two trials were performed for each ambient testing case, and one to three trials for the various fire conditions. In total, 12 samples for Series A (PUR1) and B (PUR2), and 6 samples for Series C (MUF) were tested under the same thermal but different structural load.

Table 6. Experimental matrix.

NUMBER OF TRIALS	SERIES	GLUE	CONDITIONS				
			AMBIENT	FIRE [ 50 kW/m <sup>2</sup> ]			
				MC: 9.1-10.5 %		MC: 0 %	
			Displacement 1mm/min	Lower load 100 kg	Higher load 200 kg	Lower load 100 kg	Higher load 200 kg
A	PUR1	2: A1, A2	3: A4, A3, A11	3: A5, A6, A12	3: A7, A10, A13	3: A8, A9, A14	
B	PUR2	2: B1, B2	3: B3, B6, B11	3: B4, B5, B12	3: B7, B10, B13	3: B8, B9, B14	
C	MUF	2: C1, C2	2: C3, C5	2: C6, C4	1: C7	1: C8	
TOTAL		6	8	8	7	7	
		6	30				

### 3.3 Experimental apparatus, instrumentation and procedure

The equipment used for the three types of tests performed were (1) a hydraulic testing machine (Instron 4050) for ambient shear strength tests; (2) Thermo Scientific™ Heratherm™ General Protocol Oven for moisture content measurements; and (3) a radiant panels and bespoke loading device for the shear strength tests under radiant exposure. Each apparatus is presented in Figure 25.

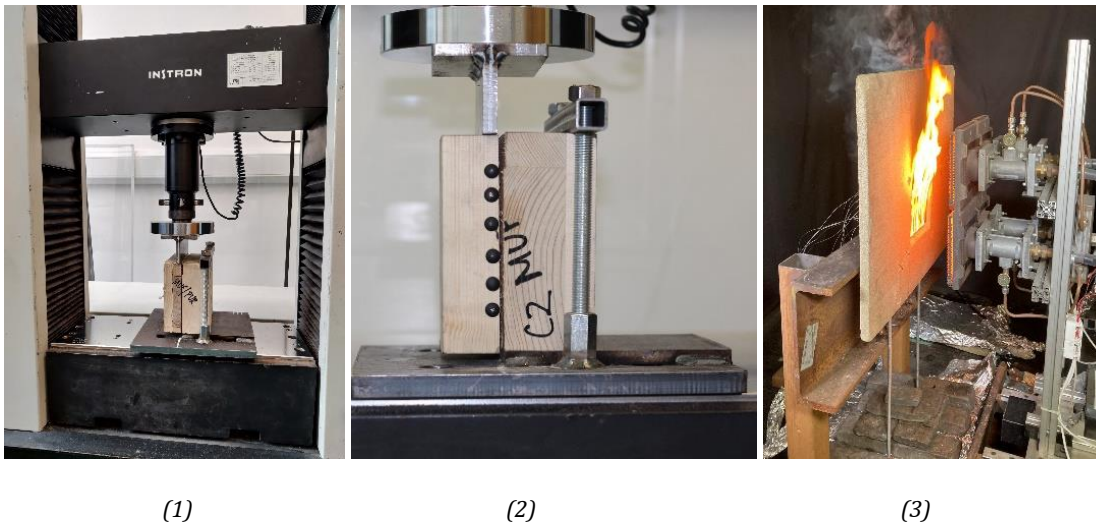


Figure 25. Apparatuses used for ambient tests to failure (1,2) and for shear strength test under fire conditions



### 3.3.1 Ambient shear strength tests

Two samples from each series were exposed to compression by applying the displacement (1mm/min) with hydraulic jack, transferred through a steel T-profile to stress the CLT bond line in shear up to failure, as shown in Figure 25-2. The aim is to define the load that causes failure (i.e. the ultimate shear strength) and to observe the failure modes.

### 3.3.2 Moisture content tests

These followed ASTM D4442 standard: Method B. Specifically, fourteen samples (six samples for Series A and Series B, and two samples for Series C) were dried to 103°C in the oven. Mass loss curves are presented in Appendix C. Afterwards, the same dried specimens were used for the shear tests in fire conditions to observe an impact of moisture migration on composite behaviour, and more specifically the adhesive. For specimens that were not dried, the initial moisture content was measured manually with Valiant FIR412 Digital Moisture Meter for Firewood Timber and Brickwork.

### 3.3.3 Shear strength tests under fire conditions

Before testing, the mass and moisture content of each specimen was measured.

In these tests, structural load was applied by using the shear rig and the loading frame presented in Figure 26. For Series B and C, a sample was placed under the clamps so that the front lamella (4 cm) was hanging from the rig. For Series A, two lamellae (2+2 cm) were hanging as presented in Figure 27. A hand spanner was used to tighten the clamps and ensure a rigid connection of the second two lamellae.

The loading frame was positioned at the hanging sample. It has an upper flange and two bars welded to it which were then holding the steel plate at the bottom. The steel plate was used to position the lead ingots, used as a load. The weight of each ingot was  $12.5 \pm 2.5$  kg. Aluminium foil was placed on the floor to allow the collection and visual observations of the possible char fall-off residues.

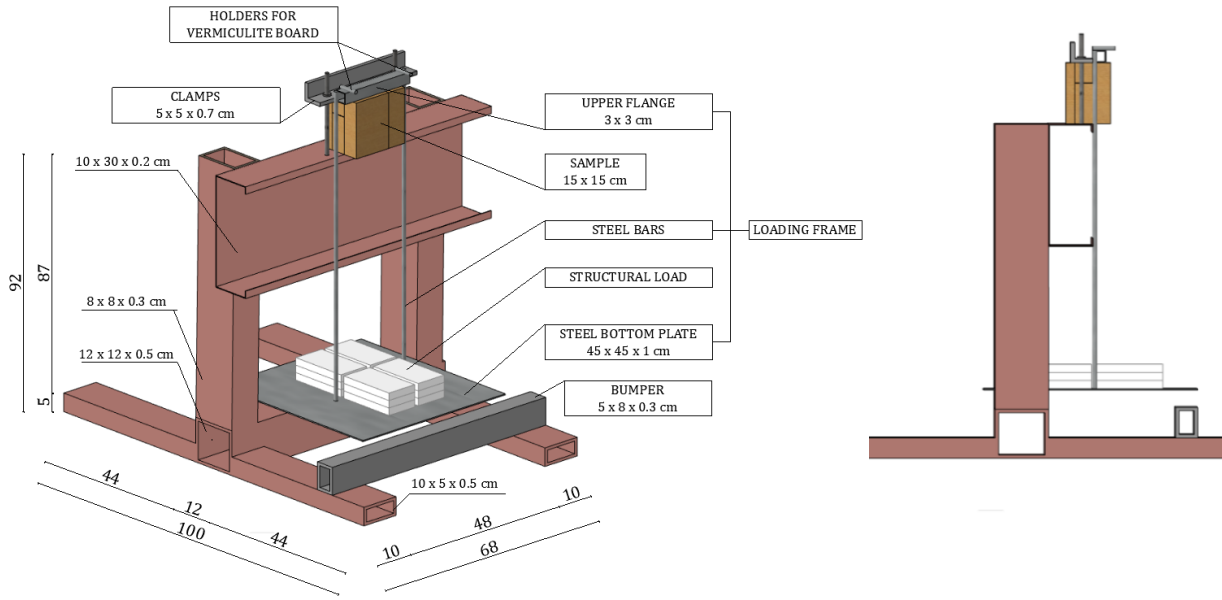


Figure 26. Shear rig geometry – 3D view with dimensions (left), side view (right)

All apparatus and instrumentation used is presented in Figure 28.

In the positioned sample, 13 Type K thermocouples ( $\varnothing 1.5$  mm) were installed from the back of the samples (cool side) in hand-drilled holes. It was aimed for the tip of the thermocouple to have a direct contact with the timber to obtain more accurate measuring and avoid the influence of air gaps. Therefore, the total length of the hole was drilled to  $\varnothing 1.5$  mm. When installed from the back, the hole depth can reach one of the three planes: 6 cm to the 1<sup>st</sup> glue line (1), 4 cm to the middle of the second lamella (M) and 2 cm to the 2<sup>nd</sup> glue line (2) (as shown in Figure 27). Although positioned throughout differing depths, all thermocouples were within the projection of the first (reduced in size) bond line area. Their purpose was to measure the bond line temperature at failure and to monitor the thermal penetration wave throughout the test. Once installed, the thermocouples were connected to the datalogger to check if the temperature readings correspond to ambient temperatures.

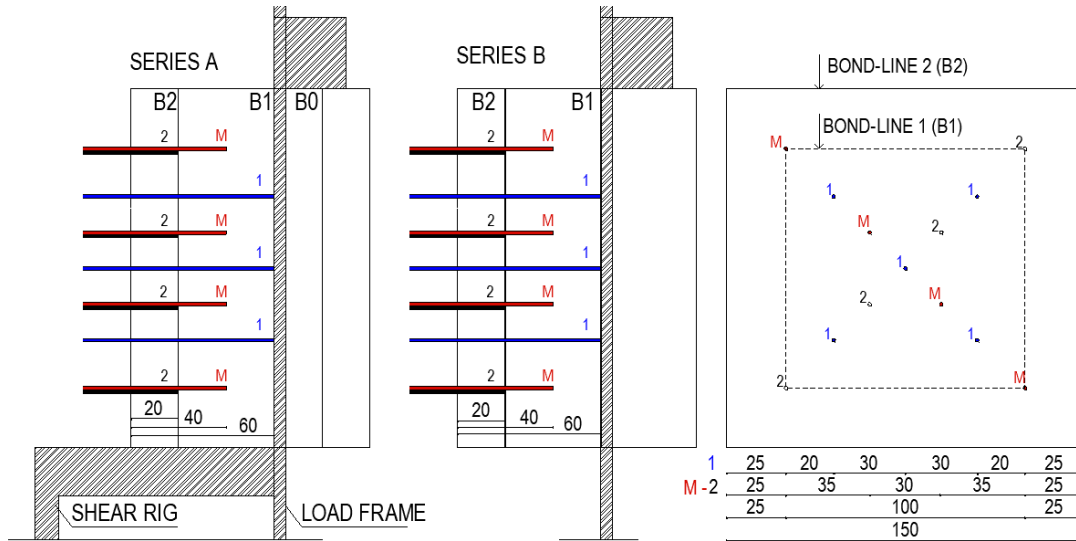


Figure 27. Position of thermocouples installed from the back of the sample (Series A and B). Dimensions are in mm.

Finally, a 2 cm thick vermiculite board was used to reduce the impact of the radiant panel heating on the sample's side surfaces; the weight of the vermiculite board was accounted for when positioning the structural load. Before the start of the test, while igniting and calibrating the radiant panel, another insulating board was placed in front of the sample as a shield to protect the sample from preheating.

As seen in Figure 28, before the test, the radiant panel distance needs to be calibrated with a heat flux gauge. The same distance is then used between the sample and the panel. Radiant panel used was an array of 4 smaller propane-fired radiant panels, positioned centrally in front of the specimen. The apparatus used was the *heat-transfer rate inducing system* H-TRIS, developed in Maluk et al. [157].

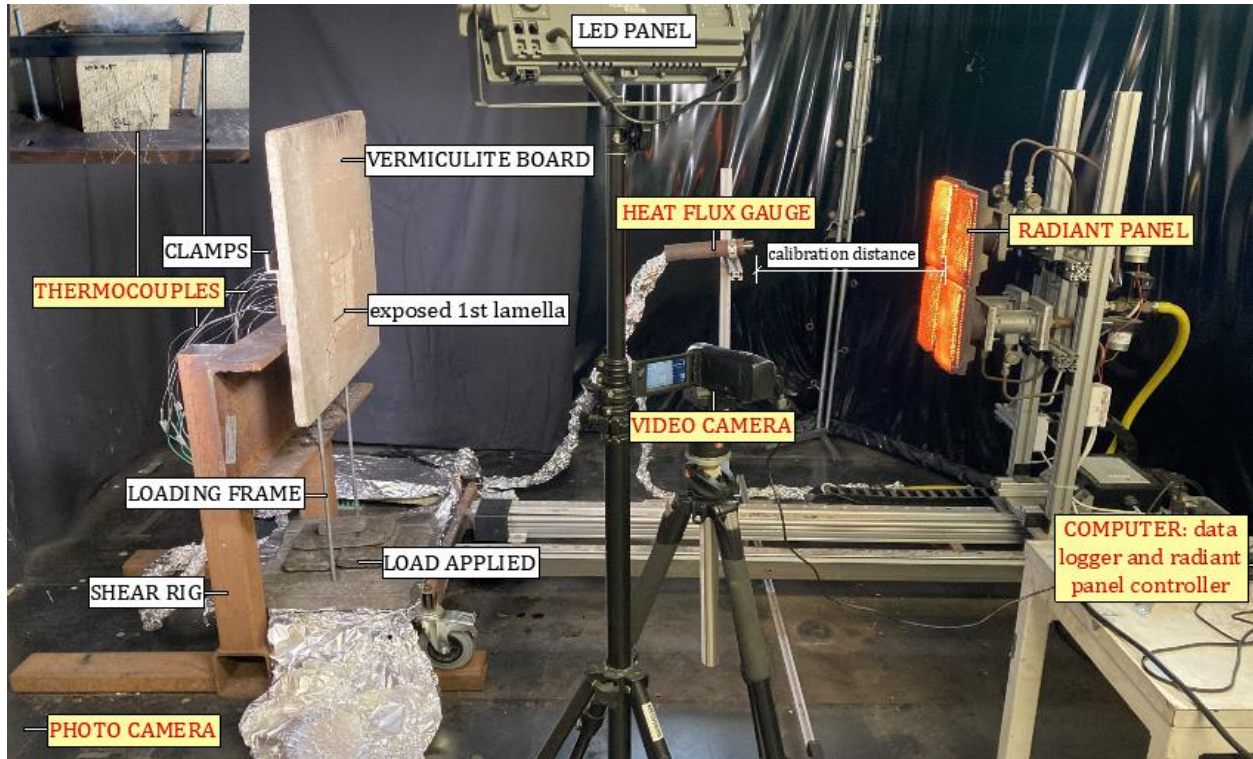


Figure 28. Instrumentation for shear strength test under fire conditions

A Hukseflux Schmidt-Boelter water-cooled heat flux gauge was positioned in front of the panel and connected to the data logger. The gauge is cooled to minimise any radiative losses. It is coated with a black high emissivity paint to maximise the absorbed radiation. For more information, work from Kidd and Nelson [158] describes the thermal response from this transducer.

The mechanical linear motion system was controlled by computer to position the H-TRIS in front of the gauge. Once the vents for the air supply of the radiant panel were on, the propane flow was distributed through the gas supply system to the radiant panel and the torch in front of the panel was used to achieve the ignition of the propane. The intensity of four smaller panels was adjusted to achieve steady and uniform radiation exposure.

Calibration distance is measured when the readings from the data logger were within 1% of the desired stabilised heat flux ( $50 \text{ kW/m}^2$ ). The heat flux gauge is then removed together with the shield in front of the specimen.

Radiant panel is moved towards the specimen and data logger to record temperatures is restarted simultaneously with the video camera. Side photo camera was started at the moment when the radiant panel is in front of the sample.

Video camera positioned in front of the specimen was used to observe the char fall off, time to ignition, time to failure, and failure modes. A Canon DSLR EOS camera was used for a 5 seconds time-lapse photography, positioned at the side of the specimen, used for post-processing to determine the failure modes. The planned image analysis for sample deflections, specified within the framework in Figure 19, is not presented within this study due to the time restrictions.

During the test, one needs to visually observe and monitor possible char fall-off and delamination. Once the sample failed, the radiant panel and vermiculite board were moved to the initial position before testing. For Trial 1, samples were left to cool down. For Trial 2 and 3, samples and fallen char were extinguished with a sprayed water. The fallen char was collected in the aluminium foil, and its and the samples' weight was measured. Photos of the specimen and the char under the light bulb were taken from all sides. Checklist for all testing is presented in Appendix C.

From the measured data, the bond line temperatures, thermal penetration wave, char propagation, failure mode, and influence of the narrow bonding can be directly assessed. This is presented within the next section. However, the methodology has some limitations that need to be addressed and well understood before drawing any conclusions. They are noted within Appendix E



## Chapter 4 Results and discussion

### 4.1 Ambient shear strength tests

The shear strength in ambient conditions was assessed by loading the samples under the hydraulic jack applying compression. From the tests performed, maximal force that sample can hold was obtained and then translated to shear stress in the bond line area 100x100 mm. Stress-displacement curve is presented in Figure 29 for two samples in each Series.

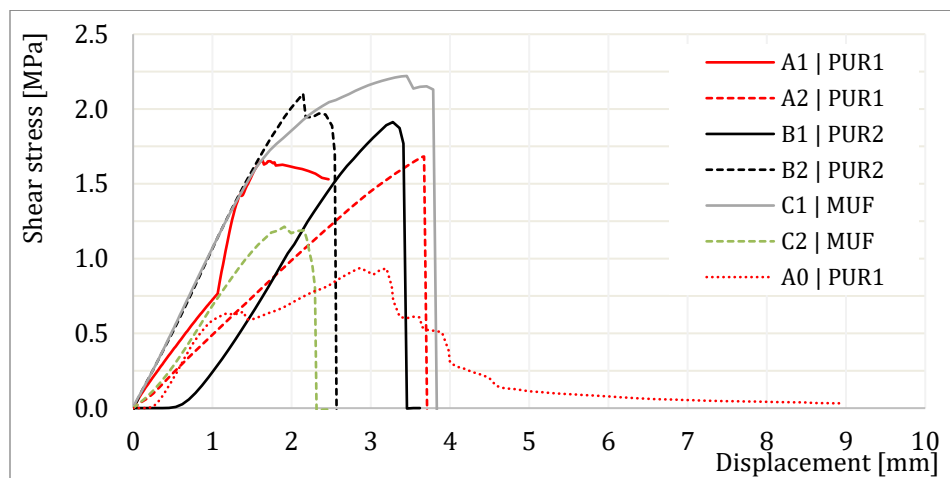


Figure 29. Stress vs. displacement curve for the ambient shear strength tests

By testing only two samples, the statistical power for any reliable conclusion is not achieved. From Figure 29, it is evident that the sample's shear strength varies greatly even at ambient temperature. All samples experienced brittle failure apart from one PUR1 A0 sample. This is because sample A0 was oriented in a way that the horizontal lamella was loaded and exposed to direct rolling shear. Failure was experienced at 0.9 MPa when a plastic behaviour was introduced. Therefore, this sample is not comparable with others.

From the three samples with different adhesive, Series A and B with 1-component polyurethane (PUR1 and PUR2) showed a repeatable result. Strength for PUR1 (A1, A2) was in both cases approximately 1.6 MPa ( $\approx 16$  kN), but the experiment A1 was terminated because the sample experienced a localised failure in the non-loaded area where it was too tightly clamped. PUR2 samples had a shear strength varying from 1.8 to 2 MPa (18 and

21kN). MUF had the greatest variation in behaviour, varying from 1.2 to 2.2 MPa ( $\approx 12$  and 22 kN).

The assumption used for this study is that a sample has no narrow bonding between two lamellae in the same layer (although in this study they mostly do) and that it will fail due to the rolling shear in the orthogonally oriented clamped lamella. For samples loaded out-plane prescribed shear strength in longitudinal layers is  $f_{v,k} = 4$  MPa. The rolling shear strength in orthogonal layers is  $f_{r,k} = 0.7$  MPa [159] (no narrow bond-line), and  $f_{r,k} = 1.25$  MPa (with narrow bond-line) when the width over lamella thickness is greater than 4. None of the tests has shown the shear strength of  $f_{v,k} = 4$  MPa. Since the tested samples in Figure 29 showed the lowest tested strength to be closer to the  $f_{r,k} = 1.25$  MPa (i.e. 1.2 MPa for MUF sample), the reference value taken for this study ( $f_{r,k} = 0.7$  MPa) could be considered to be conservative.

The various failure modes are presented in Figure 30. All samples experienced a mixed adhesive-timber failure but with a high wood failure percentage (WFP). Visually observed WFP is emphasised for samples in Series B, with PUR2 adhesive. The last, C2 sample, also experienced partial adhesive failure, which is concluded from the visible glue traces and correlates to the lowest shear strength presented in Figure 29.



Figure 30. Failure modes for ambient tests. From left to right: High wood failure percentage A2, B1, B2, C1; Partial adhesive cohesion failure C2.

The wood failure percentage (WFP) in ambient temperatures found in this study differs from the finding by Clauß et al [22], [51], who had 100% WFP for MUF and 40-90% for different 1-C-PUR adhesives. Observations are in agreement with Zelinka et al.[127] who for one of his 1-C-PUR adhesives reported 100% WFP in ambient temperatures.



## 4.2 Shear strength tests in fire conditions

Timber is sensitive to environmental changes. Before testing in fire conditions, the moisture content (MC) was assessed for 14 samples. It was then extrapolated on the other 16, which were stored in the same conditions and showed similar results when the digital moisture meter was used. Results are presented in Appendix D. Moisture content varied from 9.1 to 10.5 %. It is representative of Serviceability class 1 for softwood (<12%), used indoors according to European jurisdiction [3]. Also, as explained within the Literature review it is not too high to have a prevalent influence on the charring rate or strength decrease in the wood, meaning that those specific components could be correlated to the boundary conditions in compartment fire for i.e. residential building.

The following sections provide an analysis of the thermal behaviour experienced by samples with different moisture content under the same heat exposure. The failure modes are briefly described, followed by the temperature analysis of the first bond-line to assess whether a temperature-based criterion correlates with failure times. Ultimately, failure modes and their recurrence throughout the 30 experiments is discussed. Main findings are presented in regard to adhesive type, structural load applied, moisture content, and impact of the narrow bond line.

### 4.2.1 Thermal behaviour of the tested samples

As designed, exposing the samples to 50 kW/m<sup>2</sup> always resulted in a relatively fast auto-ignition. Once the char layer started to form, the flames became smaller and then steady-state burning (flaming) was established for all samples. Figure 31-Figure 33 present the development of temperatures in time. Five thermocouples were positioned in the 1<sup>st</sup> bond-line and the curve presents the average temperature that was developed. It stops at the point of failure. Shaded areas serve as an indication of the maximal and minimal temperature read in the bond-line.

Temperature readings from five data points in three different planes were used to develop a trend line for thermal penetration presented in Figure 34. Although the power function used had a high R<sup>2</sup> value, it is not considered to be a good approximation because of the low

number of in-depth readings made (three), which is not enough to predict an accurate thermal gradient. This function only serves for comparison among samples. In this study, only the thermal gradient in the bond line proximity will be discussed. These temperatures may be affected by a conduction error from thermocouples and are actually expected to be larger.

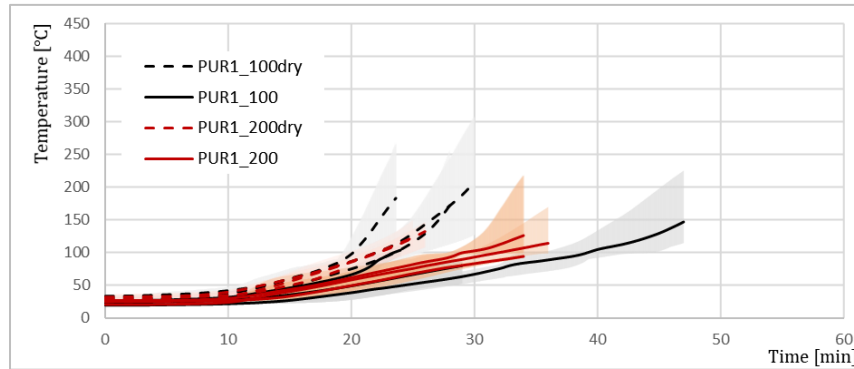


Figure 31. Average thermocouple reading at the first bond-line. Temperature-time curve for all specimens bonded with 1-C-PUR at the bond-line between layers and combination of Hotmelt and PVAc between single lamellae (narrow bonding)

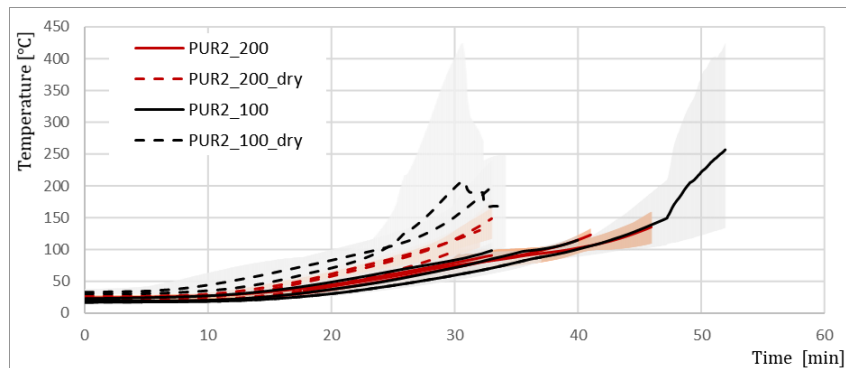


Figure 32. Average thermocouple reading at the first bond-line. Temperature-time curve for all specimens bonded with 1-C-PUR at the bond-line between layers and between single lamellae (narrow bonding)

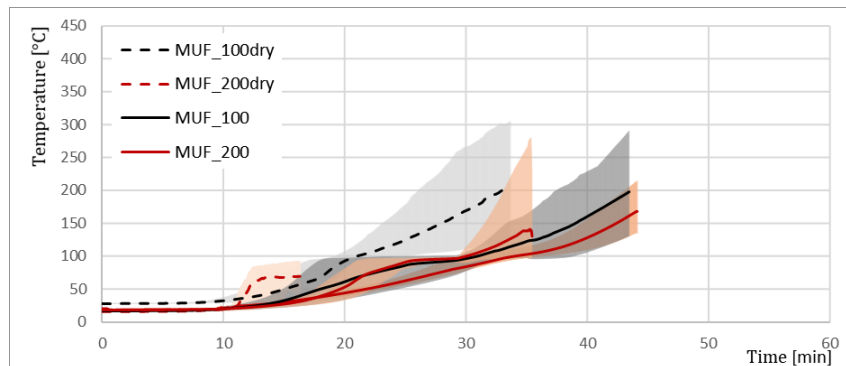


Figure 33. Average thermocouple reading at the first bond-line. Temperature-time curve for all specimens bonded with MUF at the bond-line between layers and between single lamellae (narrow bonding)

Moisture content | When compared, dried samples independent from the adhesive, had a faster developed thermal penetration than non-dried. This is due to the moisture evaporation and heat absorption represented by a developed plateau at 100°C.

Adhesive type | For all three samples, in-depth temperatures and temperature growth in time is very similar up to 30 min, independent from the adhesive. This is presented for Series A in Figure 34. Formaldehydes tend to develop moisture plateau from 25 to 35 minute and they tend to fail after passing through the plateau. For polyurethanes this phenomenon starts after 30 minutes but most of the time they fail during the evaporation, with one exception for lower load in each series, A and B. The origin for this could come from moisture movement and evaporation which degrades adhesive and timber properties.

Load and failure mode | When exposed to a lower structural load, some polyurethane samples experience the failure slightly later, but there is no clear trend. It is also noted that the lower structural load gives bigger temperature variations after passing the moisture evaporation plateau, for all three adhesive types. However, lower load could not be correlated to the specific failure mode. For higher load, uniform distribution in the bond-line is present in both, non-dried and dried samples, throughout the whole duration of the experiments. Failure modes observed were delamination and local failure.

Thermal penetration will not be widely discussed, due to the lack of data points and because the thermal profile is not expected to be affected by the structural load for the chosen experimental set-up. However, the application of higher load (200 kg) gives more uniform and repeatable profiles (indicated in Figure 34), as a result from similar failure temperatures and more similar failure modes for this group.

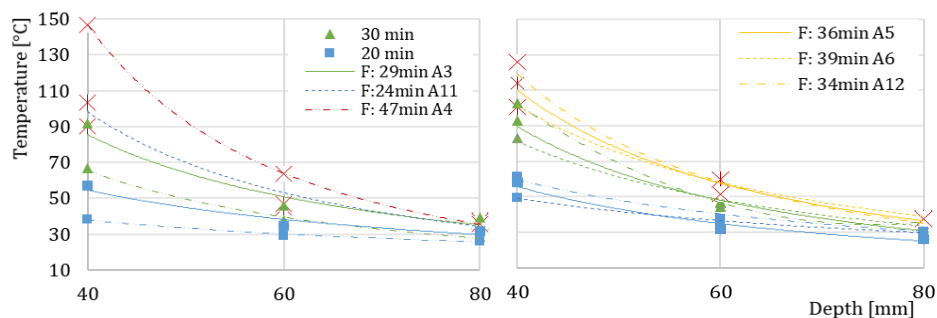


Figure 34. Samples loaded with 100kg (left) and 200 kg (right). Comparison of thermal profiles for PUR1 adhesive at 20min (blue), 30 min (green) and at the point of failure (F).

#### 4.2.2 Type of failure modes identified

Observed failure modes were delamination, local failure, mechanical failure, and char fall-off. Local failure at the top of the sample in Figure 35(1-2) is the unwanted outcome of the methodology applied for this study. Once the lamella is delaminated, preheated wood is exposed which allows for the sudden increase in the release of pyrolysis gases and reignition and flaming combustion. Delamination in Figure 35 (3-4) is further differentiated between the failure in the adhesive, bonding interface, and timber (in the vicinity of the bond-line). Char fall-off was observed *at* the adhesive line, as in Figure 35(5), or *after* reaching the adhesive line as in Figure 35(6). Char fall-off *before* reaching the adhesive line was indicated only once. When the char propagates fully to the unloaded part of the failure is named mechanical because char has no load-bearing properties.

Figure 2 in the Introduction offers a better understanding of char fall-off and delamination phenomena represented within this section.

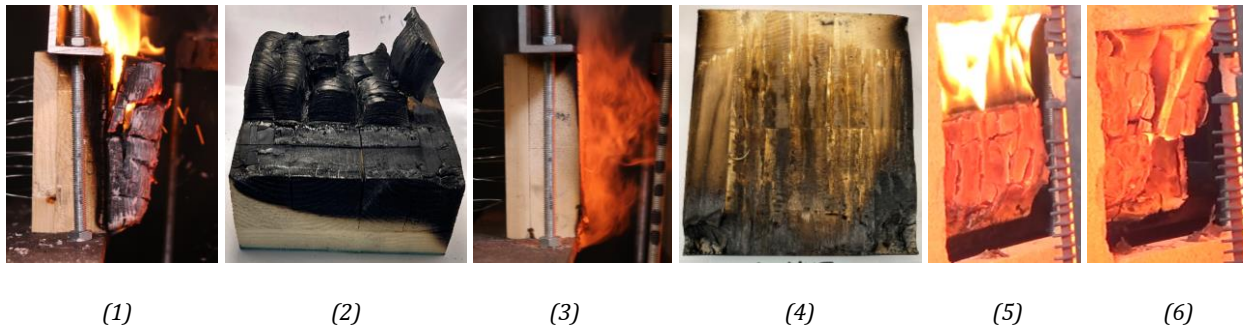


Figure 35. Failure modes: 1-2 Local failure, 3-4 Delamination, 5 Char fall off at the adhesive line, 6 Char fall off after the adhesive line

Sometimes, it is hard to distinguish between the char fall-off at the adhesive line and the delamination as both are followed by a rapid reignition and flaming combustion caused by the exposure of the new fuel. Assessment is then done by observing the fallen char residues for any preheated but not pyrolyzed wood left on the residue, which would be the case for delamination. For the local failure, the upper part of the lamella is bent toward the radiant panel. Mechanical failure appears when the lamella is completely charred.

### Origin of local failure:

For samples later specified in Table 10 two types of failure are observed; local wood failure at the top of the lamella (marked with a red circle), and shear failure through the charred lamella. The latter is a *char fall-off within the char layer*. Both are unwanted phenomena of less importance for this study. It is an outcome of the implemented Methodology and not an indicator of lamella behaviour when exposed to shear stresses in fire. All samples that experienced this type of failure are presented in Appendix D.

Since all sides of the sample were cut in-depth for 2.5 cm, the top of lamella is exposed to the concentrated stresses without bond-line to support the interaction of that lamella with the rest of the composite. That means that the top, not-bonded, part of the lamella has to carry the load by itself which is only possible if the load is perfectly positioned near the bond-line and there is no eccentricity. In that case, all the load would immediately be transferred to the bond-line.

The rig geometry indicates that a vermiculite board was eccentrically placed in front of the sample. That could be the first origin of momentum which causes the bending at the top. Secondly, the sample was positioned in the rig manually by using the spanner to achieve sufficient clamping, which was prone to human mistake depending on the force applied. Hence, this occasionally caused the leaning of the complete specimen toward the radiant panel, advancing the influence of the momentum on the final failure as explained with Figure 36 and visible in Table 10 .

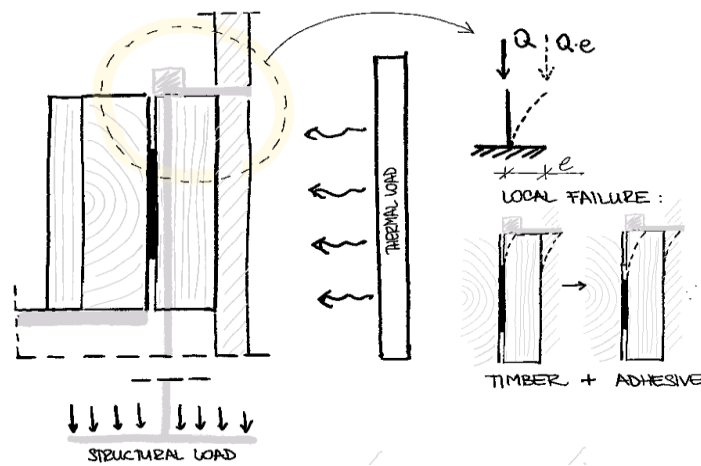


Figure 36. Local failure caused by eccentricity of load and eventual charring

Thirdly, but most detrimentally, once the lamella auto-ignites and the char starts to form, heating of the element causes a reduction in the stiffness of the wood causing the neutral axis to shift toward the unheated cool side. The bigger the char formation, higher the eccentricity. Once the top of the non-bonded lamella cannot transfer that load, it slowly starts to bend towards the radiant panel. If the bond-line preserves the composite action, lamella does not affect the adhesive (indicated as timber in Figure 36), and the shear plane is then formed in the part of the charred lamella (B6, B11, C3). One can imagine the top of the lamella as a cantilever column, where the bond-line is support.

However, since that support is not perfectly rigid because the adhesive weakens at higher temperatures, in some cases, bending lamella opens the crack at the top of the bond-line. This allows the further degradation of the adhesive (A12 in Figure 37) and it introduces peeling between two lamellae (B13, C4). Peeling is a result of concentrated tension stresses perpendicular to the grain, manifested in form of little splinters (C4 in Figure 37).

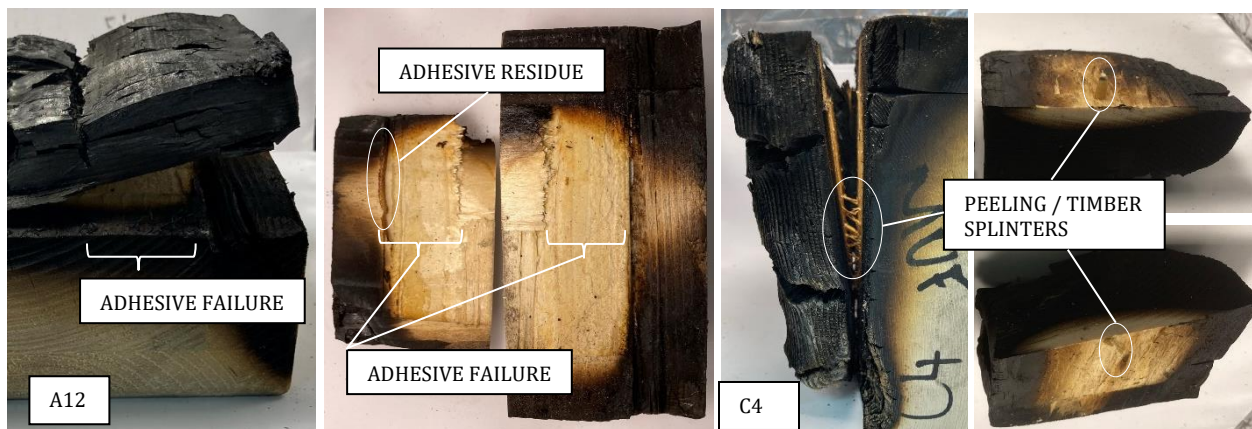


Figure 37. Adhesive degradation (A12) and peeling forces (C4) caused by local failure at the top

### 4.2.3 Failure time and temperature at the first bond line

Failure times for all experimental configurations are presented in Figure 38.

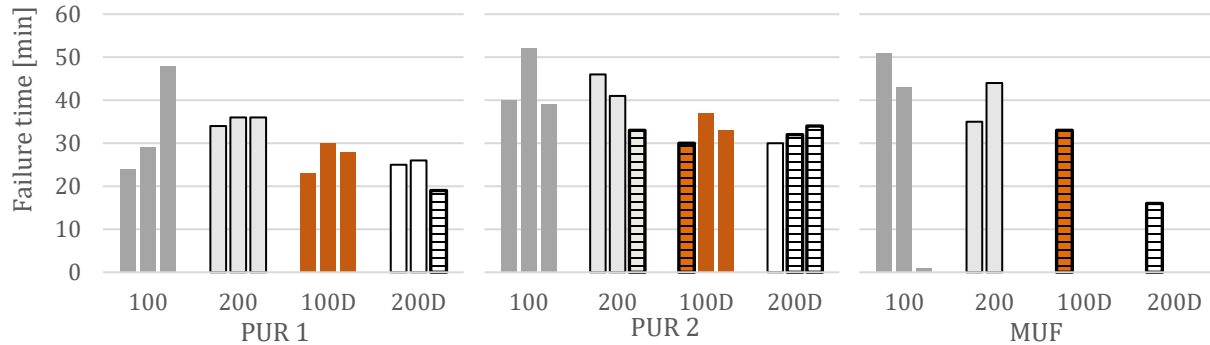


Figure 38. Failure time for three groups of adhesive and different setup

Samples with a bold outline and stripes indicate delamination.

**Adhesive type** | Average failure time is for samples with PUR1 adhesive the lowest  $\approx 30$  min. Samples with PUR 2 and MUF behave similar and experience the failure later, from approximately 30 to 40 minutes. This could be due to the geometry, and the failure mode which is for PUR1 mostly char fall off, influenced by the smaller thickness of lamellae.

**Load** | There is no trend observable when it comes to load. For non-dried PUR1 samples lower loads induced a slightly earlier failure, while in PUR2 and MUF both non-dried and dried samples have the similar average time of failure.

**Moisture content** | For all three adhesives, dried samples had the similar time to failure, from 25 to 33 min (with one exception for MUF sample which has failed after 16 min). Non-dried samples experience a delay in failure, being from 35 to 45 min (with one exception for PUR2 at 52 min).

#### Temperature:

Figure 39 presents the difference in the median 1<sup>st</sup> bond line at the point of failure between three adhesives for all tested configurations. Median is used to reduce the influence of outliers. The error bars indicate maximal and minimal temperature developed, while the orange shading represents the range of temperatures associated with timber pyrolysis.

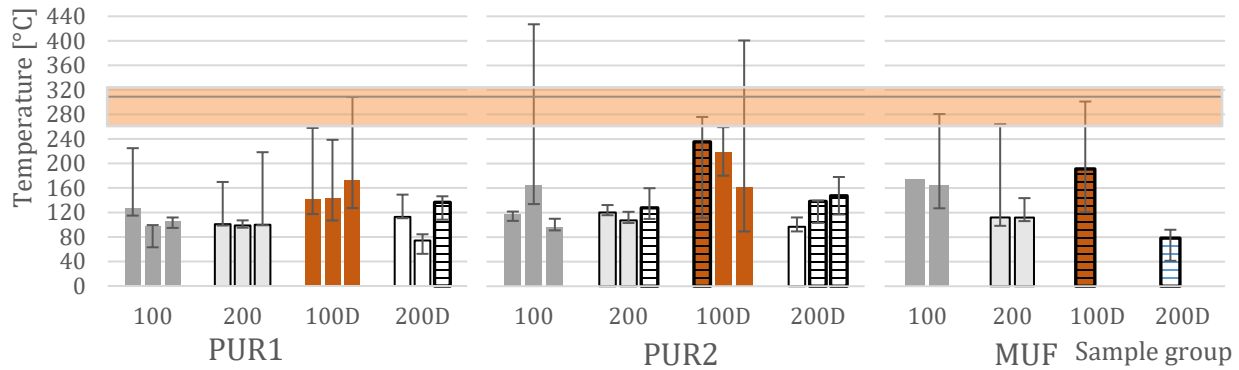


Figure 39. Median failure temperatures in the first bond-line for three groups of an adhesive and different setup. The orange area represents range of temperatures for timber pyrolysis. Samples in bold indicate delamination.

General observation | The highest median failure temperature is still under the generally adopted pyrolysis isotherm of 300°C. This confirms that the components (timber and adhesive) of the timber composites do not behave as one with the same mechanical properties in fire conditions as they do in ambient conditions.

For some samples, the error bars are large. This could be due to several factors: (1) non-uniform char penetration, (2) non-uniform failure mode and/or char fall-off before the failure, (3) increased oxidation and flaming of the sample at the sides, (4) positioning of the thermocouples (TC) which is not in the same plane due to manual drilling, where deeper placed TCs measured higher temperatures.

Adhesive type | The high variability in failure temperatures is reduced by observing the median value. The mean failure temperature was also driven by the failure mode, ranging for PUR1 from 96°C to 172°C, for PUR2 from 96°C to 235°C, and for MUF from 78°C to 191°C. This shows the importance of the chemical composition even within one adhesive family.

Samples with a bold outline in Figure 39 indicate delamination, where the mean failure temperature is 136°C (PUR1), from 127°C to 235°C (PUR2), and from 78°C to 191°C (MUF). Results are compared to data from Clauß et al. [22], Frangi et al. [45], Liu et al. [88] and Zelinka et al. [127] (shown in Figure 13 and 14 in the Literature review). In their lap shear tests for samples firstly heated at uniform elevated temperatures and then loaded, shear strength of MUF adhesive was 70% at 100°C and 40% at 200 °C. For polyurethanes, it ranged from 50 to 90% at 130°C. (Indicated strength values are a ratio of the solid wood shear



strength at ambient temperatures.) For both adhesive groups, shear strengths drop to 20-30% only after 220°C, which suggests that the failure temperatures observed in this study are not in a good correlation with the loss of shear strength by other authors. This the discussion presented within the methodology drivers and emphasise the importance of the simultaneous application of both structural and thermal load. Indicated lower temperatures in this study could be a result from transient heating that causes temperature creep, moisture movement, and differential shrinkage self-stressing due to the thermal gradients. Frangi et al. [102] discussed that oven tests at elevated temperature tend to give higher strength values in comparison to fire tests influenced by loading rate and change in wood moisture.

Load | With no distinction in moisture content, for samples loaded at a lower load (100 kg), MUF shows the highest median failure temperatures (164-191°C) and repeatable results. Polyurethanes show higher variation in behaviour (PUR1: 95-170°C, PUR2:96-235°C). However, for specific groups (e.g. non-dried lower load), median temperatures are more similar but error bars are still large.

Samples exposed to the higher load (200 kg) tend to give more uniform temperature distribution over the first bond-line at the point of failure but also more repeatable results. This can be due to the nature of the failure, which is for 200kg mostly delamination or local failure where the complete bond-line experiences the same condition at once (delamination) or it remains intact (local failure).

Failure mode | Delamination was observed after 30 minutes (shown in Figure 38), from 127 to 236°C (with one exception of 78°C) but mostly for dried samples. This finding covers the range studied by other researchers who performed small scale experiments under steady-state uniform heating and observed delamination under 100-150°C [21,22,47,114,129]. However, using 130°C as a design temperature might be over-conservative when compared to critical bond-line temperatures as 200°C in the large scale tests [30], [128].

Moisture content | For all three adhesives exposed to lower load (100 kg), dry samples tend to give the same or higher median failure temperatures than non-dried samples but lower

failure time. Lower MC provides opportunity for faster heat penetration so the ‘failure temperature’ is reached in shorter time. But without moisture movement, one assumes that both the timber and the adhesive can retain more of their strength.

Table 7 and Figure 40 present six different samples (two from each series) and their thermal penetration profile at the similar time of failure with maximum, minimum and average temperatures. All are loaded under lower load, with different moisture content (dried and non-dried). The photos are taken from the side where the char penetration was more rapid than it is in the middle of the sample and indicated temperatures are not directly behind that char layer because they would be higher. They only serve as a visual representation of the sample before the failure.

Table 7. Thermal penetration for non-dried and dried samples 5s before the failure

S	A: PUR1 [A3, A7]		B: PUR2 [B6, B7]		C: MUF [C5, C7]	
MC	10.1%	0% [dry]	9.4%	0% [dry]	9.2%	0% [dry]
F	33 min	37 min	29 min	28 min	43 min	33 min
M	Char fall-off		Local failure	Delamination	Local failure	Delamination

S – series; MC – moisture content; F – failure time; T-failure mode

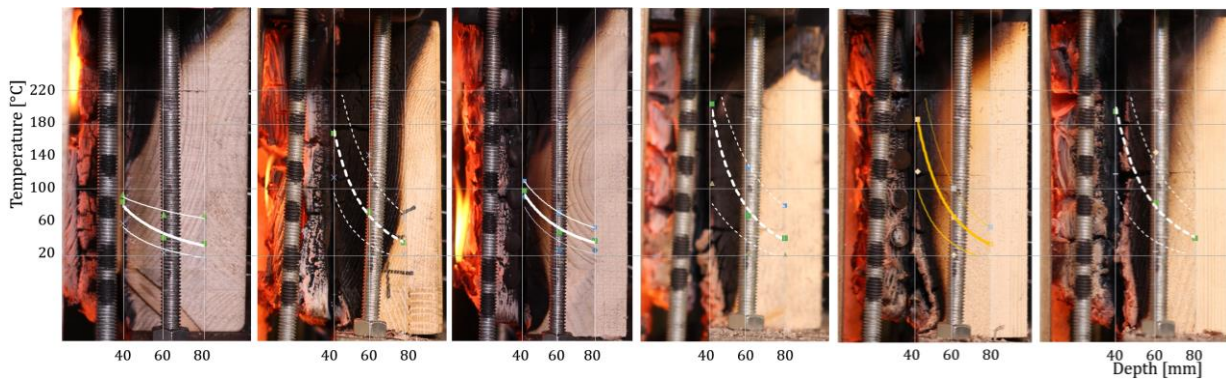


Figure 40. Thermal penetration for non-dried and dried samples 5s before the failure for A3, A7, B6, B7, C5 and C7

When compared, dried samples had a visible higher gradient between the first glue line and the middle lamella. At the time of failure ( $\approx 30$  min), the average temperature at the first bond line for dried samples went above  $180^{\circ}\text{C}$  for all three samples with different adhesives (Figure 40: A7, B7, C7 - dashed). For non-dried samples, they were around  $100^{\circ}\text{C}$  for two samples with PUR1 and PUR2 and again above  $180^{\circ}\text{C}$  for one melamine formaldehyde. With high temperatures in dry samples the bigger range from min. to max. temperature is also present. From this, one could argue that it is not only the temperature and temperatures

gradient that drives the failure of the bond line. Otherwise, it would be the same for both dried and non-dried samples as they are for MUF (but with the faster failure of the dried samples).

Also, although the dried sample with MUF presented in Figure 40 has failed only after 180°C and 33 min, another dried sample with MUF has failed already at 78°C after 16 min. One would expect lower temperatures in dried samples, because the adhesive was affected during drying. However, it seems like the lower temperatures experienced in non-dried samples result from the traveling moisture and water evaporation which weakens the adhesive and timber. To prove such hypothesis, and to use temperature as an adhesive failure parameter, more samples with improved methodology should be tested.

#### **4.2.4 Factors relevant to failure modes**

This section will briefly focus on the difference between failure modes based on the adhesive type and load applied. Moisture content is for now integrated in the latter two but it will be separately discussed in the next section, where Table 12 is introduced to present the reoccurrence of each failure mode and to deduct main driving parameters and findings.

In Table 9-Table 11, some of the samples are presented with their respective failure modes, but photographs of all failure modes are listed in Appendix D. Red numbers indicate the time of failure for sample “S” under the load “L”. Figures in Stage 2 are used to distinguish the failure mode. Figures in Stage 3 are taken after cooling. From the front and the side view, one can visually assess WFP and/or the presence of local failure. By looking at the sample sliced through the middle, the depth of the char propagation and the bond-line analysis after failure can be made. If samples were tested in the first trial, they were not extinguished (marked with “\*”) and their photos in Stage 3 are taken after experienced smouldering, further char regression, and potentially char fall-off. Hence, the WFP cannot be assessed, but one can observe if the adhesive manages to hold the char and achieve auto-extinction.

#### **Impact of the amount of structural load applied**










Local failure | The amount of load did not have a significant impact on the onset of local failure for non-dried samples where almost an equal number of samples failed under lower


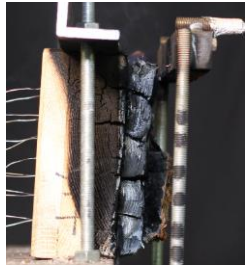


as for higher load. Dried samples failed more often under the higher load which was possibly supported by the higher eccentricity due to a faster charring rate than it was for non-dried samples.

Delamination | It was repeatable for the higher load. Series B (PUR2) and C (MUF) are mostly representatives of this failure mode. There was only one case where the non-dried sample has experienced delamination and that was when the higher load was applied. When compared to the other types of failure, most of the dried samples have experienced this type of failure (as presented in summary in Table 12).

A mechanical failure with no char fall-off was not dependent on the load applied. For sample A5 and A7 failure originated from the shear within the 2<sup>nd</sup> charred lamella with no reignition. Sample A4 experienced mechanical failure but at the 2<sup>nd</sup> bond-line with reignition as presented in Table 8 .



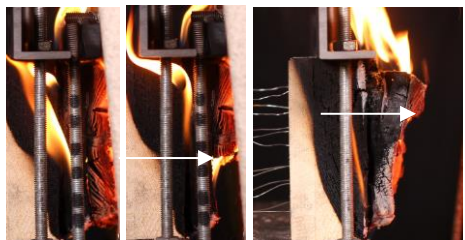
Table 8. Visual observation of samples before/after mechanical failure (MF), and after cooling.



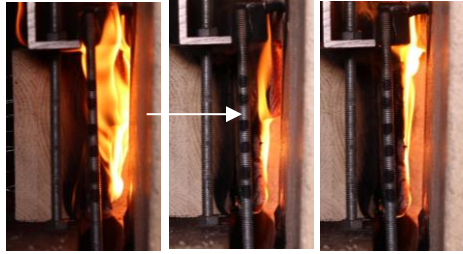
L	S	Stage 2: Testing		Stage 3: Post-processing	
100 [MC>0%]	A4* 48:04				 (Residual char fell during cutting)
		MF: Failure appears when the left lamella in the 2 <sup>nd</sup> layer completely chars and falls off at <b>2<sup>nd</sup> the adhesive line</b> , indicated by reignition.			
200 [MC>0%]	A5* 36:50				 A5 
		MF: Failure appears <b>after char reaching the 1<sup>st</sup> adhesive line</b> . Flaming combustion present in second photo is from the local failure at the top and side failure where sample has an in-depth cut in the bond-line. There was no reignition present in the bonded area.			

100D [MC=0%]	A7 28:32				
	MF: Failure appears <b>after char reaching the 1<sup>st</sup> adhesive line</b> , reignition not present. Specimen was left to smoulder which lead to regression, falling of the residual char after the failure as indicated in the photos in Stage 3, and eventual self-extinction.				

Char fall-off | The load has no impact on the appearance of char fall-off and it seems to appear arbitrary at and after the adhesive line as presented in Table 9. To define if the char fall off is more driven by the thermal than structural load, one could test the same configuration where the main variable would be the heat flux. In this case, load only defines the failure time after the char fall-off has appeared, but this is then the time of mechanical failure because char has no load bearing properties.

Table 9. Visual observation of samples before and at char fall-off (CF)






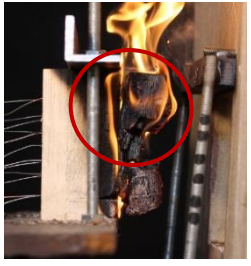


L	S	Stage 2: Testing	Stage 3: Post-processing
100D [MC=0%]	A13 25:30 26:00		
	30:53		CF: Firstly, first charred lamella falls off in parts <b>after char reaching the 1<sup>st</sup> adhesive line</b> , there is no flaming and the parts just drop. Second lamella then experiences <b>buckling</b> , failure appears partially locally at the top, after significant char regression of the second lamella.

100D [MC=0%]	<b>A10</b>		
	15:30 19:10 <b>23:40</b>		CF: Firstly, charred lower part of the 1 <sup>st</sup> lamella falls <b>at the 1<sup>st</sup> adhesive line</b> experiencing <b>buckling</b> failure and flaming combustion. Secondly, upper char falls off <b>after char reaching the 1<sup>st</sup> adhesive line</b> with no bigger reignition. Failure is local at the top due to significant char regression of the complete second lamella.

### Adhesive type

Local failure | Independent from the drying conditions, samples with PUR2 and MUF adhesive were more prone to this type of failure than the ones with PUR1. Some of the failures are presented in Table 10. Non-dried PUR2 samples failed slightly before (33 to 40 min) compared to MUF (35 to 50 min). The difference could be governed by the presence of narrow bond-line, but also by the other factors as wood's mechanical properties, its initial density and moisture content. For samples with PUR1 adhesive, this type of failure was always combined with the partial char fall-off.

Table 10. Visual observation of samples before wood failure, at the moment of wood failure, and after cooling.

L	S	Stage 2: Testing		Stage 3: Post-processing	
100 [MC>0%]	B10 34:50				
	C3* 51:17				

Delamination | When PUR2 and MUF are compared (because they have the same geometry and different adhesive), all dried MUF samples have experienced delamination, while 3 out of 6 dried PUR2 samples experienced it. Two scenarios are presented in Table 11.

Table 11. Visual observation of samples before or/and at delamination, and after cooling.

100D [MC: 0 %]	C7* 33:43				
200D [MC: 0 %]	B9 33:40				

In all the cases, the failure was brittle and sudden, which does not correlate to the plastic and ductile ambient behaviour of polyurethanes. Samples with MUF adhesive have a

combination of adhesive residual and splinters at the bonding interface of the second lamella, indicating a failure at adhesive-timber interface (AT) in Figure 41. Same was observed for B12 sample with PUR2 adhesive where the effect of the rolling shear is assumed to be present because some of the perpendicularly oriented grains from second lamella are “sticked” to the adhesive of the delaminated lamella.



Figure 41. Delamination: Adhesive-timber failure: bond-line interface with timber residues from the second lamella. From left to right: PUR2 B12; MUF C7, C8.

Conversely, PUR1 and PUR2 have experienced failure in timber (T) in the vicinity of the bond-line. More data about the similar failure modes is presented within Appendix D. In Figure 42 one can notice a failure parallel to the grain, where a pure shear failure is characterised by the sliding of the fibres in the same direction as explained by Franke et al. [160].



Figure 42. Delamination: Timber failure: sliding of fibres in the first lamella. From left to right: B9, B14, A14



Sometimes, the different type of delamination and charring rate was observed for two lamellae next to each other as visible for sample B9 (PUR2) in Figure 37. The same figure shows that the charred front has never reached the adhesive line, which was another indicator of delamination.

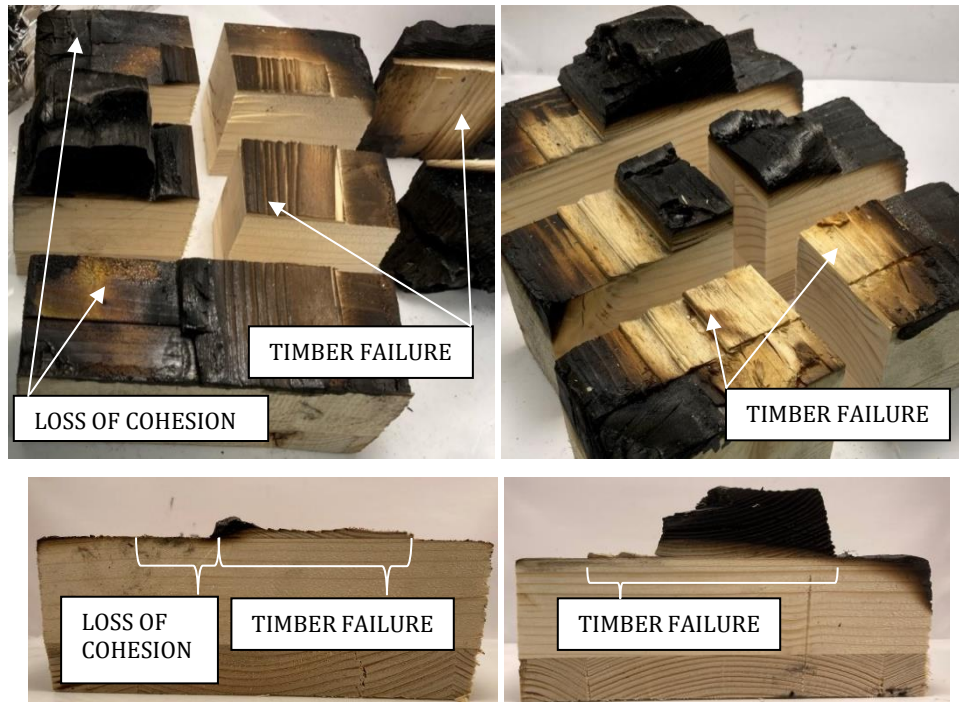


Figure 43. Failure variation within one sample. From left to right: B9, B14

Char fall-off | It was observed for eight samples, seven for Series A (PUR1) with 2x2cm lamellae and one for Series B (PUR2) 1x4cm lamella. Once the first lamella was lost, it was common that the second one experiences mechanical failure within the char layer. For PUR1 with two lamellae, char fall-off appears interchangeably at and after the 1<sup>st</sup> adhesive line. There is no trend for the specific load, which makes it hard to indicate whether the PUR1 is capable, for a specific time, to retain bondability between lamellae and allow for the char to propagate in the second lamella. Nevertheless, when it happens at the adhesive line, a failure of the first charred lamella is in big pieces that resemble the geometry of the whole lamella, with a smooth surface, which indicates the adhesive degradation influenced by the specific thermal load, rather than a loss of cohesion within the charred timber itself.

For the samples with the same geometry, only one PUR2 has experienced the char fall-off once, but MUF samples also did not have the narrow bond-line, which is indicated as a weak point for char fall-off. Figure 44 shows the charred, but still, load-bearing lamella, held by PUR2 and MUF adhesive.

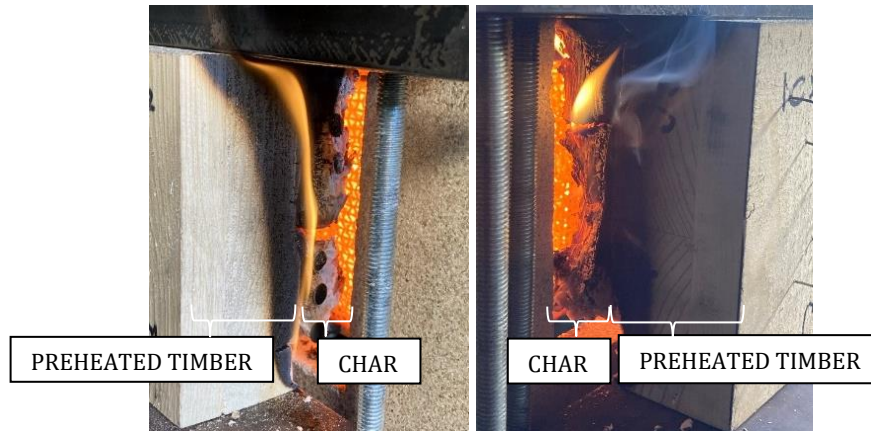


Figure 44. MUF (left) and PUR2 (right) main bond-line holding the charred lamella despite the developed cracks

#### 4.2.4.1 Discussion

Reoccurrence of different failures was assessed independently for dried (MC: 0%) and non-dried (MC: 9-10%) samples and presented in Table 12. Independently means that the ratio of reoccurrence was observed for non-dried samples separately from dried.

Table 12. Change in failure modes based on the adhesive type, the structural load applied and moisture content.

<b>Variable</b>			<b>DELAMINATION</b>		<b>CHAR FALL-OFF</b>		<b>LOCAL FAILURE</b>		<b>MECHANICAL</b>	
<b>MC</b>			<b>9-10%</b>	<b>0%</b>	<b>9-10%</b>	<b>0%</b>	<b>9-10%</b>	<b>0%</b>	<b>9-10%</b>	<b>0%</b>
<b>Failure type</b>										
			6%	43%	31%	14%	50%	21.5%	13%	21.5%
<b>Tested nr.</b>			<b>Adhesive type</b>							
<b>PUR1</b>	<b>6</b>	<b>6</b>	0%	17%	67%	33%	0%	0%	33%	50%
			0	1	4	2	0	0	2	3
<b>PUR2</b>	<b>6</b>	<b>6</b>	1%	50%	17%	0%	67%	50%	0%	0%
			1	3	1	0	4	3	0	0
<b>MUF</b>	<b>4</b>	<b>2</b>	0%	100%	0%	0%	100%	0%	0%	0%
			0	2	0	0	4	0	0	0
<b>Structural load</b>										
<b>100 kg</b>			0	2	3	2	5	1	1	1
<b>200kg</b>			1	4	1	1	4	1	1	1

### Failure type

The most common failure mode was a local failure, with 50% for the non-dried samples and 21.5% for dried samples when compared to other failure modes. It is the result of the implemented Methodology, and limitations and possible improvements will be addressed in Appendix E. **Error! Reference source not found.** Dry timber might have a higher strength than non-dried timber but it is assumed that this failure mode is highly random and might be affected by local defects of the timber.

Char fall-off was the next most common failure mode which was highly dependent on the lamella thickness. Char is not able to carry the load because it has negligible strength and stiffness, its behaviour was always unpredictable, and failure was non-uniform throughout all of the experiments. Therefore, the estimation used in standards that char has no strength, is considered as valid.

However, the indicated cases of delamination prove the importance of thermal penetration in front of the char layer front, as well as the influence of elevated temperatures on the adhesive line, and therefore the composite action and structural capacity.

Mechanical failure appears when the lamella has completely charred and it represents a successful application of the methodology and composite behaviour. However, method is considered not to be suitable for char fall-off evaluation. When two lamellae are exposed and loaded in shear for PUR1, rather than only one thick lamella, one can observe load redistribution. When the first lamella starts to char, the stresses tend to redistribute to the cooler side. Since there is still some “only” preheated timber left to bear the load, it can be observed if the char will surpass the adhesive line before falling. For two other adhesives, PUR2 and MUF, and one loaded 4cm thick lamella, a char fall-off caused by the adhesive degradation cannot be accessed. The ultimate failure will always be mechanical and appear before the char penetrates the bond-line because once the complete lamella chars, it cannot carry the load and there is no material (section) where load can be redistributed.

### Adhesive type and geometry

Adhesives were assessed individually, based on the ratio of the failure mode they experience the most for the group of non-dried, and then dried samples.

The main failure mode for the PUR1 adhesive was char fall-off and mechanical failure. Char fall-off occurred seemingly arbitrarily, sometimes at and sometimes after the adhesive line. For a successful design of the CLT composite in fire, it would be best to have the char fall-off, if present, appearing after the char reaching the adhesive line and for some char to remain below the fallen char. In this way, one can avoid reignition, the charring rate will not be increased, and in-depth temperatures will drop sufficiently to design for self-extinction. However, with no trend it was hard to indicate whether the PUR1 is capable, for a specific time, to retain sufficient bond strength between lamellae and allow for the char to propagate in the second lamella. It was not experienced for PUR2 and MUF, but this was attributed to the sample geometry. Failure for the samples with thicker 4 cm lamellae is driven by different mechanics – such as local failure and delamination.

MUF experienced delamination at the adhesive-timber interface and due to the loss of adhesion, while PUR1 and PUR2 in timber in the vicinity of the bond-line. WFP for polyurethanes was high, which is contradictory to the study by Clauß et al. [51] who observed that the gross penetration of 1-C-PUR possibly contributes to delaying wood failure by reinforcing the wood, while intracellular MUF adhesive penetration can change the wood properties and promote wood failure.

### Structural load

One cannot define load as a driving parameter for the specific type of failure. Char fall-off, local and mechanical failure do not seem to depend on the amount of load applied but the load has influenced the time of failure for char fall-off. However, it was observed that samples tend to delaminate more under higher load, with repetitive failure times and bond-line temperatures which range from approximately 120°C to 150°. Once the methodology is improved, more samples should be tested to make a better estimation and define if this could be a way to assess the critical bond-line temperature.

### Adhesive type and moisture content

The influence of the moisture movement on temperature creep cannot be assessed from these results. However, by comparing the failure time and modes in fire conditions, one can discuss if the long-term exposure to drying prior to exposure makes a difference in the behaviour of timber and adhesive.

PUR1 shows no difference in the behaviour for dried and non-dried samples. Samples PUR2 and MUF had the highest percentage for brittle delamination for dried samples. PUR2 experienced the failure in timber, while MUF showed mixed failure of adhesive and timber. During the curing and cross-linking of the adhesives, polyurethanes require water and formaldehyde heat which can make the latter more sensitive to the water impact. MUF failure could be due to the hydrolysis of formaldehyde-based adhesive as noted by Dunky and Neimz [91]. Since they were dried in the oven for two days at 103°C, this supports the finding that large preheating times might cause risk of failure in the adhesive line before any charring propagates to the bond-line [25,42]. A long-term influence on the adhesive is in agreement with the study from Burchardt *et al.* [50], and Custodio *et al.* [82].

When compared, non-dried samples tend to fail at lower temperatures. Moisture movement with simultaneous application of load might be detrimental for adhesive and timber behaviour. Since not enough samples were tested, further research on the impact of moisture content movement on delamination and char fall off is recommended.

Local failure was observed more for the non-dried samples (9) than for the dry ones (4). Non-dried PUR2 samples failed slightly before (33 to 40 min) compared to MUF (35 to 50 min).

### Influence of the narrow bonding

Narrow bonding was proved to be a significant variable for all types of failures, independent from the type of adhesive. PUR2, and MUF narrow bond-lines tended to lose the cohesion at the very beginning, where the crack allowed for a deeper flame penetration as shown in

Figure 45 Sometimes, the different type of delamination and charring rate was observed for two lamellae next to each other as visible for sample B9 (PUR2) in Figure 37.

However, for the samples in Series A where for narrow bonding the combination of Hotmelt formaldehyde-free and PVAc adhesive was used, and the surface was not sanded, the crack tended to appear in a different position. For this series and all samples with a horizontally oriented front lamella, the crack would initially happen when there was a cathedral grain or a bull's eye pattern, typical for a flatsawn board (indicated as a dashed blue line in Figure 46).

For the one additional test (A9), when the sample had the front lamella vertically oriented, the crack has not appeared at the point of the bull's eye pattern. Although one might discuss that the wood pattern and lamella orientation might not be directly connected to the objective of this study, it is still important to mention it because any type of direct flame penetration leads to faster degradation of adhesive behind that specific lamella.

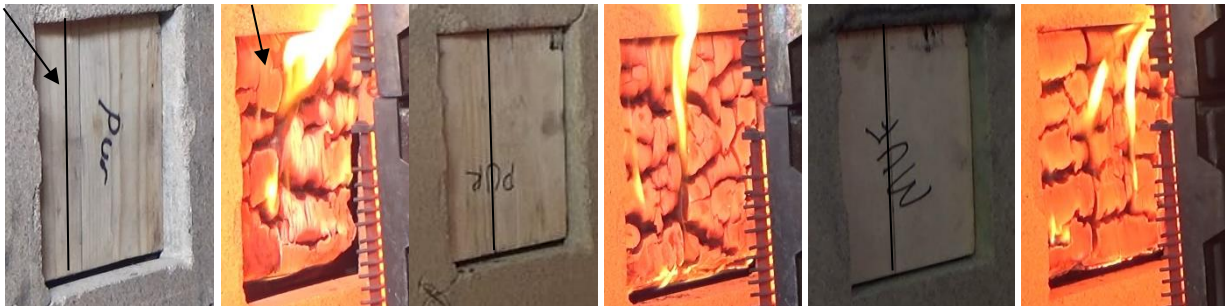


Figure 45. Narrow bond-line failure for PUR2 (B) and MUF (C) adhesive. From left to right: B9, B12 (delamination), C6 (local failure)

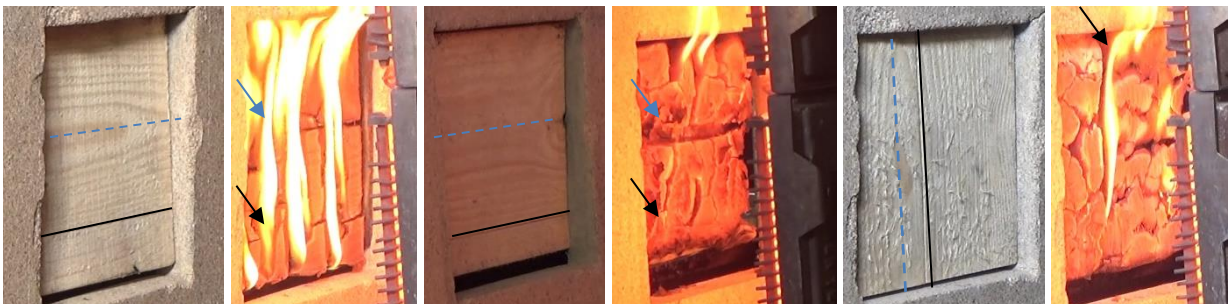


Figure 46. Narrow bond-line failure and specific wood failure for Hotmelt formaldehyde-free and PVAc adhesive From left to right: A6, A7, A9 (char fall-off)

It was reviewed by Brandner et al. [161] that in the ambient conditions and climatic variations CLT is expected to create cracks at the surface and within the lamellae, caused by swelling and shrinking. When a narrow bond-line is present between two lamellae, it is considered to be quasi-rigid, and an irregular pattern is therefore expected to appear within the lamella itself - not in the bond-line. But when there is no adhesive at the narrow surface between two lamellae in the same layer, the stresses are released at that connection, and there are no unexpected cracks within the lamellae. When exposed to fire conditions, PUR2 and MUF adhesive got disintegrated and stopped working as a rigid connection, and all the stresses in wood caused by shrinking were released in the narrow bond-line.

In the author's opinion, knowing the weak point of the composite, as the narrow bond-line can be, could be a beneficial aspect. It allows for the engineer to easier predict the behaviour and to design for it, by addressing his needs to the manufacturer. Designing the narrow bond-line to keep the rigid properties, for a specified period (i.e. up to the point that char has penetrated in the second lamella), would allow for the cracks to appear within the lamella. The author assumes that in that case the pieces of char that are falling off would be restricted to a smaller area. This hypothesis will be considered in further research since the heat release rate and the auto-extinction are the function of the area of char fall-off and the thickness of the lamella [114].

#### Influence of the ply configuration on the char fall-off

Apart from the lamella orientation (vertical/horizontal), wood pattern and finishing, and narrow bond-line, the thickness can also influence char fall-off.

It is assumed that Series A has experienced a different type of failure mode (mostly char fall-off) due to geometry (two loaded lamella 2 cm thick instead of only one 4 cm thick). Comparison of samples in Series A emphasised the importance of preserved bondability of lamella after the char reaching the adhesive line. For 100 kg, when there was no char fall-off at the 1<sup>st</sup> adhesive line, failure was postponed for 20 minutes. For 200 kg, it was postponed for 10 minutes.

No presence of char fall-off for thicker samples complies with the findings from Klippel et al. [123] and Wiesner et al. [20]. Klippel that the *non-delaminating adhesive* experienced char fall-off when lamella was 10 or 25 mm thick, but for 35 mm lamella, it did not appear. Wiesner discussed that “...for fire conditions, using the thicker outer plies delays the thermal penetration and postpones debonding, thus increasing the chances of achieving burnout and auto-extinction before the new virgin wood is involved.”

Thin lamellae seem to also be more prone to “buckling” failure than thick lamellae. The author named it this way because it looks like there is a contraction in the timber parallel to the grain, restricted by the bond-line internal stresses developed at the top and bottom of the lamella, causing the buckling failure which looks like the char has just *popped out* (shown Figure 47). This type of char fall-off mostly appeared for the already dried specimens (A9,10,11,13). The origin of such behaviour is not within the author's knowledge but it is assumed that it has to do with the slenderness of the lamellae.



Figure 47. Buckled char fall-off residue

Buckling failure of little charred bits was noted by L.Schmidt [19] who in her experiments loaded the pinned/pinned column under compression and exposed it to radiant panel. Since the failure in this study is driven by different type of loading, this effect of char just popping out might be a result of the thermal load. Another possible reason is macroscopic shrinkage effect of char pieces [36] which leads to curvature of the char pieces and subsequently to tension perpendicular to the bond lines.



## Chapter 5      Conclusions and future work

There is a recognised research gap when it comes to the design of mass timber buildings in fire conditions, due to the uncertainties this “new” material brings in the design process. To employ compartmentation as an integral part of a fire strategy, one needs to be able to achieve self-extinction, which relies on the composite action of the engineered wood products. In this study, the composite action of cross-laminated timber at elevated temperatures is assessed through the performance of the adhesive-timber bonding interface.

The novelty of this research work is that the bond line performance is assessed for the effects of the simultaneously applied thermal and structural load, i.e. the sample is being heated while loaded in shear. Also, the structural load applied is calculated according to real-life applications, and the heat flux applied allows for a transient heating of the sample.

The bond line behaviour is dictated by both the adhesive performance and the adhesive-timber interaction. The methodology is found to be applicable for this performance assessment through observing the developed bond line temperature ranges at the time of failure. It also studies the influence of the lamella thickness and narrow bonding on the char fall-off. It successfully presents delamination caused by thermal penetration.

However, it needs to be improved in terms of load application and load transfer to obtain repeatability in the failure modes. Currently, the variance in results is too big to draw definite conclusions about the bond line performance. It does not allow for the assessment of temperature-induced creep, but only the comparative analysis of the behaviour for dried and non-dried samples.

The most important findings that address the objectives will be explained in terms of: failure mode and geometry, adhesive type, moisture content, the amount of load applied, and finally the bond line failure temperature criteria.

Failure mode and geometry | More uniform failure modes were present in ambient temperatures. The method used to test for shear strength in fire conditions is useful to observe any delamination caused by the thermal wave propagation. However, a large

number of samples have experienced local failure, which restricts the comparison between the applied configurations. This is caused by the eccentricity of the load placed on the lamella due to insufficient clamping; this can be improved in future research by ensuring only a vertical application of load, as proposed in Appendix E

With an improved methodology, to test for char fall-off, the number of loaded lamellae needs to be increased. When the first lamella starts to char, the stresses need to be able to redistribute to the cooler but loaded side. Only in this way can one observe char fall off at the adhesive line and after the adhesive line as it was the case for the samples with two (2) cm thick lamellae glued with one-component polyurethane (PUR1). Conversely, if there is only one lamella in place, it will experience mechanical failure or delamination.

Char fall-off was happening arbitrarily, sometimes at and sometimes after the adhesive line. Apart from the indicated thickness, it was influenced by the lamella orientation (vertical/horizontal), wood pattern and finishing, and narrowness of the bond-line. Presence of edge gluing allowed for faster flame penetration to the next CLT layer and influenced faster char fall-off.

Adhesive type | Char fall-off was observed only for the samples with one-component polyurethane adhesives (seven PUR1, one PUR2), but not with melamine-urea formaldehyde (MUF) adhesives. However, the latter had mostly no presence of a narrow bond line. Delamination was present for both PUR2 and MUF, where the failure of PUR2 was mostly in the timber in vicinity of the bond line, and for MUF at the adhesive-timber interface.

Moisture content | Dried samples had a faster developed thermal penetration than non-dried ones, which resulted in faster failure time. Brittle delamination was indicated mostly for the dried samples, which implies the importance of moisture movement for this failure mode, but it was not quantified. A sample that was evaluated for char fall-off, with PUR1, showed no difference in the behaviour for dried and non-dried samples. Since non-dried samples tend to fail at lower temperatures, it can be assumed that both adhesive and timber are highly affected by the moisture movement and water evaporation.

Load | The thermal load applied was sufficient to prevent self-extinction of the sample. The change in structural load caused a difference only for the case of delamination, where under higher load, the samples experienced repetitive failure times with bond-line temperatures ranging from approximately 120°C to 150° for higher load.

Bond line failure temperature criteria | Delamination was observed from 127 to 236°C (with one exception of 78°C). Using 130°C as a design temperature might be over-conservative when compared to critical bond-line temperatures as 200°C in large scale tests. For other failure modes, the big variance in failure temperatures between dried and non-dried samples suggests that temperature is not the only parameter that drives the failure of the bond line. In order to use temperatures as an adhesive assessment, it should be possible to drive a correlation between dried and non-dried samples based on the influence of moisture movement. However, more samples should be tested to confirm this statement. This is addressed within further research.

There is a high demand for a harmonised small scale methodology to test the adhesive-timber interaction in both ambient and fire conditions which can be easily applied by manufacturers. This research can be used as an input for the further development of such a methodology, that could successfully address both char fall-off and delamination, whose occurrence can prevent self-extinction. To increase the understanding about the bond line behaviour in fire conditions, along with delamination and char fall-off phenomena, further research could be directed to address the following:[162]

- Impact of the load on char fall-off which currently appear to be arbitrary.
- Causes for char “buckling” phenomenon.
- Influence of sample orientation narrow bond-line, surface finishing and patterns (e.g. the bull’s eye and cathedral pattern) on char fall-off.
- Impact of the adhesive penetration depth on delamination and char fall-off.
- Impact of moisture movement on composite degradation, and delamination.
- Testing under different (and transient) heat fluxes to address the large preheating times and decay phase

## References

- [1] E. Serrano, B. Källander, "Building and construction - timber" . In: *Adhesive Bonding: Science, Technology and Applications*. (2005) , pp.328–356. <https://doi.org/10.1533/9781845690755.3.328>.
- [2] L. McNulty, "Interiors - Hereford College of Arts" (n.d). <https://www.lancemcnulty.co.uk/interiors/6iv3t5ds7i3sq0mhchwnax3iqb69al> (accessed February 3, 2021).
- [3] H.J. Blaß, C. Sandhaas, *Timber Engineering: Principles for design*, 1988. [https://doi.org/10.1016/s1474-6670\(17\)54538-3](https://doi.org/10.1016/s1474-6670(17)54538-3).
- [4] S.L. Zelinka, K. Sullivan, S. Pei, N. Ottum, N.J. Bechle, D.R. Rammer, L.E. Hasburgh, "Small scale tests on the performance of adhesives used in cross laminated timber (CLT) at elevated temperatures" . In: *International Journal of Adhesion and Adhesives*. 95 (2019). <https://doi.org/10.1016/j.ijadhadh.2019.102436>.
- [5] A.I. Bartlett, R.M. Hadden, L.A. Bisby, "A Review of Factors Affecting the Burning Behaviour of Wood for Application to Tall Timber Construction" . In: *Fire Technology*. 55 (2019) , pp.1–49. <https://doi.org/10.1007/s10694-018-0787-y>.
- [6] D. Barber, R. Gerard, "Summary of the fire protection foundation report - fire safety challenges of tall wood buildings" . In: *Fire Science Reviews*. 4 (2015). <https://doi.org/10.1186/s40038-015-0009-3>.
- [7] R. Emberley, J. Torero Cullen, Cross-laminated timber failure modes for fire conditions, in: *Proceedings of the Second International Conference on Performance-Based and Life-Cycle Structural Engineering*, School of Civil Engineering, The University of Queensland, 2015: pp. 1023–1030. <https://doi.org/10.14264/uql.2016.403>.
- [8] A. Law, R. Hadden, "We need to talk about timber: Fire safety design in tall buildings" . In: *The Structural Engineer*. 98 (2020) , pp.10–15. [https://www.research.ed.ac.uk/portal/en/publications/we-need-to-talk-about-timber\(039aa2e7-3e93-4ea2-8808-a6eaceafe5d46\).html](https://www.research.ed.ac.uk/portal/en/publications/we-need-to-talk-about-timber(039aa2e7-3e93-4ea2-8808-a6eaceafe5d46).html).

- [9] “We need to talk about timber” (n.d.). <https://www.istructe.org/resources/training/fire-safety-design-we-need-to-talk-about-timber/> (accessed September 28, 2020).
- [10] R. Emberley, T. Do, J. Yim, J.L. Torero, “Critical heat flux and mass loss rate for extinction of flaming combustion of timber” . In: *Fire Safety Journal*. 91 (2017) , pp.252–258. <https://doi.org/10.1016/j.firesaf.2017.03.008>.
- [11] J. Su, P. Lafrance, M. Hoehler, M. Bundy, “Fire Safety Challenges of Tall Wood Buildings – Phase 2: Task 2 & 3 – Cross Laminated Timber Compartment Fire Tests” (2018) , pp.396. <https://doi.org/https://doi.org/10.18434/T4/1422512>.
- [12] L. Hasburgh, K. Bourne, C. Dagenais, L. Ranger, A. Roy-Poirier, “Fire performance of mass-timber encapsulation methods and the effect of encapsulation on char rate of cross-laminated timber” . In: *WCTE 2016 - World Conference on Timber Engineering*. (2016) , pp.3964–3972.
- [13] R.M. Hadden, A.I. Bartlett, J.P. Hidalgo, S. Santamaria, F. Wiesner, L.A. Bisby, S. Deeny, B. Lane, “Effects of exposed cross laminated timber on compartment fire dynamics” . In: *Fire Safety Journal*. 91 (2017) , pp.480–489. <https://doi.org/10.1016/j.firesaf.2017.03.074>.
- [14] J. König, L. Walleij, Timber frame assemblies exposed to standard and parametric fire, 2000.
- [15] R. Crielaard, J.W. van de Kuilen, K. Terwel, G. Ravenshorst, P. Steenbakkens, “Self-extinguishment of cross-laminated timber” . In: *Fire Safety Journal*. 105 (2019) , pp.244–260. <https://doi.org/10.1016/j.firesaf.2019.01.008>.
- [16] A. Bartlett, R. Hadden, L. Bisby, B. Lane, “Auto-extinction of engineered timber as a design methodology” . In: *WCTE 2016 - World Conference on Timber Engineering*. (2016).
- [17] C.J. McGregor, Contribution of Cross Laminated Timber Panels To Room Fires, 2013. <http://newbuildscanada.ca/wp-content/uploads/2013/06/T3-3b-C7-McGregor-C-Thesis-Contribution-of-CLT-panels-to-room-fires.pdf>.
- [18] C. Gorska, J.P. Hidalgo, J.L. Torero, “Fire dynamics in mass timber compartments” . In: *Fire Safety Journal*. (2020) , pp.103098. <https://doi.org/10.1016/j.firesaf.2020.103098>.
- [19] L. Schmidt, Experimental study on the effect of char fall off on the heat transfer within loaded CLT columns exposed to radiant heating, The University of Edinburgh: College of Science and Engineering, 2020.

- [20] F. Wiesner, PhD Thesis: Structural behaviour of cross-laminated timber elements in fires, The University of Edinburgh, 2019. <https://hdl.handle.net/1842/36675>.
- [21] A. Nicolaidis, R. Emberley, D. Fernando, J. Torero, "Thermally driven failure mode changes in bonded timber joints" . In: *WCTE 2016 - World Conference on Timber Engineering*. (2016) , pp.5243–5251.
- [22] S. Clauß, M. Joscak, P. Niemz, "Thermal stability of glued wood joints measured by shear tests" . In: *European Journal of Wood and Wood Products*. 69 (2011) , pp.101–111. <https://doi.org/10.1007/s00107-010-0411-4>.
- [23] L. Hasburgh, K. Bourne, P. Peralta, P. Mitchell, S. Schiff, W. Pang, "Effect of adhesives and ply configuration on the fire performance of Southern pine cross-laminated timber" . In: *WCTE 2016 - World Conference on Timber Engineering*. (2016).
- [24] R. Emberley, Z. Yu, D. Fernando, J.L. Torero, "Delamination occurrence in engineered mass timber products at elevated temperatures" . In: *WCTE 2016 - World Conference on Timber Engineering*. (2016) , pp.5262–5268.
- [25] R. Emberley, A. Inghelbrecht, N. Doyle, "Components and consequences of CLT delamination" . In: *Fire Science and Technology 2015*. (n.d.). <https://doi.org/10.1007/978-981-10-0376-9>.
- [26] R. Emberley, A. Nicolaidis, D. Fernando, J.L. Torero, "Changing Failure Modes of Cross-Laminated Timber" . In: *9th International Conference on Structures in Fire*. (2016) , pp.643–649.
- [27] J. Konnerth, M. Kluge, G. Schweizer, M. Miljković, W. Gindl-Altmutter, "Survey of selected adhesive bonding properties of nine European softwood and hardwood species" . In: *European Journal of Wood and Wood Products*. 74 (2016) , pp.809–819. <https://doi.org/10.1007/s00107-016-1087-1>.
- [28] H. Quiquero, B. Chorlton, J. Gales, "Performance of adhesives in Glulam after short term fire exposure" . In: *International Journal of High-Rise Buildings*. 7 (2018) , pp.299–311. <https://doi.org/10.21022/IJHRB.2018.7.4.299>.
- [29] P. Niemz, K. Allenspach, D. Einfluss, "Untersuchungen zum Einfluss von Temperatur und Holzfeuchte auf das Versagensverhalten von aus - gewählten Klebstoffen bei

- Zugscherbeanspruchung” 31 (2009) , pp.296–304. <https://doi.org/10.1002/bapi.200910039>.
- [30] M. Janssens, Development of a fire performance assessment methodology for qualifying cross laminated timber adhesives, San Antonio, texas, USA, 2017. <https://doi.org/10.1210/endo-66-4-646>.
- [31] D. Brandon, C. Dagenais, “Fire Safety Challenges of Tall Wood Buildings – Phase 2: Task 5 – Experimental Study of Delamination of Cross Laminated Timber (CLT) in Fire” (2018) , pp.74. <https://doi.org/10.18434/T4/1422512>.
- [32] D. Brandon, B. Östman, “Fire Safety Challenges of Tall Wood Buildings – Phase 2: Task 1 - Literature Review” . In: *National Fire Protection Association (NFPA)*. (2016) , pp.39. <http://www.diva-portal.org/smash/get/diva2:1014998/FULLTEXT01.pdf>.
- [33] M. Klippel, A. Frangi, “Einfluss des Klebstoffes auf das Brandverhalten von Brettschichtholz” 34 (2012) , pp.142–152. <https://doi.org/10.1002/bapi.201200018>.
- [34] M. Klippel, A. Frangi, “Fire behaviour of cross-laminated timber” . In: *Bautechnik*. 93 (2016). <https://doi.org/10.1002/bate.201500070>.
- [35] A. Frangi, G. Bochicchio, A. Ceccotti, M.P. Lauriola, “Natural full-scale fire test on a 3 storey XLam timber building” . In: *10th World Conference on Timber Engineering 2008*. 1 (2008) , pp.528–535.
- [36] M. Klippel, J. Schmid, R. Fahrni, A. Frangi, Assessing the adhesive performance in CLT exposed to fire, in: WCTE 2018 - World Conference on Timber Engineering, World Conference on Timber Engineering (WCTE), 2018.
- [37] European Committee for Standardization (CEN), EN 13381-7 Test methods for determining the contribution to the fire resistance of structural members - Part 7:Applied protection to timber members, 2019.
- [38] F. Wiesner, F. Randmael, W. Wan, L. Bisby, R.M. Hadden, “Structural response of cross-laminated timber compression elements exposed to fire” . In: *Fire Safety Journal*. 91 (2017) , pp.56–67. <https://doi.org/10.1016/j.firesaf.2017.05.010>.
- [39] PRG 320-2019: Standard for Performance-Rated Cross-Laminated Timber, United States, n.d.

- [40] European Committee for Standardization (CEN), EN 302-2 Adhesives for load-bearing timber structures - Test methods - Determination of resistance to delamination, 2017.
- [41] American Society for Testing and Materials, ASTM D5824 - 98: Standard Test Method for Determining Resistance to Delamination of Adhesive Bonds in Overlay-Wood Core Laminates Exposed to Heat and Water, West Conshohocken, PA, 2017.
- [42] B. Miyamoto, N.J. Bechle, D.R. Rammer, S.L. Zelinka, "A small-scale test to examine heat delamination in cross laminated timber (CLT)" . In: *Forests*. 12 (2021) , pp.1–11. <https://doi.org/10.3390/f12020232>.
- [43] European Committee for Standardization (CEN), EN 14080 - Timber structures — Glued laminated timber and glued solid timber — Requirements, Brussels, CEN, 2013.
- [44] F. Stoeckel, J. Konnerth, W. Gindl-altmutter, "Mechanical properties of adhesives for bonding wood — A review" . In: *International Journal of Adhesion and Adhesives*. 45 (2013) , pp.32–41. <https://doi.org/10.1016/j.ijadhadh.2013.03.013>.
- [45] A. Frangi, M. Fontana, A. Mischler, "Shear behaviour of bond lines in glued laminated timber beams at high temperatures" . In: *Wood Science and Technology*. 38 (2004) , pp.119–126. <https://doi.org/10.1007/s00226-004-0223-y>.
- [46] K. Richter, R. Steiger, "Thermal stability of wood-wood and Wood-FRP bonding with polyurethane and epoxy adhesives" . In: *Advanced Engineering Materials*. 7 (2005) , pp.419–426. <https://doi.org/10.1002/adem.200500062>.
- [47] M. Klippel, Fire safety of bonded structural timber elements, ETH, 2014. <https://doi.org/10.3929/ethz-a-010782581>.
- [48] K. Grøstad, A. Pedersen, "Emulsion polymer isocyanates as wood adhesive: A review" . In: *Journal of Adhesion Science and Technology*. 24 (2010) , pp.1357–1381. <https://doi.org/10.1163/016942410X500981>.
- [49] British Standards Institution, "BS EN 301 Adhesives , phenolic and aminoplastic , for and performance requirements" (2017).
- [50] B. Burchardt, Advances in polyurethane structural adhesives, Woodhead Publishing Limited, 2010. <https://doi.org/10.1533/9781845698058.1.35>.



- [51] S. Clauß, J. Gabriel, A. Karbach, M. Matner, P. Niemz, "Influence of the adhesive formulation on the mechanical properties and bonding performance of polyurethane prepolymers" . In: *Holzforschung*. 65 (2011) , pp.835–844. <https://doi.org/10.1515/HF.2011.095>.
- [52] L. Muszynski, E. Hansen, S. Fernando, G. Schwarzmann, J. Rainer, "Insights into the global cross-laminated timber industry" . In: *Bioproducts Business*. 2 (2017) , pp.77–92.
- [53] "Nordic Structures: Technical Documents - Adhesives used in Nordic Products" (2020).
- [54] "SmartLam:Resources - CLT Specification Guide" (2020) , pp.pg.17.
- [55] "Structurlam Resources: ICC-ES Report" (n.d.).
- [56] "XLam New Zeland:Technical Specifications - XLam Panels" (2020).
- [57] R.N. Passarelli, M. Koshihara, "CLT panels in Japan from cradle to construction site gate: global warming potential and freight costs impact of three supply options" . In: *International Wood Products Journal*. 8 (2017) , pp.127–136. <https://doi.org/10.1080/20426445.2017.1317471>.
- [58] "Mayr-Melnhof Holz Holding AG" (n.d.). [http://www.mm-holz.com/fileadmin/user\\_upload/Pressemitteilungen/Newsletter\\_Architekten/MM\\_crosslam.pdf](http://www.mm-holz.com/fileadmin/user_upload/Pressemitteilungen/Newsletter_Architekten/MM_crosslam.pdf) (accessed July 30, 2020).
- [59] "HASSLACHER Holding GmbH" (n.d.). [https://www.hasslacher.com/data/\\_dateimanager/broschuere/HNT-Brettsperrholz-EN.pdf](https://www.hasslacher.com/data/_dateimanager/broschuere/HNT-Brettsperrholz-EN.pdf) (accessed July 30, 2020).
- [60] "ZÜBLIN Timber GmbH" (n.d.). [https://www.zueblin-timber.com/fileadmin/downloads/ETA\\_10\\_0241\\_eng.pdf](https://www.zueblin-timber.com/fileadmin/downloads/ETA_10_0241_eng.pdf) (accessed July 30, 2020).
- [61] "Merkle Holz GmbH" (n.d.). <https://www.merkleholz.de/en/X-Lam-10980-300.html> (accessed July 30, 2020).
- [62] Derix W. u. J. GmbH & Co., n.d. [https://www.derix.de/data/DERIX\\_X\\_Lam\\_Brosch\\_EN\\_2020\\_03\\_WEB\\_final.pdf](https://www.derix.de/data/DERIX_X_Lam_Brosch_EN_2020_03_WEB_final.pdf).
- [63] "Monnet Seve: Catalogue Produit - Technical Sheets" (2017). <https://en.calameo.com/read/003516086bc933810ff19> (accessed January 9, 2021).

- [64] “Binderholz GmbH” (n.d.). [https://www.binderholz.com/fileadmin/user\\_upload/books/en/clt\\_bbs/6/#zoom=z](https://www.binderholz.com/fileadmin/user_upload/books/en/clt_bbs/6/#zoom=z) (accessed July 30, 2020).
- [65] “Holzbau Unterrainer GmbH” (n.d.). <https://holzbau-unterrainer.at/wp-content/uploads/02-Radiusholz-Brettsperrholz-2018.pdf> (accessed July 30, 2020).
- [66] KLH Massivholz GmbH, n.d. <https://www.klh.at/wp-content/uploads/2019/10/klh-eta-certificate-en.pdf>.
- [67] “Stora Enso Oyj” (n.d.). <https://www.storaenso.com/-/media/documents/download-center/documents/product-brochures/wood-products/clt-by-stora-enso-technical-brochure-en.pdf?mode=brochure#page=4>.
- [68] “Weinberger Holz GmbH” (n.d.). <https://www.weinberger-holz.at/en/downloads/?739903589> (accessed July 30, 2020).
- [69] “Artuso Legnami: XLam Catalogue - Technical Sheets” (2015). [https://www.artusolegnami.it/images/depliant/depliant\\_catalogo\\_xlam\\_Artuso\\_2015.pdf](https://www.artusolegnami.it/images/depliant/depliant_catalogo_xlam_Artuso_2015.pdf) (accessed February 9, 2021).
- [70] “XLam Dolomiti: Quality Control - Technical Sheets” (2017). [https://www.xlamdolomiti.it/assets/site/doc/Quality\\_Control\\_en.pdf](https://www.xlamdolomiti.it/assets/site/doc/Quality_Control_en.pdf) (accessed February 9, 2021).
- [71] “Moser Holzbau GmbH: Massivholzplatten - Technical Sheets” (n.d.). <https://moser-holzbau.com/produkte/massivholzplatten> (accessed February 9, 2021).
- [72] “Bélliard Frères: Les caractéristiques techniques - Technical Sheets” (n.d.). <http://www.panneau-plicroise.fr/les-caracteristiques-techniques/> (accessed February 9, 2021).
- [73] “Egoin UK: EGO-CLT Environmental Product Declaration - Technical Sheets” (n.d.). <https://uk.egoin.com/downloads/> (accessed January 9, 2021).
- [74] “Oy CrossLam Kuhmo Ltd: Manufacturing of CLT board - Adhesive properties - Technical Sheets” (2007). <https://www.crosslam.fi/en/products/manufacturing-of-clt-board.html> (accessed February 9, 2021).

- [75] “Schillinger Holz: Declaration of performance - Technical Sheet” (2020). [https://www.schillinger.ch/wp-content/uploads/2020/05/03\\_Declaration-of-performance\\_GFP-SHI-03-01052020.pdf](https://www.schillinger.ch/wp-content/uploads/2020/05/03_Declaration-of-performance_GFP-SHI-03-01052020.pdf) (accessed February 10, 2021).
- [76] “TIMBER-ONLINE.net: The biggest glulam producers” . In: *Holzkurier*. (2020). <https://www.timber-online.net/blog/biggest-glulam-producers.html>.
- [77] W. Song, Y. Cao, D. Wang, G. Hou, Z. Shen, S. Zhang, “An investigation on formaldehyde emission characteristics of wood building materials in Chinese standard tests: Product emission levels, measurement uncertainties, and data correlations between various tests” . In: *PLOS ONE*. 10 (2015) , pp.1–38. <https://doi.org/10.1371/journal.pone.0144374>.
- [78] T. Salthammer, “The formaldehyde dilemma” . In: *International Journal of Hygiene and Environmental Health*. 218 (2015) , pp.433–436. <https://doi.org/10.1016/j.ijheh.2015.02.005>.
- [79] M.Z.M. Salem, M. Böhm, J. Srba, J. Beránková, “Evaluation of formaldehyde emission from different types of wood-based panels and flooring materials using different standard test methods” . In: *Building and Environment*. 49 (2012) , pp.86–96. <https://doi.org/10.1016/j.buildenv.2011.09.011>.
- [80] British Standards Institution, BS EN 13986 Wood-based panels for use in construction - characteristics, evaluation of conformity and marking, Brussels, 2015.
- [81] British Standards Institution, BS EN 16351 - Timber structures — Cross laminated timber — Requirements, Brussels, 2015.
- [82] J. Custódio, J. Broughton, H. Cruz, “A review of factors influencing the durability of structural bonded timber joints” . In: *International Journal of Adhesion and Adhesives*. 29 (2009) , pp.173–185. <https://doi.org/10.1016/j.ijadhadh.2008.03.002>.
- [83] Sika, “Sika: Product information Sikadur®-330 - Technical Sheets” (2017) , pp.2–5. [file:///F:/1\\_Fakultetsko\\_ obrazovanje/3\\_IMFSE/4\\_Master\\_thesis/1\\_Literature/3\\_To\\_read/5\\_Glue/Technical\\_sheet/Sikadur-330.pdf](file:///F:/1_Fakultetsko_ obrazovanje/3_IMFSE/4_Master_thesis/1_Literature/3_To_read/5_Glue/Technical_sheet/Sikadur-330.pdf) (accessed July 28, 2020).
- [84] AkzoNobel, “Product Information: Laminated beam MUF system” (2009). [https://www.huettemann-holz.de/application/files/2114/4663/1861/Glue\\_Harder\\_1249-](https://www.huettemann-holz.de/application/files/2114/4663/1861/Glue_Harder_1249-)

- 2579\_Product\_Information\_2009.pdf.
- [85] M. Sernek, M. Boonstra, A. Pizzi, A. Despres, P. Gérardin, “Bonding performance of heat treated wood with structural adhesives” . In: *Holz Als Roh - Und Werkstoff*. 66 (2008) , pp.173–180. <https://doi.org/10.1007/s00107-007-0218-0>.
- [86] C.R. Frihart, “Adhesive groups and how they relate to the durability of bonded wood” . In: *Journal of Adhesion Science and Technology*. 23 (2009) , pp.601–617. <https://doi.org/10.1163/156856108X379137>.
- [87] J. Luedtke, C. Amen, A. van Ofen, C. Lehringer, “1C-PUR-bonded hardwoods for engineered wood products: influence of selected processing parameters” . In: *European Journal of Wood and Wood Products*. 73 (2015) , pp.167–178. <https://doi.org/10.1007/s00107-014-0875-8>.
- [88] J. Liu, K. Yue, L. Xu, J. Wu, Z. Chen, L. Wang, W. Liu, W. Lu, “Bonding performance of melamine-urea-formaldehyde and phenol-resorcinol-formaldehyde adhesive glulams at elevated temperatures” . In: *International Journal of Adhesion and Adhesives*. 98 (2020) , pp.102500. <https://doi.org/10.1016/j.ijadhadh.2019.102500>.
- [89] H. Cruz, J. Custódio, “Thermal performance of epoxy adhesives in timber structural repair” . In: *9th World Conference on Timber Engineering 2006, WCTE 2006*. 2 (2006) , pp.1077–1084.
- [90] M. Knorz, P. Schmid, J.W. van de Kuilen, K. Richter, “Time to failure testing in shear of wood-adhesive bonds under elevated temperatures” . In: *Forest Products Journal*. 68 (2019) , pp.383–389. <https://doi.org/10.13073/FPJ-D-17-00071>.
- [91] M. Dunky, P. Niemz, *Holzwerkstoffe und Leime*, 2002. <https://doi.org/10.1007/978-3-642-55938-9>.
- [92] International Organisation for Standardization, ISO 527-1 Plastics — Determination of tensile properties — Part 1: General principles, 2012. <https://www.iso.org/standard/56045.html>.
- [93] British Standards Institution, BS EN 302-1 Adhesives for load bearing timber structures. Test methods. Determination of bond strength in longitudinal tensile shear strength, n.d. <https://shop.bsigroup.com/ProductDetail/?pid=000000000030112556>.
- [94] Z. Lu, H. Zhou, Y. Liao, C. Hu, “Effects of surface treatment and adhesives on bond performance and mechanical properties of cross-laminated timber (CLT) made from small diameter

- Eucalyptus timber” . In: *Construction and Building Materials*. 161 (2018) , pp.9–15. <https://doi.org/10.1016/j.conbuildmat.2017.11.027>.
- [95] European Committee for Standardization (CEN), EN 391 Glued laminated timber. Delamination test of glue lines, 2002.
- [96] European Committee for Standardization (CEN), EN 392 Glued laminated timber. Shear test of glue lines, 1995.
- [97] American Society of Testing and Materials, ASTM D2559-04 Standard Specification for Adhesives for Structural Laminated Wood Products for Use Under Exterior (Wet Use) Exposure Conditions, West Conshohocken, PA, 2004.
- [98] American Institute of Timber Construction, Test Method for Structural Glued Laminated Timber: AITC Test T110 – Cyclic Delamination Test, Centennial, Colorado, 2007.
- [99] A. Witkowski, A.A. Stec, T.R. Hull, SFPE Handbook of Fire Protection Engineering 5th Edition: Thermal Decomposition of Polymeric Materials, 5th ed., Springer, 2016.
- [100] S. Claub, K. Allenspach, J. Gabriel, P. Niemz, “Improving the thermal stability of one-component polyurethane adhesives by adding filler material” . In: *Wood Science and Technology*. 45 (2011) , pp.383–388. <https://doi.org/10.1007/s00226-010-0321-y>.
- [101] European Committee for Standardization (CEN), EN 302-1: Adhesives for load-bearing timber structures - Test methods - Part 1: Determination of longitudinal tensile shear strength, Brussels, 2004.
- [102] A. Frangi, M. Bertocchi, S. Clauß, P. Niemz, “Mechanical behaviour of finger joints at elevated temperatures” . In: *Wood Science and Technology*. 46 (2012) , pp.793–812. <https://doi.org/10.1007/s00226-011-0444-9>.
- [103] J.J. Licari, “Adhesives Technology for Electronic Applications, Second Edition: Materials, Processing, Reliability” (2011) , pp.512. <http://www.amazon.com/Adhesives-Technology-Electronic-Applications-Edition/dp/1437778895>.
- [104] M. Verdet, A. Salenikovich, A. Cointe, J.-L. Coureau, P. Galimard, W. Munoz Toro, P. Blanchet, C. Delisée, “Mechanical Performance of Polyurethane and Epoxy Adhesives in Connections with Glued-in Rods at Elevated Temperatures” . In: *BioResources*. 11 (2016) , pp.8200–8214.

- <https://doi.org/10.15376/biores.11.4.8200-8214>.
- [105] J. Custódio, H. Cruz, J. Broughton, "Preparation method and service conditions effects on the performance and durability of epoxy adhesives used in structural timber repairs" . In: *11th International Conference on Durability of Building Materials and Components – DBMC 2008*. (2008) , pp.635–642.
- [106] F. Wiesner, M. Klippel, C. Dagenais, A. Dunn, B. Östman, M.L. Janssens, K. Kagiya, Requirements for engineered wood products and their influence on the structural fire performance, in: WCTE 2018 - World Conference on Timber Engineering, 2018.
- [107] "Wood Anatomy" (n.d.). <https://careforwood.wordpress.com/wood-anatomy/> (accessed April 1, 2021).
- [108] D.R. Rammer, S.L. Zelinka, L.E. Hasburgh, S.T. Craft, "Ability of finger-jointed lumber to maintain load at elevated temperatures" . In: *Wood and Fiber Science*. 50 (2018) , pp.44–54. <https://doi.org/10.22382/wfs-2018-005>.
- [109] European Committee for Standardization (CEN), EN 302-2 Adhesives for load-bearing timber structures. Test methods. Determination of resistance to delamination, 2013.
- [110] M. Schmidt, P. Glos, G. Wegener, "Verklebung von Buchenholz für tragende Holzbauteile" . In: *European Journal of Wood and Wood Products*. 68 (2010) , pp.43–57. <https://doi.org/10.1007/s00107-009-0382-5>.
- [111] Canadian Standards Association, CSA O177-06 Qualification Code for Manufacturers of Structural Glued-Laminated Timber, Mississauga, ON, 2015. <https://www.scc.ca/en/standardsdb/standards/22939>.
- [112] C. Dagenais, L. Ranger, Revisiting heat delamination characteristics of adhesives in cross-laminated timber, in: WCTE 2018 - World Conference on Timber Engineering, 2018.
- [113] V. Babrauskas, "Journal of Fire Protection Ignition of Wood : A Review of the State of the Art" . In: *Journal of Fire Protection Engineering*. 12 (2002) , pp.81–88. <https://doi.org/10.1106/104239102028711>.
- [114] F. Wiesner, L.A. Bisby, A.I. Bartlett, J.P. Hidalgo, S. Santamaria, S. Deeny, R.M. Hadden, "Structural capacity in fire of laminated timber elements in compartments with exposed

- timber surfaces” . In: *Engineering Structures*. 179 (2019) , pp.284–295.  
<https://doi.org/10.1016/j.engstruct.2018.10.084>.
- [115] D. Morrisset, R.M. Hadden, A.I. Bartlett, A. Law, R. Emberley, “Time dependent contribution of char oxidation and flame heat feedback on the mass loss rate of timber” . In: *Fire Safety Journal*. (2020) , pp.103058. <https://doi.org/10.1016/j.firesaf.2020.103058>.
- [116] D. Drysdale, *An introduction to fire dynamics*, 3rd ed., John Wiley and Sons Ltd., Edinburgh, 2011. [https://doi.org/10.1016/0010-2180\(86\)90037-4](https://doi.org/10.1016/0010-2180(86)90037-4).
- [117] J. ichi Suzuki, T. Mizukami, T. Naruse, Y. Araki, “Fire Resistance of Timber Panel Structures Under Standard Fire Exposure” . In: *Fire Technology*. 52 (2016) , pp.1015–1034.  
<https://doi.org/10.1007/s10694-016-0578-2>.
- [118] A. Frangi, M. Fontana, E. Hugi, R. Jübstl, “Experimental analysis of cross-laminated timber panels in fire” . In: *Fire Safety Journal*. 44 (2009) , pp.1078–1087.  
<https://doi.org/10.1016/j.firesaf.2009.07.007>.
- [119] M. Klippel, C. Leyder, A. Frangi, M. Fontana, F. Lam, A. Ceccotti, “Fire tests on loaded Cross-laminated timber wall and floor elements” . In: *Fire Safety Science*. 11 (2014) , pp.626–639.  
<https://doi.org/10.3801/IAFSS.FSS.11-626>.
- [120] European Committee for Standardization (CEN), EN 1995-1-2: Eurocode 5 Design of timber structures - Part 1-2: General - Structural fire design, Brussels, 2004.
- [121] C. Dagenais, R.H. White, K. Sumathipala, “CLT Handbook (US Edition) Chapter 8 - Fire Performance of Cross-Laminated Assemblies” . In: *CLT Handbook*. (2012) , pp.1–55.
- [122] M. Klippel, J. Schmid, “Design of cross-laminated timber in fire” . In: *Structural Engineering International*. 27 (2017) , pp.224–230.  
<https://doi.org/10.2749/101686617X14881932436096>.
- [123] M. Klippel, J. Schmid, R. Fahrni, M. Kleinhenz, A. Frangi, “Vorschlag einer Standardprüfmethode für Brettsperrholz im Brandfall” . In: *Bautechnik*. 96 (2019).  
<https://doi.org/10.1002/bate.201900019>.
- [124] B. Östman, E. Mikkola, R. Stein, A. Frangi, J. König, D. Dhima, T. Hakkarainen, J. Bregulla, *Fire safety in timber buildings - Technical guideline for Europe*, 2010.

- [125] J. Wallner-Novak, M., Koppelhuber, K. Pock, *Cross-Laminated Timber Structural Design - Basic design and engineering principles according to Eurocode*, 2013.
- [126] R. Harris, A. Ringhofer, G. Schickhofer, "Focus Solid Timber Solutions - European Conference on Cross Laminated Timber (CLT)" (2013).
- [127] S.L. Zelinka, K. Sullivan, S. Pei, N. Ottum, N.J. Bechle, D.R. Rammer, L.E. Hasburgh, "Small scale tests on the performance of adhesives used in cross laminated timber (CLT) at elevated temperatures" . In: *International Journal of Adhesion and Adhesives*. 95 (2019). <https://doi.org/10.1016/j.ijadhadh.2019.102436>.
- [128] S.L. Zelinka, L.E. Hasburgh, K.J. Bourne, D.R. Tucholski, J.P. Ouellette, "Compartment Fire Testing of a Two-Story Mass Timber Building" (2018) , pp.476. <https://doi.org/10.13140/RG.2.2.26223.33447>.
- [129] R. Emberley, "Fundamentals for the Fire Design of Cross Laminated Timber Buildings" (2017) , pp.147.
- [130] T.H. Yang, S.Y. Wang, M.J. Tsai, C.Y. Lin, Y.J. Chuang, "Effect of fire exposure on the mechanical properties of glued laminated timber" . In: *Materials and Design*. 30 (2009) , pp.698–703. <https://doi.org/10.1016/j.matdes.2008.05.022>.
- [131] E. Borgström, ed., *Design of timber structures - Structural aspects of timber construction: Volume 1, 2nd ed.*, Swedish Forest Industries Federation, Stockholm, 2016. <https://doi.org/10.1201/9781315368221-15>.
- [132] T. Ehrhart, R. Brandner, "Rolling shear: Test configurations and properties of some European soft- and hardwood species" . In: *Engineering Structures*. 172 (2018) , pp.554–572. <https://doi.org/10.1016/j.engstruct.2018.05.118>.
- [133] American Society of Testing and Materials, *ASTM D905-03 Standard Test Method for Strength Properties of Adhesive Bonds in Shear by Compression Loading*, West Conshohocken, PA, 2003. <https://www.astm.org/DATABASE.CART/HISTORICAL/D905-03.htm>.
- [134] American Society of Testing and Materials, *ASTM D905 - 08 Standard Test Method for Strength Properties of Adhesive Bonds in Shear by Compression Loading*, West Conshohocken, PA, 2013. <https://www.astm.org/Standards/D905.htm>.



- [135] American Society of Testing and Materials, ASTM D3737-03 Standard Practice for Establishing Allowable Properties for Structural Glued Laminated Timber (Glulam), West Conshohocken, PA, 2003. <https://www.astm.org/DATABASE.CART/HISTORICAL/D3737-03.htm>.
- [136] American Society of Testing and Materials, ASTM D3737 - 18e1 Standard Practice for Establishing Allowable Properties for Structural Glued Laminated Timber (Glulam), West Conshohocken, PA, 2018. <http://www.astm.org/cgi-bin/resolver.cgi?D3737-18e1>.
- [137] International Organisation for Standardization, ISO 527-1 Plastics — Determination of tensile properties — Part 1: General principles, 2019.
- [138] American Society of Testing and Materials, ASTM D143-14 Standard Test Methods for Small Clear Specimens of Timber, West Conshohocken, PA, 2014. <http://www.astm.org/cgi-bin/resolver.cgi?D143-14>.
- [139] Deutsches Institut für Normung, DIN 52187:1979-05 Prüfung von Holz; Bestimmung der Scherfestigkeit in Faserrichtung, Germany, Berlin, 2005. <https://doi.org/https://dx.doi.org/10.31030/1260180>.
- [140] P. Santos, J.R. Correia, L. Godinho, A. Dias, “Bonding quality assessment of cross-layered Maritime pine elements glued with one-component polyurethane adhesive” . In: *Construction and Building Materials*. 211 (2019) , pp.571–582. <https://doi.org/10.1016/j.conbuildmat.2019.03.064>.
- [141] H. Lim, S. Tripathi, J.D. Tang, “Bonding performance of adhesive systems for cross-laminated timber treated with micronized copper azole type C (MCA-C)” . In: *Construction and Building Materials*. 232 (2020) , pp.117208. <https://doi.org/10.1016/j.conbuildmat.2019.117208>.
- [142] C.A. Vick, E.A. Okkonen, “Strenght and Durability of One-Part Adhesive Bonds to Wood” . In: *Forest Products Journal*. 48 (1998) , pp.71–76.
- [143] American Society for Testing and Materials, ASTM D2559 12a Standard Specification for Adhesives for Bonded Structural Wood Products for Use Under Exterior Exposure Conditions, West Conshohocken, PA, 2018.
- [144] European Committee for Standardization (CEN), EN 14292: Adhesives - Wood adhesives - Determination of static load resistance with increasing temperature, CEN, Brussels, 2005.

- [145] S.T. Craft, R. Desjardins, L.R. Richardson, "Development of small-scale evaluation methods for wood adhesives at elevated temperatures" . In: *10th World Conference on Timber Engineering 2008*. 2 (2008) , pp.583–590.
- [146] M. Klippel, A. Frangi, E. Hugi, "Experimental Analysis of the Fire Behavior of Finger-Jointed Timber Members" . In: *Journal of Structural Engineering*. (2014). [https://doi.org/10.1061/\(ASCE\)ST.1943-541X.0000851](https://doi.org/10.1061/(ASCE)ST.1943-541X.0000851).
- [147] American Society of Testing and Materials, ASTM D3535 - 07a Standard Test Method for Resistance to Creep Under Static Loading for Structural Wood Laminating Adhesives Used Under Exterior Exposure Conditions, West Conshohocken, PA, 2013. <https://doi.org/10.1520/D3535-07AR13>.
- [148] European Committee for Standardization (CEN), EN 302-8 Adhesives for load-bearing timber structures. Test methods. Static load test of multiple bond line specimens in compression shear, Brussels, BE, 2017.
- [149] European Committee for Standardization (CEN), EN 15416-3 Adhesives for load bearing timber structures other than phenolic and aminoplastic. Test methods. Creep deformation test at cyclic climate conditions with specimens loaded in bending shear, Brussels, BE, 2019.
- [150] C.-J. Johansson, T. Pizzi, M. Van Leemput, COST Action E13 Wood Adhesion and Glued Products, 2002.
- [151] American Society of Testing and Materials, ASTM D7247-6 Standard Test Method for Evaluating the Shear Strength of Adhesive Bonds in Laminated Wood Products at Elevated Temperatures, West Conshohocken, PA, 2006. <https://doi.org/10.1520/D7247-06>.
- [152] Canadian Standards Association, CSA O112.9-10 Evaluation Of Adhesives For Structural Wood Products (Exterior Exposure), Mississauga, ON, 2014. <https://webstore.ansi.org/standards/csa/csao11220102014>.
- [153] R. Emberley, A. Inghelbrecht, Z. Yu, J.L. Torero, "Self-extinction of timber" . In: *Proceedings of the Combustion Institute*. 36 (2017) , pp.3055–3062. <https://doi.org/10.1016/j.proci.2016.07.077>.
- [154] J. Cuevas, J.L. Torero, C. Maluk, "Flame extinction and burning behaviour of timber under

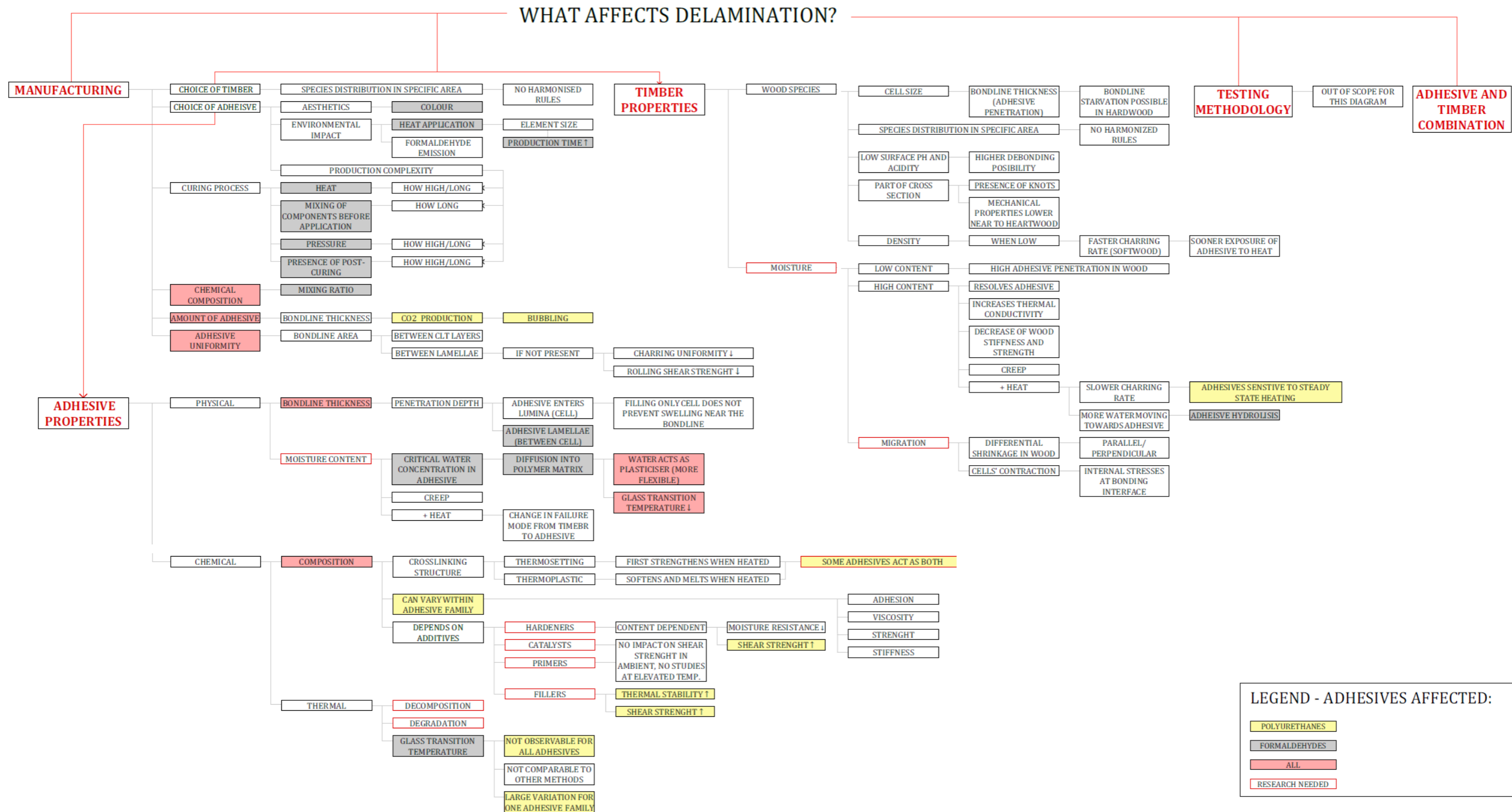
- varied oxygen concentrations” . In: *Fire Safety Journal*. 120 (2021) , pp.103087. <https://doi.org/10.1016/j.firesaf.2020.103087>.
- [155] A. Bartlett, R. Hadden, L. Bisby, B. Lane, Auto-extinction of engineered timber: the application of firepoint theory, in: Interflam, 2016.
- [156] R. Fjellgaard Mikalsen, K. Storesund, A. Steen-Hansen, N.K. Reitan, S. Aicher, M. Klippel, “FIREWOOD - Improved fire design of engineered wood systems in buildings - Small scale CLT testing: [www.researchgate.net/project/FIREWOOD-Improved-fire-design-of-engineered-wood-systems-in-buildings](http://www.researchgate.net/project/FIREWOOD-Improved-fire-design-of-engineered-wood-systems-in-buildings)” (2021). <https://www.researchgate.net/project/FIREWOOD-Improved-fire-design-of-engineered-wood-systems-in-buildings> (accessed April 26, 2021).
- [157] C. Maluk, L. Bisby, M. Krajcovic, J.L. Torero, “A Heat-Transfer Rate Inducing System (H-TRIS) Test Method” . In: *Fire Safety Journal*. 105 (2019) , pp.307–319. <https://doi.org/10.1016/j.firesaf.2016.05.001>.
- [158] C.T. Kidd, C.G. Nelson, “How the Schmidt-Boelter gage really works” . In: *41st International Instrumentation Symposium*. (1995) , pp.347–368.
- [159] H. Unterwieser, G. Schickhofer, “Characteristic Values and Test Configurations of CLT with Focus on Selected Properties: Determination of the basis of design and material properties of CLT” . In: *European Conference on Cross Laminated Timber*. (2013) , pp.53–73.
- [160] S. Franke, B. Franke, A.M. Harte, “Failure modes and reinforcement techniques for timber beams-State of the art” . In: *Construction and Building Materials*. 97 (2015) , pp.2–13. <https://doi.org/10.1016/j.conbuildmat.2015.06.021>.
- [161] R. Brandner, “Production and Technology of Cross Laminated Timber (CLT): A state-of-the-art Report” . In: *Focus Solid Timber Solutions - European Conference on Cross Laminated Timber (CLT)*. (2014) , pp.3–36.
- [162] J.M. Allwood, J.M. Cullen, “Steel , aluminium and carbon : alternative strategies for meeting the 2050 carbon emission targets” . In: *R'09 Conference*. (2009). [https://www.researchgate.net/publication/242582149\\_Steel\\_aluminium\\_and\\_carbon\\_alternative\\_strategies\\_for\\_meeting\\_the\\_2050\\_carbon\\_emission\\_targets](https://www.researchgate.net/publication/242582149_Steel_aluminium_and_carbon_alternative_strategies_for_meeting_the_2050_carbon_emission_targets).

- [163] M. Klippel, A. Frangi, M. Fontana, "Influence of the adhesive on the load carrying capacity of GLT Members in fire" . In: *Fire Safety Science*. (2011). <https://doi.org/10.3801/IAFSS.FSS.10-1219>.
- [164] M. König, J., Norén, J., Sterley, Effect of adhesives on finger joint performance in fire, in: Proceedings of 41st CIB-W18 Meeting, St. Andrews, Canada, 2008.
- [165] E.L. Schaffer, "A Simplified Test for Adhesive Behavior in Wood Sections Exposed to Fire" (1968).
- [166] N. Mohd Yusof, P. Md Tahir, S.H. Lee, M.A. Khan, R. Mohammad Suffian James, "Mechanical and physical properties of Cross-Laminated Timber made from Acacia mangium wood as function of adhesive types" . In: *Journal of Wood Science*. 65 (2019). <https://doi.org/10.1186/s10086-019-1799-z>.
- [167] L. Muszyński, R. Gupta, S. hyun Hong, N. Osborn, B. Pickett, "Fire resistance of unprotected cross-laminated timber (CLT) floor assemblies produced in the USA" . In: *Fire Safety Journal*. 107 (2019) , pp.126–136. <https://doi.org/10.1016/j.firesaf.2018.12.008>.
- [168] European Committee for Standardization CEN, EN1991-1-1: Eurocode 1: Actions on Structures: Part 1-1: Densities, self-weight and imposed loads, European Standards (ES), Brussels, Belgium, 2002.
- [169] M. Jeleč, D. Varevac, V. Rajčić, "Cross laminated timber (CLT) - A state of the art" . In: *Gradjevinar*. 70 (2018) , pp.75–95. <https://doi.org/10.14256/JCE.2071.2017>.
- [170] D. Morrisset, G. Thorncroft, R. Hadden, A. Law, R. Emberley, "Statistical uncertainty in bench-scale flammability tests" . In: *Fire Safety Journal*. 122 (2021) , pp.103335. <https://doi.org/10.1016/j.firesaf.2021.103335>.
- [171] I. Pope, J.P. Hidalgo, J.L. Torero, A correction method for thermal disturbances induced by thermocouples in a low- conductivity charring material, in: IAFSS, 2020.
- [172] American Society of Testing and Materials, ASTM D7247-17 Standard Test Method for Evaluating the Shear Strength of Adhesive Bonds in Laminated Wood Products at Elevated Temperatures, West Conshohocken, PA, 2017. <http://www.astm.org/cgi-bin/resolver.cgi?D7247-17>.

- [173] Canadian Standards Association, CSA O112.9-2010 Evaluation Of Adhesives For Structural Wood Products (Exterior Exposure), Mississauga, ON, 2019.  
<https://webstore.ansi.org/Standards/CSA/CSA01122010R2019>.

# Appendix A

## Properties affecting delamination



Some of the main differences in structural and thermal performance are:

#### Polyurethanes

- ductile, high fracture energy [1] [51],
- the long-term durability of PUR adhesives is not well known [1],
- resistance to heat poorer than for formaldehydes [23],
- structural performance highly reliant on its chemical composition, manufacturer and fillers [22,44,46,47], and the methodology used to test the specimen [46,47],
- if well adapted it can reach the PRF adhesive strength and WFP [22],
- based on the small-scale shear tests, increased elongation, WFP reduction, and temperature induced creep is expected from 80°C to 150°C [21,26,108],
- low heat flux as 6 kW/m<sup>2</sup> can also cause 1-C-PUR adhesive failure [24],
- char fall-off observed in several full-scale tests [11,13,30,31,38],
- “Non-delaminating” PUR [11,30,31] could be used to avoid CLT delamination in furnace tests,
- shows good results when combined with 35 mm thick lamella, but not with 25 mm where it experienced char fall-off [123] in furnace tests.
- EPI adhesive
- has a high thermal stability but it varies within the family [44,47,48].

#### Urea-formaldehyde (UF)

- has a low cost, but due to its’ low durability, it is not recommended for outdoor usage,
- performs bad at elevated temperatures,
- combined with melamine (MUF) shows improved behaviour in fire [3] and higher durability [88].

#### Melamine-urea-formaldehyde (MUF)

- High shear strength, brittle behaviour, and the high wood percentage failure,

- compared to PRF, it can absorb more deformation energy, but strength and stiffness in tensile shear test tends to be higher than for all 1-C PUR adhesives [88],[51],
- change in failure mode expected after 150°C [88], but can also depend on the test duration [90],
- at 220°C can undergo significant chemical breakdown [88],
- no reports of char fall-off for MUF were found [131].

#### Phenol-Resorcinol Formaldehyde (PRF)

- The best structural response in terms of required shear strength,
- not influenced by duration of load,
- experiences brittle failure behaviour [1][34][51],
- high temperature resistance with only minor changes in mechanical performance [1,44] with a same shear strength as solid wood at all temperatures [127],
- high wood failure percentage in shear tests [22,127],
- high timber failure in tensile tests at elevated temperatures [47],
- behaviour is also depended on the methodology [88],
- cohesion in glue line possible at elevated temperature higher than 150°C [45],
- experiences only little or no char fall-off [23].

#### Epoxy adhesive

- available in a great variety of formulated products- exhibits different properties, in terms of adhesion to wood, viscosity, reaction and cure time, strength and stiffness
- can experience great dimensional stability after hardening, excellent mechanical resistance and high resistance to chemical products and water
- high sensitivity of to heat at temperatures ranges from 30 to 80°C [82,89,105].

#### PVAc adhesives

- if not integrated in a two-component adhesive system, tends to creep
- bond strength reduced when exposed to high moisture and/or temperature [90]
- not widely used in structural design and therefore it was less studied than other adhesives in this study.



## Appendix B

## Studies observed

Year	Author	Test description	Adhesive	Adhesive producer	Timber species	EWP	Heat / Load	Sample dimensions [mm]
<b>SMALL SCALE TEST</b>								
[46]	2005	K. Richter, R. Steiger	1-C-PUR: DMA Dynamic shear-tension mode GABO Explorer 800, Empa Heat resistance test: Longitudinal tensile shear strength test EPX: Torsion pendulum test Myrenne ATM 3, Tensile strength test Zwick 1417	1-C-PUR (5) 1-C-EPX (3) 2-C-EPX (8)	Not specified	Beech wood (1-C-PUR) Norway spruce (EPX)	Glued joints wood-wood Wood-FRP	H/L PUR: 9 samples: bond thickness 0.1 mm, 9 samples: bond thickness 1 mm EPOXY: wood specimen bonded with 2 FRP splices (cured (11), post-cured(11))
[45]	2004	A. Frangi, M. Fontana	The specimens were heated in an oven to the required constant temperature and the transferred to the three point bending test in heated loading arrangement.	RF (1) 1-C-PUR (5) 2-C-EPX (1)	Specified*	Spruce 456-533 kg/m <sup>3</sup>	GLT beam + Concrete slab	H/L 112 x 40 x 40 mm
* Türmerleim AG, CH-Basel (RF Kauresin 460 + Hardener 466, 1-C-PUR Kauranat 970)   Forbo-CTU AG, CH-Schönenwerd (1-C-PUR Balcotan 107 TR, Balcotan 60 190)   Collano AG, CH-Sempach-Station (1-C-PUR Purbond HB 110, Purbond VN 1033)   ASTORit AG, CH-Einsiedeln (2-C-EPX, Araldite AW 136 H, Hardener HY 991)								
[21]	2016	Nicolaidis et al.	Lap heated shear test. Environmental chamber to get the constant temperature in the bond line. Once heated, chamber removed and loading immediately started.	1-C-PUR	Not specified	Radiata pine	Glued joints	H/L 1400x89x19 mm Bond-line surface: 600 x 89 mm
[104]	2016	Verdet et al.	DMA used to assess glass transition temperature T <sub>g</sub> and observe correlation to static tensile load tests results.	PUR, EPX	Specified*	Black spruce (560 kg/m <sup>3</sup> )	Glued in rods GLT	H H/L 50 x 50 x 245 mm Glued in length: 50 or 92 mm (t = 2 mm)
* Purbond AG, Sempach station, Switzerland (1-C-PUR Purbond CR 421)   Sika, Le Bourget, Switzerland (EPX Sikadur 330)								
[20]	2019	F. Wiesner	1. Uniformly heated small scale samples, once a steady state distribution through specimen is observed, compression applied. 2. The applied compressive load held at a constant value and the specimen was heated until failure occurred (transient heating).	MUF, 1-C-PUR	Not specified	Spruce (460 kg/m <sup>3</sup> )	CLT cubes	H/L L/H 100 x 200 x 100-150 mm (Layers: 40-20-40 mm (LCL) and 5x20 mm (LCLCL))
[33]	2012	M. Klippel, A. Frangi	Furnace test 1000 x 800 mm, ISO curve	1-C-PUR	Not specified	Spruce 420 kg/m <sup>3</sup>	CLT panels Homogeneous panels	H w x d = 385 mm x 1000 x 54 mm; Layers: 54 mm homogen. and 3x18 mm Layers: 2x27 mm homogen. and 2x3x9 mm
[22]	2011	Clauß et al.	1: Bonding lap heated shear test: Specimen tempered in a drying chamber and tested in tensile shear strength machine Zwick Z100 2: Solid wood shear strength test	1-C-PUR (3) PVAc UF, MUF, MF PRF, EPI	Not specified	Beech 756 kg/m <sup>3</sup>	Glued joints	H/L 150x20x5 mm Bond-line surface: 10 x 20 mm
[24]	2016	Emberly et al.	Conical heater applied at the one side of the sample	1-C-PUR	Not specified	European spruce 425 kg/m <sup>3</sup>	CLT, block 5 layers	H 120x120x145 mm
[27]	2015	Konnerth et al.	1. Tensile shear strength Zwick Z020 and Z100: Two bonded lamellas compared to One solid lamella 2. Delamination test in dry and wet conditions	MUF 1-C-PUR PRF.	Specified*	Hardwood** Softwood	GLT beam	L 1. Shear lap: t = 5 mm, Bondline surface: 200 mm <sup>2</sup> 2. GLT delamination: 500 mm x 30 mm Layers: 6 x 5 mm

* AkzoNobel, CASCO ADHESIVES AB, Stockholm, Sweden (MUF: GripPro™ Design Adhesive A002 and GripPro™ Design Hardener 002)   Henkel & Cie AG, Sembach Station, Switzerland (1-C-PUR: LOCTITE HB S309)   PURBOND/ LOCTITE HB S309 PURBOND+primer LOCTITE PR 3105 PURBOND)   Dynea AS–Synthesa Chemie GmbH, Perg, Austria (1-C-PUR: Aerodux 185 and hardener HRP 150)									
** Hardwood (Deciduous): European ash 670 kg/m <sup>3</sup> , European beech 743 kg/m <sup>3</sup> , European silver birch 682 kg/m <sup>3</sup> , Sessile oak 698 kg/m <sup>3</sup> , Common hornbeam 533 kg/m <sup>3</sup> , Poplar 775 kg/m <sup>3</sup> , Black locust 775 kg/m <sup>3</sup>   Softwood (Coniferous): Norway spruce 445 kg/m <sup>3</sup> , European larch 632 kg/m <sup>3</sup>									
[29]	2009	P. Niemz, K. Allenspach	Lap heated tensile shear test	UF, PUR, PVAc	Not specified	Beech	Glued joints	H/L	Lamella: 20 x 5 x 150 mm Bondline surface: 10 x 20 mm
[10]	2017	Emberly et al.	Specimens exposed to external heat flux until ignition. Calorimeter positioned vertically.	1-C-PUR	Not specified	**	CLT blocks, 5 layer Solid wood	H	CLT: 100x100 x 145 or 150 mm Layers: 5x29 or 5x30 mm Solid wood (SW): 100 x 100 x 48 or 90 or 43 or 57 mm
** CLT: European Spruce 400 kg/m <sup>3</sup> , Radiata Pine 400 kg/m <sup>3</sup>   SW: Red Ironbark (Eucalyptus sideroxylon) 1100 kg/m <sup>3</sup> , Balsa (Ochroma pyramidale) 200 kg/m <sup>3</sup> , Kumaru (Dipteryx odorata) 900 kg/m <sup>3</sup> , Blackbutt (Eucalyptus pilularis) 950 kg/m <sup>3</sup>									
[4]	2019	Zelinka et al.	1. Tensile tests on solid wood 2. Lap shear tests At elevated temperatures below the char temperature of wood (300°C) are studied to better understand delamination.	1-C-PUR(2) MF PRF	Not specified	1. Southern yellow pine, Douglas fir, Spruce-pine-fir 2. Douglas fir	Glued joints	H/L <300	One lamella: 139.7 x 22.2 x 21 mm Bond-line surface: 22.2 x 25.4 mm
[112]	2018	Dagenais C., Ranger L.	1. Flame test 2. Cone calorimeter test	1-C-PUR 2-C-PUR MF, PRF	Not specified	Black spruce 480-580 kg/m <sup>3</sup>	GLT and CLT blocks	H	Small scale: 150 x 40 x 160 mm Layers: 8x20 mm Cone calorimeter: 100x100x80 mm Layers: 4x20 mm
[51]	2011	Clauß S., Gabriel J.	1. Tensile shear tests: Bonded wood joints Zwick/Roell Z1010 2. Tensile tests: Adhesive films Zwick/Roell Z100 3. Nanoindentation: micro-mechanical properties Hysitron Triboindenter	Commercial: MUF, PRF, 1-C-PUR(1); Prepolymer: 1-C-PUR (3) Lab adhesive: 1-C-PUR(3)	Specified*	Beech 735 kg/m <sup>3</sup>	Glued joints Adhesive films	L	Bond-line length: 10 mm
* Bayer Material Science Leverkusen, Germany (PUR prepolymers)   Purbond AG, Sempach-Station, Switzerland (1-C-PUR: PUR prepolymers + defoamer, pyrogenic silica and amine catalyst)									
[88]	2020	Liu et al.	1. Tensile solid wood test 2. Tensile double lap shear strength test 3. FTIR: Adhesive cured, grounded and heated to assess chemical and microscopic changes in various temperatures.	PRF MUF	Dynea (Shanghai, China) (PRF)	Larch 604 kg/m <sup>3</sup>	Solid wood vs. Glued joints	H/L	Lamella: 20 mm x 80 mm x 5 mm Bondline surface: 20 x 10 mm
[90]	2018	Knorz et al.	Specimens immersed in water at 60°C and 90°C 1. Short duration tensile shear test 2. Long duration TTF test at load levels between 30 and 90 % of their mean wet short-term strength	MUF	Not specified	Beech 717 kg/m <sup>3</sup>	Glued joints	H/L	Lamella: 90 x 20 x 5 mm Bondline surface: 20 x 10 mm
[141]	2020	Lim et al.	1. Block shear test 2. Delamination test (aging cycles: vacuum, soaking, oven-drying)	MF RF 1-C-PUR	Specified*	Southern yellow pine	CLT blocks, 3 layers	L	Block shear test: 667 mm x 400 mm x 107 mm Delamination test: 76 mm x 127 mm x 105 mm
* Hexion, Ohio, USA (MF: TM 4720 with Wonderbond TM Hardener 5025A)   Specialty Chemicals, Inc., New York, USA (RF: Cascophen G-1131)   Purbond AG, Sempach station, Switzerland (1-C-PUR HB E452).									
[108]	2018	Rammer et al.	4 point bending test inside the oven with a target sample temperature 204°C	MF, PRF, 1-C-PUR (4), PVAc(2)	Not specified	Douglas fir	Finger joint	H/L	

[94]	2017	Lu et al.	The effects of priming surface of eucalyptus: 1. Block shear test 2. Cyclic temperature delamination test 3. Interlaminar shear strength bending test	EP EPI PRF 1-C-PUR	Specified*	Eucalyptus ** 580 kg/m <sup>3</sup>	CLT block, 3 layers	L	1: 100x100x54 mm t =18mm 2: 100x100x54 mm t =18mm 3: 580x150x54 mm t =18mm
* Internet Wood Glue, Guangdong, China (EPX: EP resin (901S)+polyamide resin (901B), EPI: PG368)+a mixture of polyvinyl alcohol (PVA) water-based emulsion and an isocyanate hardener (C15))   Dynea, Guangdong, China (PRF: phenol-resorcinol emulsions (PR-1HSE) and paraformaldehyde (PFA) compound power (PRH-10A))   Purbond AG, Sempach station, Switzerland (1-C-PUR)									
** Hydroxymethylated resorcinol (HMR) and hygroscopic organic solvent N,N dimethylformamide (DMF) primers									
[140]	2019	Santos et al.	1. Block shear test 2. Cyclic temperature delamination test	1-C-PUR	Specified*	Maritime pine 669 kg/m <sup>3</sup> Australian blackwood 622 kg/m <sup>3</sup>	CIT (Cross insulated timber)	L	140 x 140 x 15 mm
* Henkel & Cie AG, Sembach Station, Switzerland (1-C-PUR LOCTITE PURBOND HB S709, polyol primer LOCTITE PR 3105 PURBOND)									
[118]	2009	Frangi et al.	Standard furnace test 800 x 1000 mm	1-C-PUR (5) 1 MUF	Not specified	Spruce 405-486 kg/m <sup>3</sup>	CLT panels, 5 layers	H	1.1500 x 950 x 60 mm Layers: 10-10-10-10-20, 30-30, 20-20-20 mm
[163]	2011	Klippel et al.	Numerical model of GLT with finger joints performance in fire. The results compared to fire tests performed by König et al. [164] who did four-point bending tests on GLT beams exposed to ISO-fire on three sides.	PRF MUF 1-C-PUR(2)	1-C-PUR in GLT [164], Finger joint [102]	Spruce 435+/-31 kg/m <sup>3</sup>	GLT beam 3 layers Finger joints at the bottom	H/L	135 x 90 mm
[145]	2008	Craft et al.	New elevated temperature adhesive tension test that builds on the current methods.	1-C-PUR(7) PVA	Not specified	Spruce	Finger joints	H/L	ASTM D4688-99
[165]	1968	E.L.Shaffer	Sections cut from GLT blocks, exposed to fire on one surface, transversely cut to see separation depth and broken along the glue joints to determine residual bonded area.	PRF, PVAc MF, MUF, UF CASEIN	Not specified	Southern pine Douglas-fir	Plywood blocks	H	139 mm x 25 mm x 200 mm Layers: 8 x 25 mm
[85]	2007	Sernek et al.	Shear test of the bond line (after heat treatment) tested dry and wet	MUF PRF 1-C-PUR	Not specified	Norway spruce, Douglas fir, Poplar, Birch, Alder	GLT blocks, 4 layers	H/L	35x43x72 mm
<b>INTERMEDIATE SCALE TEST</b>									
[20]	2019	F.Wiesner	Applied compression load to a proportion of manufactured capacity of CLT walls and exposed to a radiative heat flux at their mid height. Three different scenarios of heat exposure were assessed.	MUF, 1-C-PUR	Not specified	Spruce 460 +/- 22 kg/m <sup>3</sup>	CLT walls	L/H	300 x 1700 x 100 mm (Layers: 40-20-40 mm (LCL) and 5x20 mm (LCLCL))
[23]	2016	Hasburgh et al.	Horizontal furnace test (1.83 x 1.09 x 1.27 m)	PUR,MF,PRF,EPI	Not specified	Southern pine	CLT panels: 3-layers (11), 5-layers(2)	H	1194 x 965 x 105 and 175 mm (Layers: 3x35 mm and 5x35 mm)
[36]	2018	M. Klippel, J. Schmid	Standard furnace testing	1-C-PUR, MUF	Not specified	Spruce 453 +/- 20 kg/m <sup>3</sup>	CLT panel, 5 layers	H	1000 x 800 mm Layers: 5x10 mm, 5x25 mm, 5x20 mm, 5x35 mm
[31]	2019	Brandon et al.	Furnace testing but temperature-time curve approximated from compartment testing [11]	MF, PRF, EPI, 1-C-PUR [11], Improved 1-C-PUR	Not specified	Spruce-Pine-Fir lumber	CLT panels, 5 layers, no finger joints	H	1400 mm x 600 mm x 175 mm Layers: 5x35 mm

[166]	2019	Norwahyuni et al.	1. Cyclic temperature delamination test 2. Water absorption test 3. Four point bending test 4. Single span bending test 5. Compression test	PRF 1-C-PUR		Acacia magnum 673 kg/m <sup>3</sup>	CLT panels, 3 layers	L	1. 90 mm × 90 mm × 54.5 mm 2. 70 mm × 70 mm × 54.5 mm 3. 1000 mm × 70.5 mm × 54.5 mm in size 4. 470 mm × 70.5 mm × 54.5 mm 5. 327 mm × 70 mm × 54.5 mm
*AkzoNobel, Stockholm, Sweden (PRF 1734 + Hardener 2734)   Jowat Ltd., Thailand (1-C-PUR Jowapur 687.22)									
[102]	2012	Frangi et al.	Tensile tests at elevated temperatures on finger jointed specimens	1-C-PUR(4) MUF	Not specified	Not specified	Finger joints	H/L	800 × 140 × 40 mm
[119]	2014	Klippel et al.	Standard furnace testing + Compression load applied on columns (2 different supports) and Four point bending test applied on floors	1-C-PUR	Not specified	Spruce-Pine-Fir lumber	CLT walls:3 layers, 5layers CLT panels: 5 layers	H/L	Walls: PCP: 4285 x 102 mm (Layers: 34-34-34) PCPCP: 5550 x 140 mm (Layers: 34-19-34-19-34) PPCPP:5550 x 140 mm (Layers: 34-24-24-24-34) Floor: 1200 x 4800 mm
[18]	2020	Gorska et al.	Compartment fire test	1-C-PUR	Not specified	Radiate Pine XLam	CLT walls 5 layers	H	CLT element:45-20-20-20-45 mm Compartment: 500 x 500 x 370 mm Opening: 300 x 280 mm
<b>COMPARATIVE STUDY: 1. SMALL SCALE TEST 2.LARGE SCALE TEST</b>									
[28]	2018	H.Quiqueiro, J. Gales	Small: Cone calorimeter to diff. fire severities Large: Heated locally at shear and moment locations along the length of the beam	PUR, PRF	Canadaian	Spruce pine fir	GLT beam	H/L	Small scale: 100 x 100 x 45 mm Large scale: 45 x 195 x 4200 mm Carved 5 mm, 1000 mm long - mid and sides
[117]	2016	Suzuki et al.	1. Unloaded panel standard furnace test 2. Loaded standard column furnace test	API (aqueous polymer-isocyanate adhesive) PRF	Not specified	Japanese cedar, Japanese larch	1. CLT panels, LVL panels 3,5,7 layers 2. CLTcolumns, 3 and 5 layers	1. 2. H/L	H 1. CLT: 450x1500x135 mm (Layers: 3x35 mm, 5x27 mm, 7x19.3 mm) 2. 3300x500x150 and 210 mm
[47]	2014	M. Klippel	1. Finger joints: tensile strength test Zwick 1484 in a climate chamber at the exact target temperature 2. GLT beam with one finger jointed lamella in the middle tested under tensile load and applied Standard ISO 834 curve	Structural: EPI, 1-C-PUR (4), MUF (2), PRF Non-structural: UF, MUF (1), PVAc, 1-C-PUR	Not specified	Spruce 412 kg/m <sup>3</sup>	Finger joints	H/L	1. 150 x 40 mm 2. 140 x 280 x 3500 mm (Layers: 8x40 mm)
<b>LARGE SCALE TEST</b>									
[33]	2012	M.Klippel, A.Frangi	Vertical furnace test 2000 x 2000 mm, ISO curve	1-C-PUR (not the same as in small scale)	Not specified	Spruce	CLT wall elements	H	w x d = 2000 x 2000 x 84 and 85 mm (Layers: 3x28 mm and 5x17 mm)
[20]	2019	F.Wiesner	Effect of transient slow heating on four point bended elements	MUF, 1-C-PUR	Not specified	Spruce 460 +/- 22 kg/m <sup>3</sup>	CLT beams	L/H	300 x 3000 x 100 mm, Layers: 40-20-40 mm (LCL) and 5x20 mm (LCLCL)
[26]	2016	Emberly et al.	Heated with a radiant panel, afterwards three-point bend test until failure	1-C-PUR	Not specified	European spruce 425 kg/m <sup>3</sup>	CLT, beam 5 layers	H/L	145 x 100 x 1500 mm

[167]	2019	Muszyński a et al.	Standard furnace testing	1-C-PUR(2) 2-C-MF	Not specified	Spruce-Pine-Fir lumber Douglas-fir larch	CLT panels: 472 kg/m <sup>3</sup> , 532 kg/m <sup>3</sup> , 554 kg/m <sup>3</sup> , 5 layers	H/L	2794×4267 x 175mm (halp joint)
<b>FULL SCALE TEST</b>									
[128]	2018	Zelinka et al.	Compartment fire test: 4 hours, sprinkler activated, sprinkler delayed 20 min	1-C-PUR	Not specified	Douglas Fir Larch	CLT panels and walls, 5 layers	H/L	t =175 mm, room size varies, h= 2.75 m
[30]	2017	Janssens et al.	Compartment fire test	1-C-PUR (same in [11]), MF Improved 1-C-PUR	Not specified	Spruce-Pine-Fir lumber Douglas fir lumber	CLT panels and walls average 497 kg/m <sup>3</sup>	H/L	Room size: 2750x5800x2430 mm Ceiling CLT panel: 2430x4870x175 mm Layers: 5x35 mm
[11]	2018	Su et al.	Compartment fire test	1-C-PUR	Not specified	Spruce-Pine-Fir lumber	CLT panels, 5 layers, no finger joints	H/L	Room size: 9100 x 4600 x 2700 mm Test1-1, 1-2:all CLT surfaces protected; Test1-3, 1-5:one CLT wall exposed; Test 1-4 one ceiling exposed, Test 1-6:wall and ceiling exposed
[13]	2017	Hadden et al.	Five full-scale compartment fire experiments on CLT compartments (Three configurations of exposed CLT surfaces)	1-C-PUR	Not specified	Spruce	CLT panels and walls	H/L	Room size: 2720 ×2720 × 2770 mm Layers: 5 x 20 = 100 mm Opening:1840×760 mm .
[114]	2019	Wiesner et al.	Five full-scale compartment fire experiments on CLT compartments (Three configurations of exposed CLT surfaces)	1-C-PUR	Not specified	Spruce	CLT panels and walls	H/L	Room size: 2720 ×2720 × 2770 mm Layers: 5 x 20 = 100 mm Opening:1840×760 mm .



## Appendix C

### Structural load design and testing procedure checklist

The designed slab is taken to be between two storeys in the shopping area (Category D [168]), because that type of occupancy offers the highest design imposed load (5 kN/m<sup>2</sup>) in European Standards. Combined with self-weight it will give the highest requirements for design load combination. The chosen load serves as a reference value for designers with no scientific basis that can be directly correlated to this study, but still to avoid taking arbitrary values. Once the imposed load and the self-weight are known, one can calculate the deflections for different span lengths (4-12 m) but the same height (20 cm). The 5.5 m long span is chosen to be representative.

Table C. 1.. Designed slab trials - geometry

Width [m]	1		
Length [m]	5.5	6	8
Layer thickness [m]	0.04		
Total thickness [m]	0.2		
Density [kg/m <sup>3</sup> ]	470		
G <sub>k</sub> : Self-weight [kN/m <sup>2</sup> ]	1		
Q <sub>k</sub> : Imposed load [kN/m <sup>2</sup> ]	5		

Characteristic values from the self-weight and imposed load are multiplied with partial factors according to EN 1990 and EN 1991-1 to obtain the design load  $E_d$ .

$$E_d = 1.35G_k + 1.5Q_k \rightarrow q \quad \text{Eq. 1}$$

First, serviceability limit state is calculated in the middle of the span using a software CLT Designer based on the Eq 2-5. Stiffness is calculated by using the effective cross-section method.

$$\text{Deflection } w < l/250 \quad w(l/2) = (5 \cdot q \cdot L^4 / 384K_{CLT}) + (q \cdot L^2 / 8 \cdot S_{CLT}) \quad \text{Eq. 2}$$

$$\text{Bending stiffness} \quad K_{CLT} = \sum E_i \cdot I_i + \sum E_i \cdot A_i \cdot e_i^2 ; i = 0,90; \quad \text{Eq. 3}$$

Shear stiffness  $S_{CLT} = S_{tot} \cdot \kappa$  Eq. 4

Rigid shear stiffness  $S_{tot} = \sum G_i \cdot b_i \cdot t_i$  Eq. 5

Correction coefficient  $\kappa \approx 1/4$ , for exact procedure follow [159]

Vibration According to Eurocode and/or Hamm Richter [159]

$w$	deflection [mm]
$L$	Length [m]
$E_i$	modulus of elasticity of layer $i$ , ( $E_{0,i}$ or $E_{90,i}$ )
$I_i$	moment of inertia of layer $i$ in reference to its neutral axis
$A_i$	cross-sectional area of layer $i$
$e_i$	distance between the centre of gravity $S_i$ of layer $i$ and the centre of gravity $S$ of the CLT element
$\kappa$	shear correction coefficient,
$G_i$	shear modulus of layer $i$ ( $G_i$ or $G_{r,i}$ )
$b_i$	width of layer $i$
$t_i$	thickness of layer $i$

Span is reduced from 8m, to 6m and eventually to 5.5 m when the requirements for instantaneous, the final and net final deflections, as well as the vibrations were fulfilled. Only results for 5.5. m span are presented within this study. A five-layer CLT slab, 1 m wide, has the first bottom lamella exposed to fire oriented in the direction of the span (longitudinally). The slab has three longitudinally oriented load-bearing layers, while the other two orthogonally oriented do not contribute to the total bending stiffness  $K_{CLT}$  and  $E_{90}$  is taken as zero.

Table C. 2.. Serviceability design

Span [m]	5.5	6	8
$M_{Ed}$ [kNm]	33.4	39.8	70.8
$V_{Ed}$ [kN]	24.3	26.5	35.4
	Used capacity [%]		
SLS: Deflections	88	115	261
SLS: Vibrations EN 1995-1	pass	pass	fail



Once the span is defined, the design load is used to calculate the bending moment in the middle of the span and the shear force at the support.

$$M_{Ed} = q \cdot L^2/8 \quad \text{Eq. 6}$$

$$V_{Ed} = q \cdot L/2 \quad \text{Eq. 7}$$

For the elements loaded out-of plane maximal normal stresses are on the top and bottom of the section and they have to be lower than the bending strength. Timoshenko beam theory is used for this calculation.

More important for this thesis is shear stress over the cross-section, which follows quadratic distribution for longitudinal layers ( $0^\circ$ ) and has constant values in orthogonal ( $90^\circ$ ) layers where elastic modulus  $E_{90}$  is 0.

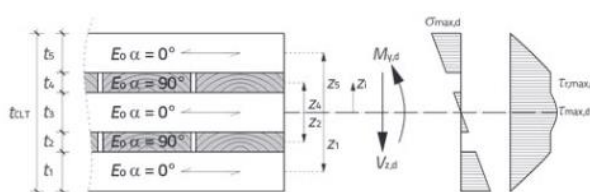


Figure C. 1. Normal and shear stress distribution over the cross-section with longitudinally oriented outer layers [169]

As the deflection is governing parameter for failure, calculated shear stress in longitudinal layer is lower than pure shear strength  $f_{v,k} = 4$  MPa, and in orthogonal layers lower than the rolling shear strength  $f_{r,k} = 0.7$  MPa (no narrow bond-line) or  $f_{r,k} = 1.25$  MPa (with narrow bond-line). Their difference was discussed within Literature review. Values are prescribed in European standards and characteristic, which means that they will be slightly reduced depending on material safety factor ( $\gamma_M$ ), load-duration class and moisture content ( $k_{mod}$ ).

Bending stresses 
$$\sigma(z) = M_y \cdot z \cdot E(z)/K_{CLT} \quad \text{Eq. 8}$$

Shear stresses 
$$\tau(z) = \left( V_y \int E(z) \cdot z \cdot dA \right) / K_{CLT} \cdot b(z) \quad \text{Eq. 9}$$

Table C. 3. Serviceability design in ambient conditions

Span [m]	5.5	6	8
MEd [kNm]	33.4	39.8	70.8
VEd [kN]	24.3	26.5	35.4
USL: Bending [%]	38	40	72
USL: Shear [%]	22	22	29

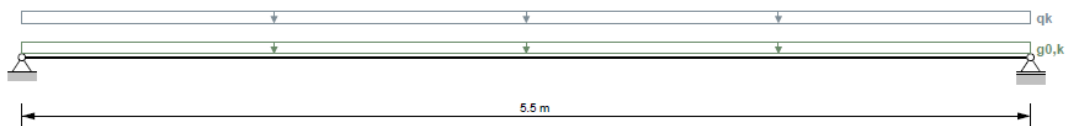
Once the shear stress is obtained it is applied on the bond-line of the specimen (100x100 mm) to design the needed load to perform the experiment. Procedure was repeated for the case when the first lamella has fallen off. Below one can find the report from CLTdesigner used for faster calculation of vibrations and deflection, where specific manufacturer can be chosen and then the material properties are directly proposed by the software. For this study, Stora Enso material properties were used.

## 1 General

Service class 1

## 2 Structural system

Single span girder



### 2.1 Supports

Support	x	Width
A	0.0 m	0.06 m
B	5.5 m	0.06 m

## 3 Cross section

CLT-Product with technical approval of the company Stora Enso: 200 L5s

5 layers (thickness: 200 mm)

### 3.1 Layer composition

Layer	Thickness	Orientation	Material
# 1	40 mm	0	C24-STORA ENSO ETA 2019
# 2	40 mm	90	C24-STORA ENSO ETA 2019
# 3	40 mm	0	C24-STORA ENSO ETA 2019
# 4	40 mm	90	C24-STORA ENSO ETA 2019
# 5	40 mm	0	C24-STORA ENSO ETA 2019

### 3.2 Material parameters

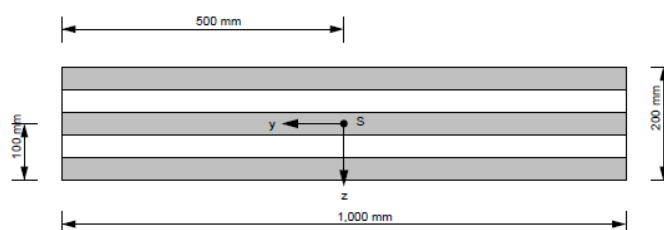
Partial safety factor  $\gamma_M = 1.25$

System factor for CLT  $k_{SYS} = 1.0$

Material parameters for	C24-STORA ENSO ETA 2019
bending strength [N/mm <sup>2</sup> ]	$1 / k_{SYS} \cdot 26.4$
tensile strength parallel [N/mm <sup>2</sup> ]	14.0
tensile strength perpendicular [N/mm <sup>2</sup> ]	0.12
compressive strength parallel [N/mm <sup>2</sup> ]	21.0
compressive strength perpendicular [N/mm <sup>2</sup> ]	2.5
shear strength [N/mm <sup>2</sup> ]	4.0
rolling shear strength [N/mm <sup>2</sup> ]	1.05
Youngs modulus parallel [N/mm <sup>2</sup> ]	12,000.0
5%-quantile from Youngs modulus parallel [N/mm <sup>2</sup> ]	10,000.0
Youngs modulus perpendicular [N/mm <sup>2</sup> ]	370.0 (0.0)
shear modulus [N/mm <sup>2</sup> ]	690.0
rolling shear modulus [N/mm <sup>2</sup> ]	50.0
density [kg/m <sup>3</sup> ]	350.0
density mean value [kg/m <sup>3</sup> ]	500.0

### 3.3 Cross-sectional values

$EA_{ef}$	1.44E9 N
$EI_{ef}$	6.336E12 N·mm <sup>2</sup>
$GA_{ef}$	1.595E7 N



### 4 Loads

Field	$g_{0,k}$	$g_{1,k}$	$q_k$	Category	$s_k$	Altitude/Region	$w_k$
1	0.981 kN/m		5 kN/m <sup>2</sup>	D			

#### Partial safety factors:

$\gamma_G = 1.35$

$\gamma_Q = 1.5$

#### Load position:

Plate weight: Total

Permanent loads: Total

Imposed loads: Field-by-field

Snow: Field-by-field

Wind: Total

**Combinations:**

Combination factors: according to EN

Combinations of distributed and concentrated loads:

$q_k$  and  $Q_k$  will be considered as one load group

s and S will be considered as one load group

$w_k$  and  $W_k$  will be considered as one load group

**5 Specification concerning structural fire design**

No specifications are available

**6 Information concerning vibrations**

normal requirements

Damping factor: 1.0 %

Support: 2-sided

Width perpendicular to the main load bearing direction: 1.0 m

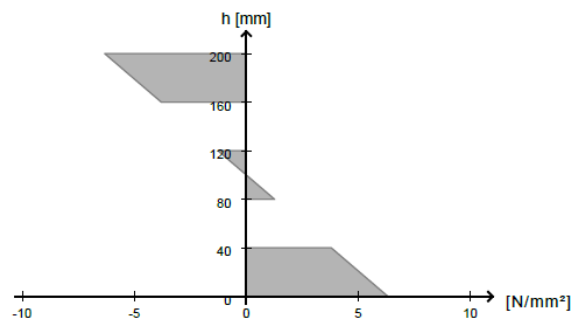
**7 Results**

Referenced standards: EN 1995-1-1:2009

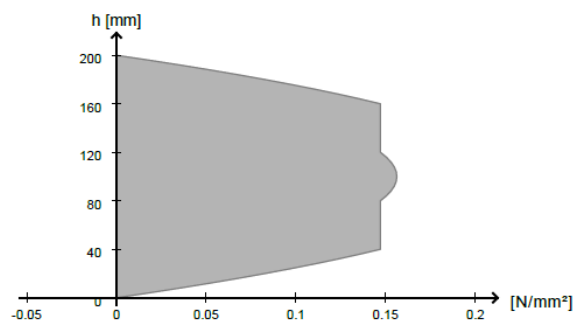
Underlying calculation method: Timoshenko

**7.1 ULS****7.1.1 Bending**

Utilisation ratio	37.4 %
$k_{mod}$	0.8
at x	2.75 m
Ek	2
Fundamental combination	$1.35 \cdot q_{0,k} + 1.50 \cdot 1.00 \cdot q_k$

**7.1.2 Shear**

Utilisation ratio	21.9 %
$k_{mod}$	0.8
at x	0.0 m
Ek	2
Fundamental combination	$1.35 \cdot q_{0,k} + 1.50 \cdot 1.00 \cdot q_k$



### 7.1.3 Bearing pressure

Utilisation ratio	17.9 %
$k_{mod}$	0.8
at x	0.0 m
$E_k$	2
Fundamental combination	$1.35 \cdot g_{0,k} + 1.50 \cdot 1.00 \cdot q_k$



## 7.2 SLS

### 7.2.1 Deflection

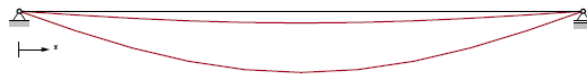
Limit values according to EN 1995-1-1

Instantaneous deformation  $w_{inst} t = 0$ :  $l/300$  (12.7 mm, 69.1 %)

Final deformation  $w_{net,fin} t = inf$ :  $l/250$  (19.4 mm, 88.2 %)

Final deformation  $w_{fin} t = inf$ :  $l/150$  (19.4 mm, 52.9 %)

Utilisation ratio	88.2 %
$w_{max}$	19.4 mm
$k_{def}$	0.8
at x	2.75 m
$E_k$	8
Final deformation $w_{net,fin} t = inf$ ( $l/250$ )	



### 7.2.2 Vibration

The verification is only valid for residential ceilings!

#### 7.2.2.1 Verification corresponding to EN 1995-1-1

Eigenfrequency:  $f_1 = 12.32 \text{ Hz} > 8.0 \text{ Hz}$

Stiffness:  $w_{1kN} = 0.633 \text{ mm} < 2.00 \text{ mm}$

Velocity/Unit impuls:  $v = 5.333 \text{ mm/s} < 12.97 \text{ mm/s}$

---> Vibration verification fulfilled (65.0 %)

## 8.1 Combinations

$E_k$	$k_{mod} / k_{def}$	Combination
Fundamental combination		

$E_k$	$k_{mod} / k_{def}$	Combination
1	0.6	$1.35 \cdot g_{0,k}$
2	0.8	$1.35 \cdot g_{0,k} + 1.50 \cdot 1.00 \cdot q_k$
3	0.6	$g_{0,k}$
4	0.8	$g_{0,k} + 1.50 \cdot 1.00 \cdot q_k$

Accidental combination		
SLS combinations according to EN 1995-1-1		
6	0.8	$g_{0,k} + 1.00 \cdot q_k$
7	0.8	$g_{0,k} + (g_{0,k})_{\text{creep}} + 1.00 \cdot q_k + (0.60 \cdot q_k)_{\text{creep}}$
8	0.8	$g_{0,k} + (g_{0,k})_{\text{creep}} + 1.00 \cdot q_k + (0.60 \cdot q_k)_{\text{creep}}$
SLS combinations according to EN 1995-1-1:NA		

## 8.2 Internal forces

Field	x	$M_{y,d}$	$V_{z,d}$
	[m]	[kN·m]	[kN]

Ek 2: $1.35 \cdot g_{0,k} + 1.50 \cdot 1.00 \cdot q_k$			
1	0.0	0.0	24.267
1	0.55	12.012	19.414
1	1.1	21.355	14.56
1	1.65	28.028	9.707
1	2.2	32.032	4.853
1	2.75	33.367	-0.0
1	3.3	32.032	-4.853
1	3.85	28.028	-9.707
1	4.4	21.355	-14.56
1	4.95	12.012	-19.414
1	5.5	-0.0	-24.267

## 8.3 Deformations

Field	x	$w_{z,\min}$	$w_{z,\max}$
	[m]	[mm]	[mm]
Load case group $g_{0,k}$			
1	0.0	0.00	0.00
1	0.55	0.66	0.66
1	1.1	1.24	1.24
1	1.65	1.70	1.70
1	2.2	1.98	1.98
1	2.75	2.08	2.08
1	3.3	1.98	1.98
1	3.85	1.70	1.70
1	4.4	1.24	1.24
1	4.95	0.66	0.66
1	5.5	0.00	0.00

Load case group $q_k$			
1	0.0	0.00	0.00
1	0.55	0.00	3.38
1	1.1	0.00	6.34
1	1.65	0.00	8.64
1	2.2	0.00	10.09
1	2.75	0.00	10.59
1	3.3	0.00	10.09
1	3.85	0.00	8.64
1	4.4	0.00	6.34
1	4.95	0.00	3.38
1	5.5	0.00	0.00

#### 8.4.1 Characteristic supporting forces

Load case group	Support	x	$F_{z,k,min}$	$F_{z,k,max}$
		[m]	[kN]	[kN]
$g_{0,k}$	A	0.0	2.698	2.698
	B	5.5	2.698	2.698
$q_k$	A	0.0	0.0	13.75
	B	5.5	0.0	13.75

#### 8.4.2 Design supporting forces

Support	x	$F_{z,d,min}$	$E_k$	$F_{z,d,max}$	$E_k$
	[m]	[kN]		[kN]	
A	0.0	2.698	3	24.267	2
B	5.5	2.698	3	24.267	2

#### 8.5.1 Bending

Field	x	$E_k$	$k_{mod}$	$M_{y,d}$	$\sigma_{max,d}$	$f_{m,d}$	$\eta$
	[m]		[-]	[kN-m]	[N/mm <sup>2</sup> ]	[N/mm <sup>2</sup> ]	[%]
1	0.0	1	0.6	0.00	0.00	12.67	0.0
1	0.55	2	0.8	12.01	2.28	16.90	13.5
1	1.1	2	0.8	21.35	4.04	16.90	23.9
1	1.65	2	0.8	28.03	5.31	16.90	31.4
1	2.2	2	0.8	32.03	6.07	16.90	35.9
1	2.75	2	0.8	33.37	6.32	16.90	37.4
1	3.3	2	0.8	32.03	6.07	16.90	35.9
1	3.85	2	0.8	28.03	5.31	16.90	31.4
1	4.4	2	0.8	21.35	4.04	16.90	23.9
1	4.95	2	0.8	12.01	2.28	16.90	13.5
1	5.5	2	0.8	-0.00	0.00	16.90	0.0



## 8.5.3 Bearing pressure

Support	x	Ek	$k_{mod}$	$F_d$	$A_{sec}$	$k_{c,90}$	$\sigma_{c,90,d}$	$f_{c,90,d}$	$\eta$
	[m]		[-]	[kN]	[mm <sup>2</sup> ]	[-]	[N/mm <sup>2</sup> ]	[N/mm <sup>2</sup> ]	[%]
A	0.0	2	0.8	24.27	60,000	1.41	0.40	2.26	17.9
B	5.5	2	0.8	24.27	60,000	1.41	0.40	2.26	17.9

## 8.5.2 Shear

Field	x	Ek	$k_{mod}$	$V_{z,d}$	$\tau_{v,d}$	$f_{v,d}$	$\eta$
					$\tau_{r,d}$	$f_{r,d}$	
	[m]		[-]	[kN]	[N/mm <sup>2</sup> ]	[N/mm <sup>2</sup> ]	[%]
1	0.0	2	0.8	24.27	0.16	2.56	6.1
					0.15	0.67	21.9
1	0.55	2	0.8	19.41	0.13	2.56	4.9
					0.12	0.67	17.5
1	1.1	2	0.8	14.56	0.09	2.56	3.7
					0.09	0.67	13.1
1	1.65	2	0.8	9.71	0.06	2.56	2.4
					0.06	0.67	8.8
1	2.2	2	0.8	4.85	0.03	2.56	1.2
					0.03	0.67	4.4
1	2.75	1	0.6	-0.00	0.00	1.92	0.0
					0.00	0.50	0.0

## 8.5.4 Deformations

Field	x	Ek	$k_{def}$	$w_{max}$	$w_{limit}$	$\eta$
	[m]			[mm]	[mm]	[%]
1	0.0	6	0.8	0.00	18.33	0.0
1	0.55	8	0.8	6.19	22.00	28.1
1	1.1	8	0.8	11.63	22.00	52.9
1	1.65	8	0.8	15.84	22.00	72.0
1	2.2	8	0.8	18.50	22.00	84.1
1	2.75	8	0.8	19.41	22.00	88.2
1	3.3	8	0.8	18.50	22.00	84.1
1	3.85	8	0.8	15.84	22.00	72.0
1	4.4	8	0.8	11.63	22.00	52.9
1	4.95	8	0.8	6.19	22.00	28.1
1	5.5	6	0.8	0.00	18.33	0.0

## Testing procedure checklist

- Turn on the hood to extract the smoke produced.
- Turn on the water to cool the heat flux gauge.
- Check if the thermocouples and heat flux gauge are connected to the datalogger.
- Turn on the data logger and check if the temperatures readings are close to the ambient temperature.
- Turn on the stepper motor and control the mechanical linear motion system to move the radiant panel sufficiently far away from the specimen and measure the distance from the specimen.
- Centrally position the heat flux gauge in front of the radiant panel. Measure if the initial physical distance from the gauge to the radiant panel corresponds to the one presented in the software to control the motion of the radiant panel. Presented as calibrated distance in Figure 28.
- Turn on the fans for the air supply system to the radiant panel.
- Turn the lever ball valve to release the propane flow through the gas supply system to the radiant panel. Use the torch in front of the panel to achieve ignition of the propane. Adjust the intensity of four smaller panels to achieve steady and uniform radiation exposure.
- Wait for the radiant heat flux reading to stabilise. Move the position of the radiant panel in front of the heat flux gauge and calibrate to get the reading within 1% of the desired heat flux ( $50 \text{ kW/m}^2$ ).
- Once a constant incident heat flux boundary condition is achieved, remove the heat flux gauge.
- Remove the radiant shield from the specimen.
- Simultaneously restart the data logger to measure temperatures, start the video recording, and press the command for the radiant panel to move towards the specimen for the calibrated distance.

- Turn on the photo camera when the radiant panel is positioned in front of the specimen.

During the test, one needs to visually observe and monitor possible char fall-off and delamination. Once the sample fails, the following steps are required:

- Turn off the radiant panel and move it to the initial position before testing.
- Move the vermiculite board.
- For Trial 1 leave the samples to cool down by themselves. For Trial 2 and 3, extinguish the samples and fallen char with sprayed water.
- Once the samples are extinguished, turn off the data logger, the photo, and video camera.
- Take photos of the specimen and the fallen parts on the floor immediately after failure.
- Collect the fallen char in the aluminium foil and measure its weight.
- Take the sample from the frame and measure its weight.
- Take photos of specimen and char under the light bulb from all sides.
- Cut the samples in several slices to observe the char penetration depth.
- Take photos of the sliced samples.
- Store the sample and prepare the setup for the next testing.

# Appendix D

## Results

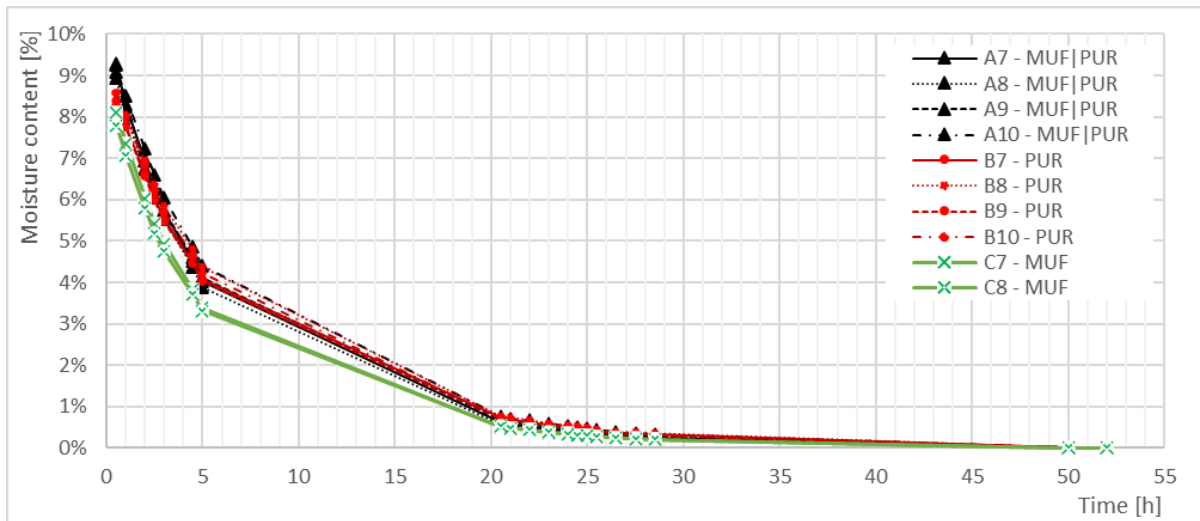


Figure D. 1. Change of moisture content for samples exposed to drying conditions at 103°C

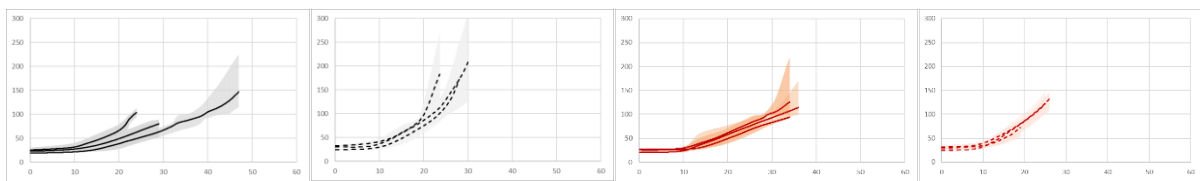


Figure D. 2. Average thermocouple reading at the first bond line. Temperature-time curve for all specimens bonded with 1-C-PUR (PUR1) at the bond-line between layers and combination of Hotmelt and PVAc between single lamellae (narrow bonding). From left to right: 100 kg, 200 kg, 100 kg dry, 200 kg dry.

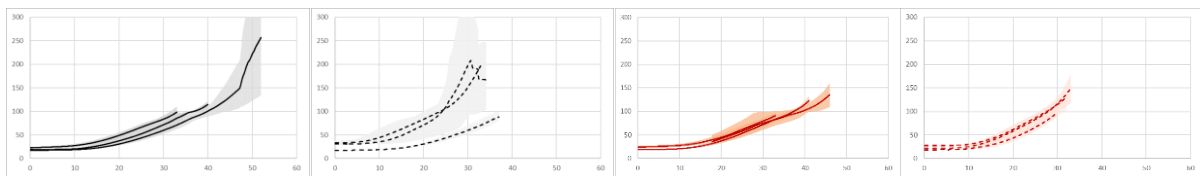


Figure D. 3. Average thermocouple reading at the first bond line. Temperature-time curve for all specimens bonded with 1-C-PUR (PUR2) at the bond-line between layers and between single lamellae (narrow bonding). From left to right: 100 kg, 200 kg, 100 kg dry, 200 kg dry.

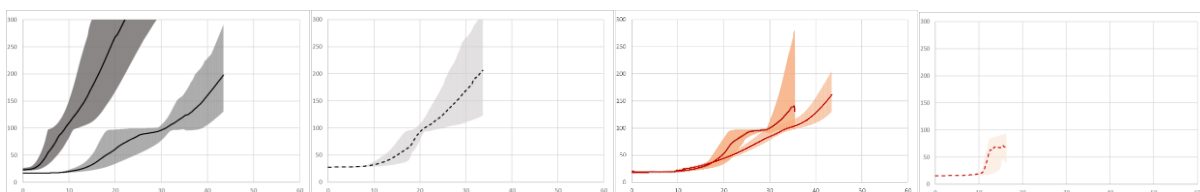


Figure D. 4. Average thermocouple reading at the first bond line. Temperature-time curve for all specimens bonded with MUF at the bond-line between layers and between single lamellae (narrow bonding). From left to right: 100 kg, 200 kg, 100 kg dry, 200 kg dry.

For non-dried MUF adhesive loaded under 100 kg in Figure D.4., thermocouples were accidentally drilled through the first bond-line and they are representative of the behaviour in the middle of the front lamella.

Table D. 1. Visual observation of samples before wood failure, at the moment of wood failure, and after cooling.

L	S	Stage 2: Testing		Stage 3: Post-processing	
100	B6 33:09				
	B11 40:45				
	C3* 51:17				
	C5 43:30				

L	S	Stage 2: Testing		Stage 3: Post-processing	
200	B4* 41:1 3				
	B5 39:4 8				
	C4 35:0 3				
	C6* 44:1 0				
100D	B13 30:3 4				
	B10 34:5 0				

200D	B8*				
	32:4 4				

















Table D. 2. Visual observation of samples before or/and at delamination, and after cooling.

L	S	Stage 2: Testing		Stage 3: Post-processing	
200	B12				
	46:46				
100D [MC: 0 %]	B7*				
	37:00				
100D [MC: 0 %]	C7*				
	33:43				
200D [MC: 0 %]	A14				
	26:49				


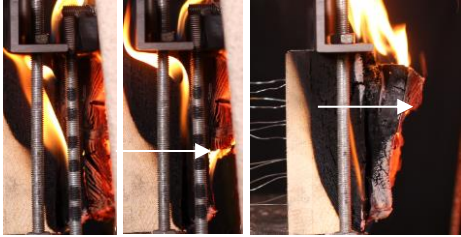




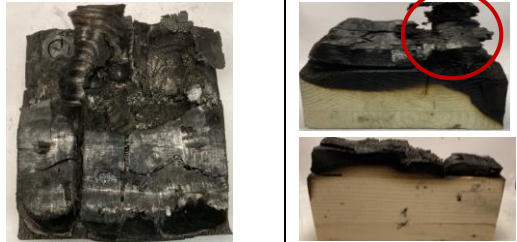
	<p>B9 33:40</p>				
<p style="writing-mode: vertical-rl; transform: rotate(180deg);">200D [MC: 0 %]</p>	<p>B14 41:13</p>				
	<p>C8* 16:22</p>				



Table D. 3. Visual observation of samples before and at char fall-off (CF)/mechanical failure (MF), and after cooling.

L	S	Stage 2: Testing		Stage 3: Post-processing	
100	<p><b>A3</b> 23:50  29:19</p>				
		CF: Upper part of the 1 <sup>st</sup> layer chars and falls off <b>at the 1<sup>st</sup> adhesive line</b> , indicated by the reignition. Followed by a local failure of the charred lamella at the top.			
	<p><b>B3*</b> 47:00  52:00</p>				
		CF: Right part of the 1 <sup>st</sup> layer chars and falls off <b>at the 1<sup>st</sup> adhesive line</b> , indicated by the reignition. Followed by a local failure of the remaining lamella at the top.			
<p><b>A4*</b>   48:04</p>					
	MF: Failure appears when the left lamella in the 2 <sup>nd</sup> layer completely chars and falls off <b>at 2<sup>nd</sup> the adhesive line</b> , indicated by reignition.				
<p><b>A11</b> 18:00  24:50</p>					
	CF: In the 1 <sup>st</sup> layer, lamella chars and experiencing <b>buckling</b> falls off <b>at the 1<sup>st</sup> adhesive line</b> , indicated by reignition. Followed by a local failure at the top of the 2 <sup>nd</sup> charred lamella.				

200	<p><b>A5*</b></p> <p>36:50</p>					<p>MF: Failure appears <b>after char reaching the 1<sup>st</sup> adhesive line</b>. Flaming combustion present in second photo is from the local failure at the top and side failure where sample has an in-depth cut in the bond-line. There was no reignition present in the bonded area.</p>
	<p><b>A6</b></p> <p>35:00</p> <p>36:19</p>					<p>CF: Firstly char falls off <b>after char reaching the 1<sup>st</sup> adhesive line</b> (no reignition); Failure appears when most of the 2<sup>nd</sup> charred layer uniformly falls down. Failure happened <b>before char reaching the adhesive line</b> (last figure), but still allowing for reignition. <b>This is not delamination because the lamella was completely charred before falling.</b></p>
	<p>A12</p> <p>34:27</p>					<p>CF: Firstly, charred lower part of the 1<sup>st</sup> lamella falls after the 1<sup>st</sup> adhesive line. Followed by a shear within the 2<sup>nd</sup> charred lamella.</p>
100D	<p><b>A10</b></p> <p>15:30</p> <p>19:10</p> <p>23:40</p>					<p>CF: Firstly, charred lower part of the 1<sup>st</sup> lamella falls <b>at the 1<sup>st</sup> adhesive line</b> experiencing <b>buckling</b> failure and flaming combustion. Secondly, upper char falls off <b>after char reaching the 1<sup>st</sup> adhesive line</b> with no bigger reignition. Failure is local at the top due to significant char regression of the complete second lamella.</p>

L	S	Stage 2: Testing	Stage 3: Post-processing
100D	<p>A13</p> <p>25:30 26:00</p> <p>30:53</p>	 	 <p>CF: Firstly, first charred lamella falls off in parts <b>after char reaching the 1<sup>st</sup> adhesive line</b>, there is no flaming and the parts just drop. Second lamella then experiences <b>buckling</b>, failure appears partially locally at the top, after significant char regression of the second lamella.</p>
	<p>A7</p> <p>28:32</p>		 <p>MF: Failure appears <b>after char reaching the 1<sup>st</sup> adhesive line</b>, reignition not present. Specimen was left to smoulder which lead to regression, falling of the residual char after the failure as indicated in the photos in Stage 3, and eventual self-extinction.</p>
200D	<p>A8*</p> <p>25:06</p>		 <p>MF: Failure appears <b>after char reaching the 1<sup>st</sup> adhesive line</b> , reignition not present.</p>

## Appendix E

### Limitations and recommendations

Table E. 1 Limitations in methodology (continued)

Methodology and results		
	Limitation	Consequence
Statistical power	The number of thermocouples close to the centre of the bond line might be insufficient.	Thermocouples do not represent well the developed temperature profiles and gradients before and after the bond-line. Lack of statistical power can restrict the author to draw definite conclusions from the study, but it still allows for comparison among trials.
	Two samples for each series were tested in ambient conditions under hydraulic jack.	Not enough to obtain the reference value of shear strength for the specific group of samples.
	A lower number of the dried and non-dried MUF samples (2+4) than PUR1 and PUR2 samples (6+6) was tested in fire conditions.	The experimental matrix allows for the comparison of adhesives with the same geometry (PUR2 and MUF) which do not have the same number of samples.
	The extinguishing method in Trial 1 differs from the one in Trial 2 and 3.	Wood failure percentage and char residue after failure in Trial 1 cannot be compared with Trial 2 and 3.
	Geometry	Restricted comparison of PUR1 with other adhesive due to different geometries.
Heat transfer	Non-uniform heating from the four smaller radiant panels, and the unknown/unquantified convective component in the heat transfer from the radiant panel.	Time to ignition and rate of thermal penetration
	Side oxidation of the sample due to the imperfect alignment of the vermiculite board.	Faster charring from the sides. A possible increase in temperatures read by the thermocouples in the first bond line closer to the edge. It also makes it difficult to address the charring rate with certainty.

Table E. 2 Limitations in methodology (continued)

<b>Methodology and results</b>		
<b>Limitation</b>	<b>Consequence</b>	
<b>Heat transfer</b>	A sample has different boundary conditions at the sides, a metal plate at the top of the sample and ambient air at the side and bottom surfaces	Possible non-uniform 1D heat transfer.
	Thermocouple holes were drilled manually.	Depth accuracy is prone to human error, i.e. reading of the temperatures might not be from the same plane. The wrong installation of thermocouples can lead to a time delay and a lower temperature reading [36], [31].
	Thermocouple holes were drilled manually.	For one MUF sample, thermocouples were penetrated too deep into the front lamella which restricted observation of bond-line temperatures at the time of failure and hence they were estimated through linear interpolation. Since Series C is the group with the least number of samples, this contributed to statistical uncertainty in results.
	High conductivity of the thermocouples.	When compared to the timber, creates a heat sink and influences the temperature readings of the thermocouple itself, which are then different than they would be in the wood when the thermocouple is not there
	Aleatoric uncertainties over which we have no control (i.e. exact chemical composition of the adhesive unknown, smoke extraction was never the same and might have changed the boundary conditions for burning; Timber is a natural organic material, and its thermal and chemical properties are randomly distributed variables)	

Table E. 3 Limitations in methodology (continued)

<b>Load transfer</b>	Possibly non-uniformly distributed load, which was positioned manually each time by one (or two) person on the steel plate at the bottom of the loading rig.	Eccentricity in load transfer. As a result of human mistake, undesirable momentum affecting the load transfer can appear, while the authors' intention is only to observe pure shear.
	A sample is positioned in the rig manually, by using the spanner and only the human force to achieve the clamping.	If the force is insufficient, developed momentum in the clamped specimen can cause the leaning of the sample which can influence the failure mode.
	The top of the front lamella which has to transfer the load to the bond line is not bonded (cut is made to obtain the 1D heating),	Localised stresses might develop.
	The specimens' initial strength is unknown.	Standardised strength values for the design of load application are taken as a reference and they can be higher depending on the timber species, moisture content etc. In that case, higher load would be required.

Table E. 4 Limitations in results

<b>Results and data analysis</b>		
<b>Data interpretation</b>	Change in the experimental condition among trials	Extinguishing in Trial 1 can have an impact on data interpretation. This is done to assess the mass loss with no influence of water.
	Insufficient clamping Unstable position of loading frame Structural load eccentricity	Local failure at the top of lamella. Restricts the comparison between MUF and PUR2 adhesives when it comes to char fall-off and delamination. Local failure at the top of the lamella is not the objective of this study.

	Hand drilling of thermocouple holes	For one MUF sample, thermocouples were penetrated too deep into the front lamella which restricted observation of bond-line temperatures at the time of failure and hence they were estimated through linear interpolation. Since Series C is the group with the least number of samples, this contributed to statistical uncertainty in results.
	Geometry	Char fall-off evaluation is not possible when only one lamella is present and completely loaded.
	Visual observation	The charring rate cannot be measured from the photos taken from the sides because the boundary conditions are not the same as in the middle of the samples.
<b>Other</b>	An intermediate-scale test	It might not directly address the behaviour of a system, but it can be used as an indicator for the necessity of further testing and upscaling.
	Cognitive bias	Author has first done literature review and created expectation about samples behavior based on the experimental setup.
	Time constraints (<4 months) The original intention was to measure also the deflection and movement of the first front lamella with a data image correlation (DIC) method and circle tracking script created in MatLAB.	Some parts of data analysis might have been neglected which influences the completeness of the study. Deflection measurements based on the data image correlation to track the possible creep and plastic behaviour of the samples were not performed.

Since the methodology is in the developing phase, an outcome of the study will serve as an input for possible improvement for both epistemic and statistical uncertainty.

Although it cannot be completely avoided, one can design for a specific threshold in statistical uncertainty, which is expected to drop with a higher number of trials [170]. However, this can only be done once the methodology is improved, optimised, and streamlined. Potential improvements are addressed within the following table.

Table E. 5 Recommendations for improvement

Limitation	Mitigation
Statistical uncertainty	To obtain the confidence interval, a larger number of tests should be performed once the methodology is improved. Testing more samples with the same variables: same adhesive different number of plies, same number of plies different adhesive.
	Testing more samples in ambient conditions to get the representative design shear strength.
	Extinguishing all samples to observe failure modes.
	Drill all thermocouple holes by the exact depth with a robot to have an even distribution along the plane.
	Install more thermocouples, and more centrally in the bond line to avoid side effects.
Methodology: char fall-off evaluation	To assess the behaviour of the char fall-off at the adhesive line two lamellas need to be loaded under the shear so that the load can be transferred in the second one once the first one has charred. This will also allow for the evaluation of the charring rate.
Methodology: local failure at the top	Load needs to be introduced centrally and any momentum caused by eccentricity should be avoided.
	If clamping is done by human it should be ensured with a torque wrench.
	Cuts should still be preserved so that the glue line is not affected by any side effect (e.g. flaming), but one should consider insulating the holes.



Methodology: heat transfer	Better representation of the thermal profiles can be obtained by heating the sample without loading it and introducing more thermocouples in different planes.
	Pope et al. [171] measured errors associated with the thermal disturbance created when a thermocouple is inserted perpendicular to a thermal wave in a charring material of low conductivity and presented a correction method.
	Testing under different and transient heat fluxes
	Consider insulating the sides to prevent increased oxidation.
Methodology: structural load transfer	Measuring deflections with image analysis module GeoPIV.
	Apply the type of load that allows for uniform distribution, i.e. plates.
Other	Consider method for tracking the moisture movement and temperature-creep dependence